6-2014

Predictive Modeling in the Search for Vertebrate Fossils: Geographic Object Based Image Analysis (GEOBIA) in the Eocene of Wyoming

Bryan Bommersbach

Predictive Modeling in the Search for Vertebrate Fossils: Geographic Object Based Image Analysis (GEOBIA) in the Eocene of Wyoming

by

Bryan Bommersbach

A thesis submitted to the Graduate College
in partial fulfillment of the requirements
for the degree of Master of Arts
Geography
Western Michigan University
June 2014

Thesis Committee:

Charles Emerson, Ph.D., Chair
Robert Anemone, Ph.D.
Kathleen Baker, Ph.D.

Predictive Modeling in the Search for Vertebrate Fossils: Geographic Object Based Image Analysis (GEOBIA) in the Eocene of Wyoming

Bryan L. Bommersbach, M.A.

Western Michigan University, 2014

The development and testing of predictive models for identifying productive fossil localities represents a promising interdisciplinary endeavor among geographic information scientists, paleoanthropologists, and vertebrate paleontologists. This thesis analyzed high resolution (2m spatial resolution) commercial satellite imagery from the Worldview-2 satellite of five areas of the Great Divide Basin using a GEographic Object-Based Image Analysis (GEOBIA) technique, which segments the image into spectrally homogeneous, multi-pixel image objects. In addition to allowing statistical analysis of the spectral characteristics of the image objects, GEOBIA techniques also let analysts incorporate expert knowledge and contextual information to improve classification accuracy. The spectral characteristics of the image objects that represent a highly productive sandstone locality (Tim's Confession, WMU-VP-220) were used to create a classification scheme to pinpoint areas in the Great Divide Basin that were highly likely of being fossiliferous. During the summer field season of 2013, thirty one locations across five satellite images with clusters of predicted fossil localities were surveyed. At thirteen of these locations fossils were recovered, leading to the documentation of twenty five new fossil localities.

ACKNOWLEDGMENTS

I would like to thank my wife, Suzette, for all the love and support she has provided me during my quest for higher education. Without her help I would never have been able to complete this thesis. I would like to thank my family, my parents John and Barb and my sister Nicole, for always having faith that I could actually pull this off. I would also like to thank Jay Emerson for his guidance and support in the development of this thesis. I would also like to thank Bob Anemone for allowing me to join his team of misguided miscreants. Lastly, I would like to thank my fellow graduate students, Rudy Bartels, Anne Santa Maria, and Shannon McEwen for the camaraderie and help on our path.

Bryan Bommersbach

TABLE OF CONTENTS

Table of Contents---Continued

LIST OF TABLES

LIST OF FIGURES

List of Figures- continued

CHAPTER I

INTRODUCTION

The history of life on our planet is studied by paleontologists and paleoanthropologists through the medium of fossil remains. The evolution of animal life in general and vertebrate mammals specifically, is elucidated through the intense study of these remains. Animals evolve and migrate in response to our ever changing planet, and species often fail to adapt and become extinct. There have been many mass extinction events in the history of the earth, such as the dinosaurs, and some believe that we are in the midst of another great extinction event (Kolbert, 2014). An important period in history where mass extinction occurred was during the transition from the Paleocene to the Eocene epochs approximately 55 million years ago (mya). Evidence points to a relatively short period of geologic time (approx. 20,000 years) where the temperature of the planet reached a thermal maximum, during which global temperatures increased by 5 degrees Celsius, followed by a 100,000 year period of a global greenhouse climate (Gingerich, 2006). This has come to be known as the Paleocene-Eocene Thermal Maximum (PETM) and marks the beginning of a change in the forms of life that inhabited our planet. Many species died off and new species, the ancestors of the mammalian fauna that exist today, became dominant. These species include the first Perissodactyls (odd-toed ungulates like horses), Artiodactyls (even-toed ungulates like cattle), hyaenodontid Creodonts (extinct carnivorous mammals), and the first Primates (Johnson, 2005; Gingerich, 1989 & 2006; Rose et al., 2012). These ancient animals are known solely through the fossil remains they left behind, therefore, the recovery and

analysis of these fossils is of utmost importance for the continued expansion of knowledge of evolutionary change.

The primary method of locating fossils in the landscape is through intensive, and time consuming, field surveys. Vertebrate mammal fossils are typically found in sandstone outcrops throughout the Great Divide Basin (GDB). Survey teams spend large amounts of time traversing the landscape in search of these sandstone outcrops. The techniques of field survey have remained constant for the last century (Anemone, Conroy & Emerson, 2011b) and there remains today a certain element of luck in the location of fossil localities. In an effort to reduce the role of chance in the location of fossil sites, geographic information techniques (Geographic Information Systems- GIS) can be utilized to create a predictive model to aid in pinpointing sandstone outcrops (and ultimately the fossils that they may contain) in the Great Divide Basin, Wyoming. This thesis aims to answer the question: Can GIS and predictive modelling using high resolution satellite imagery aid in the location of fossils?

Past research has been performed in the Great Divide Basin by Dr. Robert Anemone and Dr. Charles Emerson exploring the use of GIS techniques in hunting fossils (Anemone, Conroy & Emerson, 2011a; Anemone, et al., 2011b; Emerson & Anemone, 2012). This work used Landsat 7 Enhanced Thematic Mapper (ETM+) imagery and an artificial neural network (ANN). By training the ANN to recognize the spectral signatures of known fossil localities they created a predictive model of potential new localities throughout the GDB. It was found that the medium resolution Landsat imagery was adequate for a general reconnaissance of the 10,000 square kilometer basin, and, to provide a multi-scale approach to work in the GDB, higher resolution imagery of

areas of interest in the Basin should be analyzed with new analytical methods. Using higher resolution imagery allows for more refined results and ultimately a better tool for guiding field survey teams.

A new alternative to pixel based analysis of RS images is Geographic Object Based Image Analysis (GEOBIA) (Hay & Castilla, 2008). This technique was applied to the high resolution Worldview 2 images using eCognition Developer 64™ version 8 software. A multi-scale segmentation/object relationship modeling (MSS/ORM) methodology based on a theoretical framework called Hierarchical Patch Dynamics was adopted (Blaschke, Lang & Möller, 2005). A hierarchical image segmentation was performed, breaking the image into nested image objects at multiple scales. A known highly productive fossil locality called Tim's Confession (WMU-222, Emerson & Anemone, 2012) was used as a training site for creating a classification rule set. This rule set was based on a heuristic process of analysis of the spectral signature of the training site combined with expert knowledge (pers. comm., R.L. Anemone and C.W. Emerson). Once the rule set was established it was used to classify all image objects that meet these criteria. Additional information, such as a digital elevation model (DEM) and a surficial geology map, was incorporated into the final classification.

The resulting images contained various image objects that were classified as potentially fossiliferous localities. The images were exported as vector files and imported into a GIS to create detailed maps of areas in the GDB to be surveyed. This data was loaded onto Topcon Global Positioning System (GPS) receivers using ArcPad software in order to guide field survey. During the summer field season of 2013, thirty-one locations across five satellite images with clusters of predicted fossiliferous image

objects were surveyed. At thirteen of these locations fossils were recovered for a success rate of 42 percent, which resulted in the documentation of twenty-five new fossil localities.

The next section of this thesis will be a background section detailing the geology and typical fossil fauna of the Great Divide Basin. Chapter III will be a literature review of relevant works. Following this will be a detailed description of the methodology adopted for this work. The results from this research will be explained in Chapter V. The last section will contain conclusions and suggestions for future work.

CHAPTER II

BACKGROUND

Geography of the Great Divide Basin

The Great Divide Basin (GDB) is an endorheic, or internally draining, basin that is part of the Greater Green River basin located in southwestern Wyoming. The boundary of the basin is formed by the Continental Divide, which splits at South Pass and rejoins near Rawlins, WY, thereby encircling the GDB. This line separates the hydrological basins on the North American continent between those that flow into the Pacific Ocean and those that flow into the Gulf of Mexico, Atlantic Ocean, Caribbean Sea, and the Arctic Ocean in the north. This dividing line runs from Alaska in the north to Central America in the south and continues to the southern tip of South America. There are several internal drainage basins along this dividing line, of which the Great Divide Basin is the only one in North America.

Located in the southwestern portion of Wyoming, the GDB falls mostly within Sweetwater County, but also extends into Fremont County to the north and Carbon County to the east. The GDB is one of several sub-basins that make up the Greater Green River Basin. Other basins include the Green River, Bridger and Fossil Basins to the west, and the Washakie and Sand Wash Basins to the south (see figures 1 and 2). The GDB is bounded by the Wamsutter Arch in the south, the Rock Springs Uplift to the west, the eastern portion of the Wind River Mountains and the Sweetwater Arch to the north, and the Rawlins Uplift to the east. Interstate 80 follows the Wamsutter Arch along the

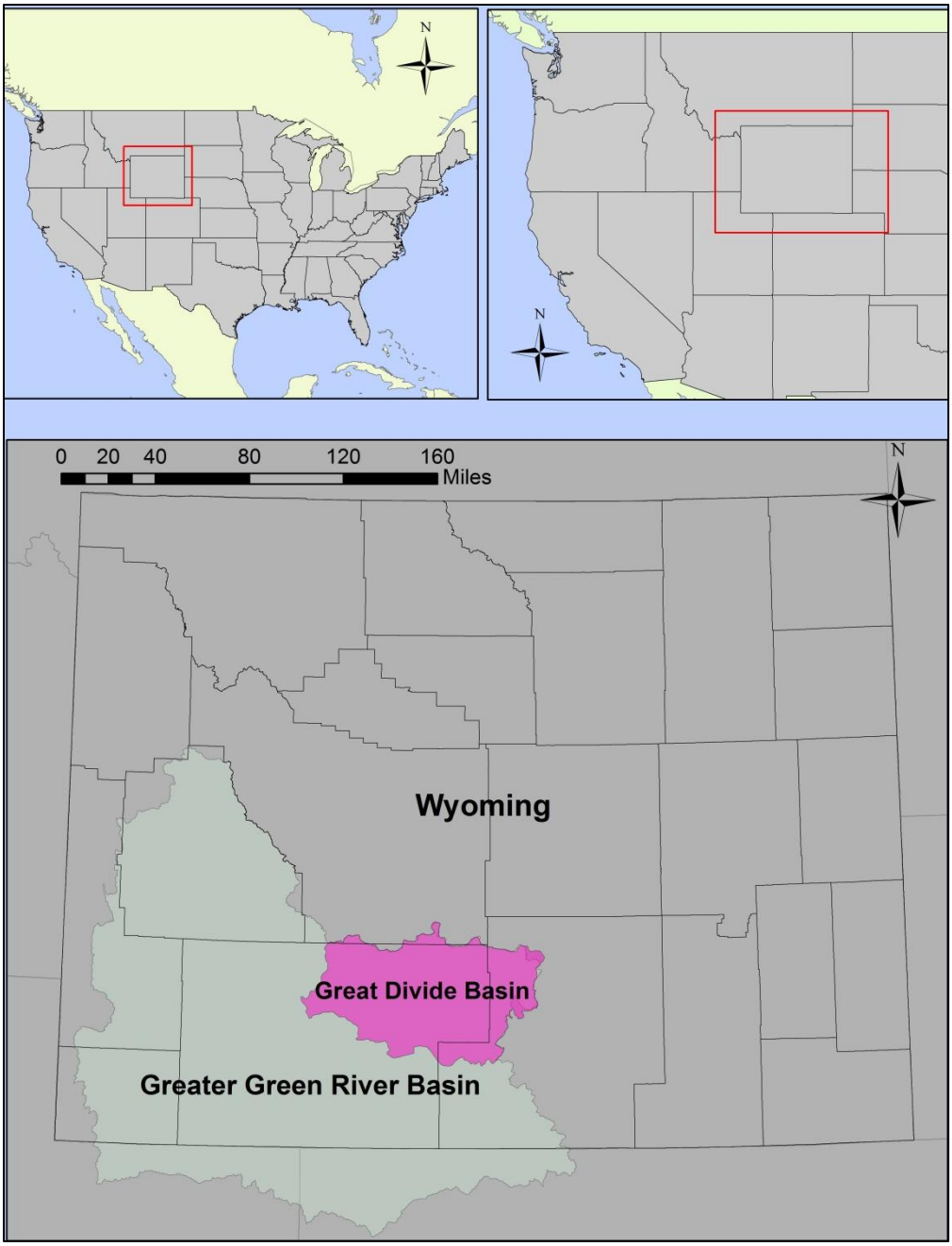

Figure 1. Greater Green River Basin and its sub-basin, the Great Divide Basin. Showing relative position within Wyoming.

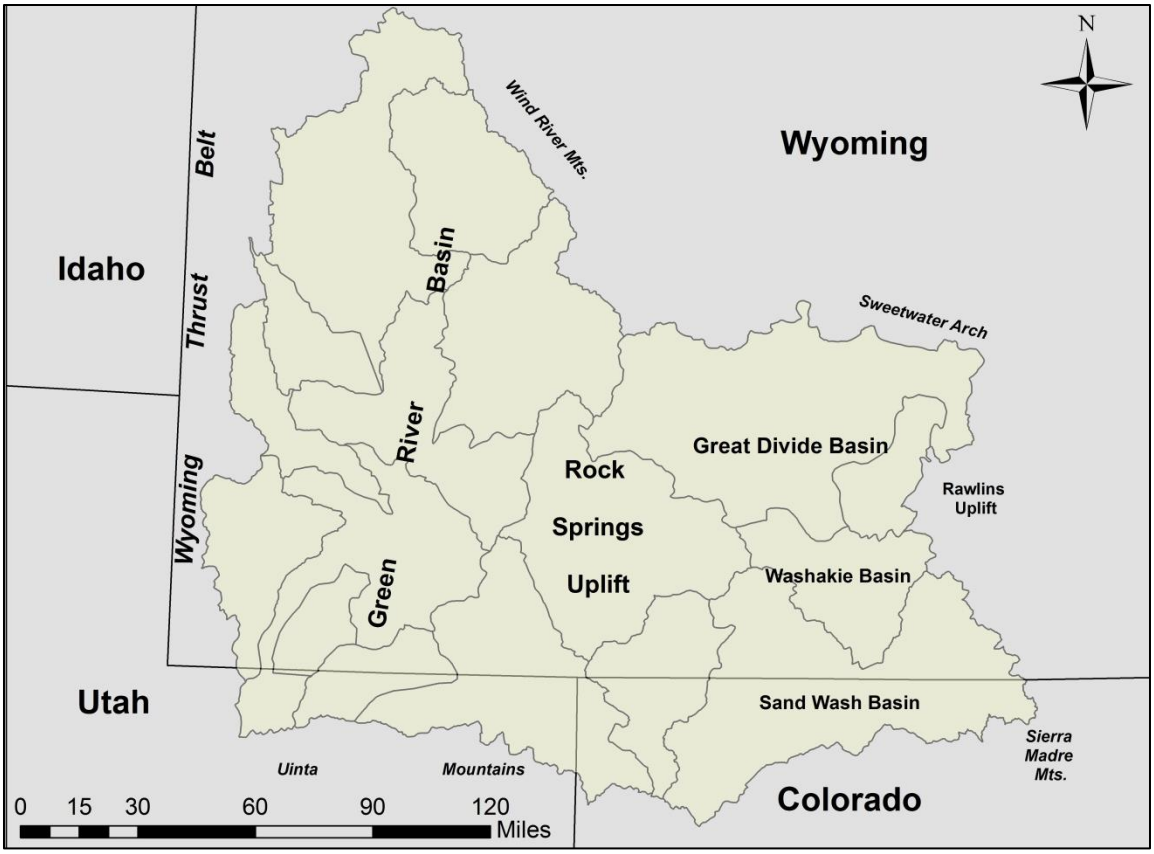

Figure 2. Sub-basins of the Greater Green River Basin.

southern edge of the GDB between the cities of Rawlins in the east and Rock Springs in the west.

The Great Divide Basin is a region of high altitude desert. The average altitude of the low lying areas is around 6500-6700 feet with the higher areas reaching around 7300-7500 feet (Pipiringos, 1962). High temperatures in the GDB average in the mid-80's, however, they can reach the high 90's to 100 degrees Fahrenheit during the warmest months when field work is typically performed. Rainfall is minimal with an average of 8.5 inches and 9 inches per year in Rock Springs and Rawlins respectively (www.noaa.gov). The primary forms of vegetation in the basin are grasses and sagebrush. The

modern fauna of the GDB includes pronghorn antelope, elk, mule deer, feral horses, and other mammals such as coyotes, prairie dogs, badgers, and mice. Avian species include sage grouse, pheasant, and notably, the golden eagle.

Geology of the Great Divide Basin

Brief history. The earliest geological work in the Great Divide Basin was performed by Hayden (1869) and King (1878). Hayden was the first to define the Green River Formation as shale with a fresh water origin and King was the first to name Lake Gosiute, which was the massive lake that covered large portions of this region in the past (Roehler, 1993). Preliminary geologic work was performed by Veatch (1907), Bradley (1925, 1929), and Nace (1939). W.H. Bradley wrote about the depositional environments of the Greater Green River Basin (1925) and even calculated the average rainfall and evaporation for Lake Gosiute (1929).

The first systematic survey of the GDB was performed by Pipiringos in the 1950's and 1960's (1955, 1962). Pipiringos' work focused on the geology of the Great Divide Basin for the purpose of mapping coal beds in search of uranium. His work also began the process of detailed description of mammalian fossils in the Basin, which will be discussed in depth later. Smithsonian Institution paleontologist C.L. Gazin (1962, 1965) built upon the work of Pipiringos and performed additional paleontological work in the region. Geologic work in the GDB was expanded immensely by Roehler in the 1990's (1991, 1992, 1993).

Stratigraphy. This region of Wyoming is drastically different today than it was during the Eocene Epoch of 55- 38 million years ago (mya). The climate was tropical and therefore significantly warmer and wetter than today. Throughout the Eocene the Greater Green River Basin was filled with a massive lake known as Lake Gosiute (King, 1878). The lake expanded and contracted several times throughout the Eocene due to climate change and tectonic activity (Johnson, 2005; Roehler, 1991, 1992), resulting in a complex inter-tonguing geology. At various times throughout the Eocene, Lake Gosiute extended to different parts of the Greater Green River Basin and was often divided into multiple, smaller lakes (Roehler, 1992). There are three primary Eocene formations in the GDB; the Wasatch, the Green River, and the Bridger. The Fort Union Formation of the Paleocene epoch (66 – 55 mya) underlies the formations of the Eocene.

The Wasatch and Green River Formations are sub-divided into tongues and members. The Wasatch formation consists of the main body, the Niland Tongue, and the Cathedral Bluffs tongue. The Green River formation consists of the Luman Tongue, the Tipton Shale Member, the Wilkins Peak Member, and the Laney Member (Roehler, 1992; Pipiringos, 1962). Figure 3 shows a stratigraphic depiction of the various tongues and members of the GDB. The Wasatch Formation and the Luman Tongue, Tipton Shale Member, and Wilkins Peak Member of the Green River Formation are typically dated to the Lower Eocene, while the Laney Member of the Green River Formation is considered Middle Eocene. The Bridger Formation ranges from the Middle Eocene to the Upper Eocene in age (Roehler, 1992). Figure 3 depicts the general stratigraphy of the GDB from the Paleocene Fort Union Formation to the Oligocene White River Formation. This

varies, however, as the eastern portions of the basin grade into the Battle Springs formation (Pipiringos, 1962).

The Fort Union formation is composed of sandstone, siltstone, clay shale, and coal beds with a thickness of around 1,000 feet and is mostly covered by younger sedimentary rocks throughout the basin (Pipiringos, 1962). This formation is the oldest

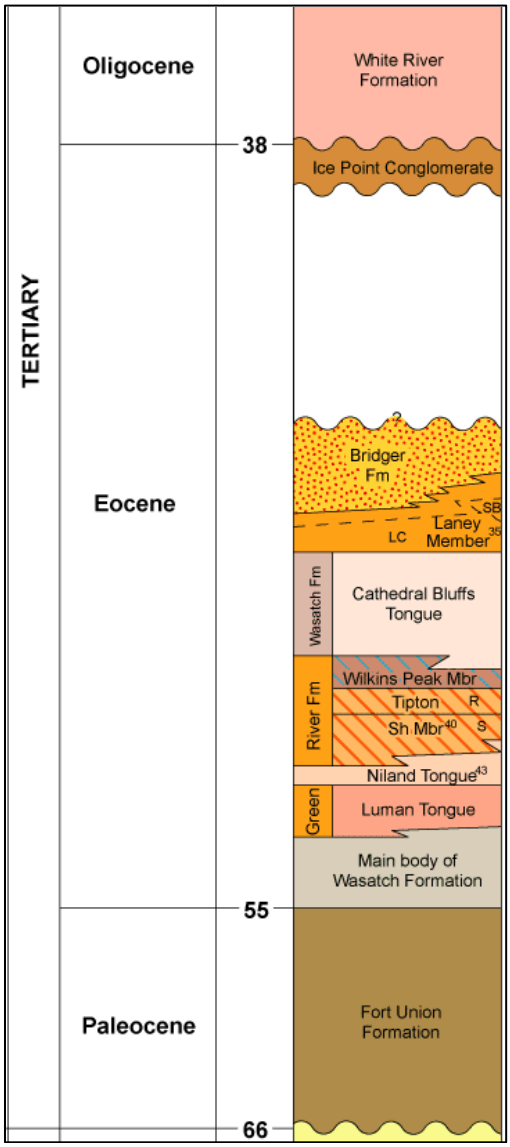

Figure 3. General stratigraphy of the Great Divide Basin. Adapted from Wyoming State Geological Survey; *Great Divide Basin (Entire Geological Time Period)*; Web; 15 Jan. 2014.

in the GDB and therefore the lowest stratigraphically. A sequence of early and middle Eocene beds unconformably overlay the Fort Union formation with a thickness of approximately 3,400 feet (Pipiringos, 1962). These beds are the various members of the Wasatch and Green River Formations and are composed of sandstone, claystone, siltstone, oil shale, clay shale, limestone, conglomerate, and coal beds (Pipiringos, 1962). There are also surface deposits of Quaternary age within the GDB. These include alluvium from dry lakes and streams, delta and fan deposits, gravel deposits, and sand dunes (Pipiringos, 1962).

The main body of the Wasatch formation was described by Pipiringos (1962) as being composed of a "sequence of clay shale, siltstone, low-grade oil shale, biotitic sandstone, and coal beds" (p. 14). This formation underlays the majority of the southern portion of the basin and overlays the Fort Union Formation, with the Luman Tongue of the Green River Formation directly above it. Around 400 feet of the main body is exposed throughout the southern GDB with around 1000 feet of exposure along the eastern portion of the Rock Springs Uplift (Pipiringos, 1962).

The Luman Tongue is described as a series of oil shale, fossiliferous muscovitic calcareous sandstone, varved siltstone (a series of layers of silt deposited by a body of still water over many years), clay shale, and some coal beds (Pipiringos, 1955). This tongue overlays the main body of the Wasatch and underlays the Niland Tongue of the Wasatch. The Luman Tongue is around 180-200 feet thick at Luman Butte and Tipton respectively, but is thicker, around 270-390 feet, to the east at Lost Creek Butte and Frewen (Pipiringos, 1962). The Luman Tongue contains fine-grained sandstone that contains muscovites and the base of the Tongue is described as'wormy' sandstone

containing mollusk impressions and "borings possibly made by worms" (Pipiringos, 1962, p. 24). These mollusk remains are thought to date to the early Eocene.

The Niland Tongue of the Wasatch Formation is the next tongue in the stratigraphic sequence of the GDB. It typically is composed of coal beds, oil shale, siltstone, sandstone, and clay shale (Pipiringos, 1955). This tongue rests on top of the Luman tongue and is below the Tipton tongue. The Niland tongue has been eroded away in the central part of the GDB and is therefore only typically found along the edges of the Basin (Pipiringos, 1962). The Niland tongue is around 400 feet thick in the vicinity of Niland Spring and thins to the west around Luman Butte to 325 feet.

The next tongue is the Tipton Tongue, or Tipton Shale Member, of the Green River Formation. This tongue is found between the Niland tongue and Wilkins Peak member. Pipiringos (1962) described the Tipton Tongue as being composed of an upper and lower division. Roehler (1968) later renamed the lower portion of the Tipton Tongue the Tipton Shale Member and the upper portion the Wilkins Peak Member. The Tipton Shale Member was later divided into two beds; Scheggs Bed and Rife Bed (Roehler, 1991). The Tipton Shale Member consists of oil and clay shales and sandstones. This member is, like the Luman and Niland, primarily found in the southern portions of the GDB as it has been eroded away from the central portions of the GDB (Pipiringos, 1962). Pipiringos (1962) describe the Tipton Tongue as being 280 feet thick in the vicinity of the town of Red Desert, which is presumably the total thickness of the Tipton Shale Member and the Wilkins Peak Member. He went on to describe the lower portion (Tipton Shale Member) as being 160 feet thick at this location and composed of oil shale and dolomitic limestone concretions (1962).

The lower bed of the Tipton Shale Member, Scheggs Bed, has a distinct "five foot bed of coquina consisting of loosely cemented mollusk fragments" (Pipiringos, 1962, p. 29) separating it from the underlying Niland tongue, which is not visible in the northern portions of the GDB, but is apparent in the southern and western areas (ibid). The two beds are separated by Roehler (1991) based on differences of depositional environments. Scheggs Bed is the lower oil shale and is believed to have been deposited in a saltwater environment while the upper oil shale Rife Bed was deposited in a freshwater environment. The Scheggs Bed is described as being composed of tan to brown oil shale and thin, very fine-grained sandstone. The Rife Bed is described as a medium to dark brown dolomitic oil shale (Roehler, 1991). The upper portion of the Rife Bed is defined by a ten foot algal-ball zone separating it from the Wilkins Peak Member which is easily seen throughout the eastern portion of the Niland Basin while the southern edge of the Basin is defined by a bed of arkosic (course grained and rich in feldspar) sandstone (Pipiringos, 1962).

The Wilkins Peak Member is 120 feet thick near the town of Red Desert and composed of sandstone, clay shale, fine-grained calcareous sandstone and algal reefs (Pipiringos, 1962). This member is defined by a thick algal-ball zone of approximately 50 feet separating it from the Cathedral Bluffs Tongue. The Wilkins Peak Member consists of fine-grained sandstone, small amounts of greenish paper shale, and considerable amounts of arkosic sandstone (Pipiringos, 1962).

The next stratigraphic layer is the Cathedral Bluffs Tongue of the Wasatch Formation. This tongue is a very distinct series of red and green claystone that forms extremely steep slopes, called the Cathedral Bluffs, going up to the Laney Rim

(Pipiringos, 1962). In the Cyclone Rim area the Cathedral Bluffs tongue is around 1,100 to 1,300 feet thick and includes a base of 300 feet of arkosic sandstone (Pipiringos, 1962). This tongue is eroded from the central portions of the GDB and is therefore typically found along the margins of the basin. Fossils are considered to be scarce in the Cathedral Bluffs Tongue (Pipiringos, 1962; Morris, 1954; Honey, 1988), however, some fossils found by Nace (1939), Morris (1954), and Gazin (1962) seem to suggest a late early Eocene age for the Cathedral Bluffs Tongue.

The last portion of the Green River Formation is the Laney member that is exposed along the Laney Rim. This member sits atop the Cathedral Bluffs tongue and is composed of green and brown oil shale, oolitic sandstone, marl, and cherty algal deposits (Pipiringos, 1962). The Laney member is sub-divided into three beds: the LaClede Bed, The Sand Butte Bed, and the Hartt Cabin Bed. The LaClede Bed is composed of saltwater lacustrine oil shale deposits and is the lowest bed stratigraphically (Roehler, 1992). The Sand Butte Bed is a lacustrine sandstone deposit that extends from the Green River Basin, across the Rock Springs Uplift, and partially into the GDB (Roehler, 1992). The Sand Butte Bed has very little presence in the GDB. The third bed is the Hartt Cabin Bed that is composed of freshwater lacustrine and flood plain deposits that are gray and green in color (Roehler, 1992). The combined beds of the Laney member are approximately 1,300 feet thick.

The Battle Spring formation is located in the eastern portions of the GDB and is a thick formation of arkosic sandstone. This formation has not been mapped extensively, but has an inferred thickness of around 3,300 feet (Pipiringos, 1962). This formation inter-tongues with all members of the Wasatch and Green River Formations along the

eastern portion of the GDB. This formation is thought to be a continuous depositional environment from the early to middle Eocene and is composed of deltaic and fluvial deposits (Pipiringos, 1962).

The last geologic formation of interest in the GDB is the Bridger Formation. This formation overlays the Laney member of the Green River Formation and is composed primarily of gray-green claystone and shale, as well as some limestone and algal deposits (Pipiringos, 1962). This formation is not typically found within the GDB as it has been eroded away, however, it is found along the edges of the basin. It is between 60 and 250 feet in thickness where found and is correlated with the Bridger formation found in the nearby Green River and Washakie basins (Pipiringos, 1962; Roehler, 1992). The Bridger Formation is thought to be of middle Eocene age. Figure 4 shows the surficial geology of the GDB and figure 5 shows the underlying geology in more detail.

Depositional environments. A description of the depositional environments that lead to the various geologic formations of the GDB is particularly useful. According to Roehler (1993), there are eight different kinds of depositional environments in the Greater Green River Basin. They are fluvial, paludal (swamps and marshes), freshwater lacustrine, saltwater lacustrine, ponds, salt pans, mudflats, and volcanic. Three different kinds of depositional environments resulted from Lake Gosiute. Fluvial deposits were created by streams and rivers that flowed into the lake while paludal deposits are associated with wetlands and marshes that formed around the shores of the lake. Lacustrine deposits were created by deposition at the bottom of the lake. The fluvial and palustrine deposits correspond with the Wasatch, Battle Springs, and Bridger Formations while the lacustrine deposits correspond with the Green River Formation (Roehler, 1992).

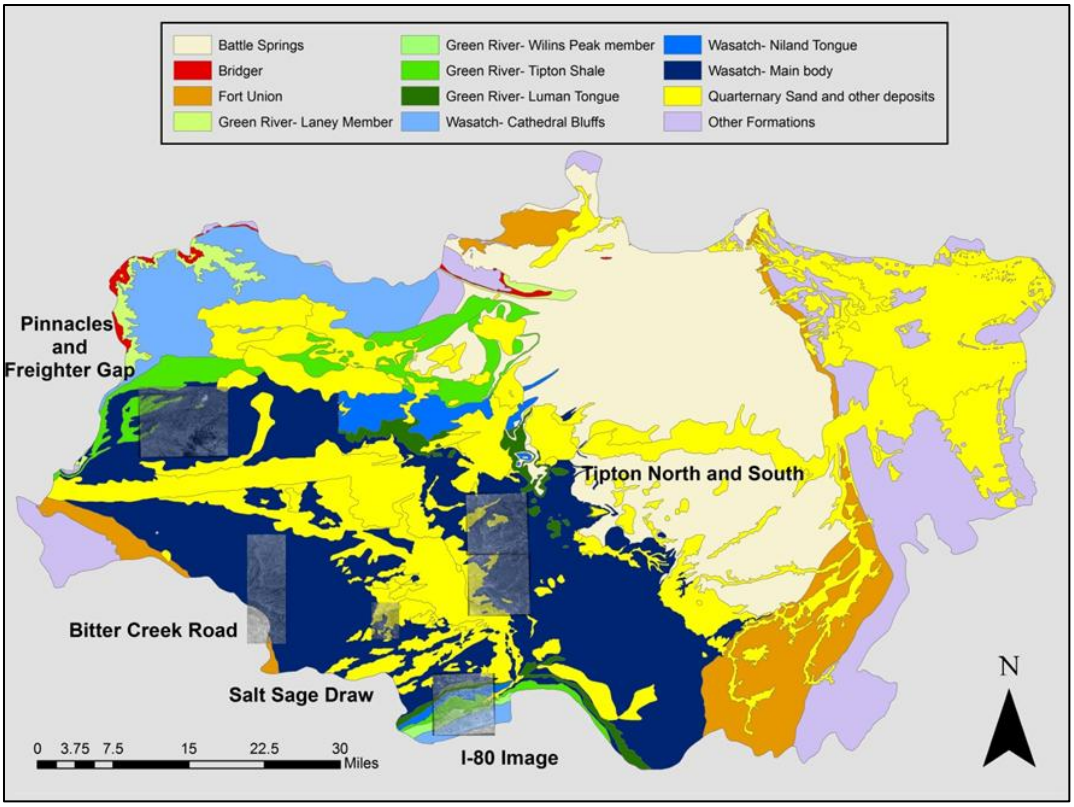

Figure 4. Surficial geology of the Great Divide Basin. The six satellite images used in this study are displayed on the map to illustrate the underlying geology in each image.

The geology of the GDB is quite complex because climatic change and tectonic activity caused the extent of Lake Gosiute to change several times throughout the Eocene epoch.

Of particular interest to this work are the depositional environments, and resulting geologic formations in which mammals of the early Eocene lived. Mammalian species fossils are not typically found within geologic formations that have lacustrine or paludal (having to do with marshes) depositional environments. The Wasatch formation is described as being composed primarily of geologic tongues that have fluvial depositional environments; therefore, mammalian fossils should be sought out in this formation.

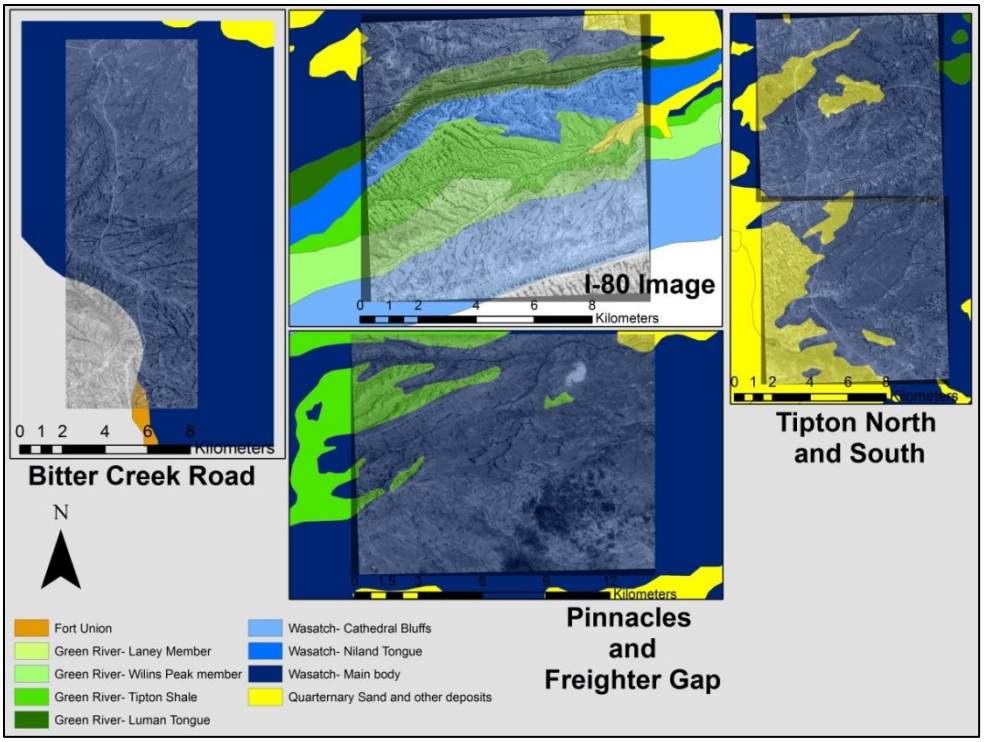

Figure 5. Surface geology of the five study areas. The Salt Sage Draw image was excluded as it was not surveyed.

Fossil Fauna

A description of the typical fossil fauna of the Eocene is of particular use at this point. A significant amount of work has been performed in basins around and within the Greater Green River Basin resulting in a relatively well understood biostratigraphic sequence of mammal fossils. The early Eocene has been labelled as the Wasatchian North American Land Mammal Age (NALMA) and is important because it is the earliest appearance of the Orders Primate, Perissodactyla, Artiodactyla, and hyanodontid creodonts (Johnson, 2005). Table 1 depicts the epochs of the Cenozoic Era and the corresponding divisions of the NALMA's. Of primary interest are the Wasatchian NALMA of the early Eocene and the Clarkforkian NALMA of the late Paleocene.

Table 2 details the typical genus that are found within the Wasatchian NALMA of the GDB, while table 3 describes the typical genus of the Clarkforkian. Other mammalian Orders found within the GDB include Rodentia and Insectivora and a large number of reptilian Orders can be recovered from the GDB. The focus of this research is on the mammalian fossil fauna recovered from the GDB.

Table 1

Epochs of the Cenozoic Era and corresponding North American Land Mammal Ages

Era	Epoch	Age	NALMA
Cenozoic	Pleistocene	1.8 mya	
	Pliocene	5.3 mya	
	Miocene	23.8 mya	
	Oligocene	33.7 mya	
	Eocene	54.8 mya	Chadronian
			Duchesnian
			Uintan
			Bridgerian
			Wasatchian
	Paleocene	65.0 mya	Clarkforkian
			Tiffanian
			Torrejonian
			Puercan

Table 2

Typical Eocene mammal fauna

Wasatchian NALMA		
Order	**Family**	**Genus**
Extant Orders		
Primates	Adapidae	*Cantius*
	Omomyidae	*Tetonius*
Perissodactyla	Equidae	*Hyracotherium*
Artiodacyla	Dichobunidae	*Diacodexis*
Carnivora	Miacidae	*Miacis*
	Viverravidae	*Viverravus*
	Viverravidae	*Didymictis*
No Living Descendants		
Condylarthra	Hyoposodontidae	*Hyopsodus*
	Hyoposodontidae	*Haplomylus*
	Meniscotheriidae	*Meniscotherium*
Pantodonta	Coryphodontidae	*Coryphodon*
Tillodontia	Esthonychidae	*Esthonyx*

Source: Adapted from Emerson & Anemone, 2012.

Table 3

Typical Paleocene mammal fauna

Clarkforkian NALMA		
Order	**Family**	**Genus**
Condylarthra	Hyoposodontidae	*Hyopsodus*
	Hyoposodontidae	*Haplomylus*
	Phenacodontidae	*Ectocion*
		Phanacodus
Pantodonta	Coryphodontidae	*Coryphodon*
Tillodontia	Esthonychidae	*Esthonyx*
Primatomorph	Plesiadapidae	*Plesiadapis*
	Paraomomyidae	*Phenacolemur*
Rodentia	Ischyromyidae	*Paramys*

Source: Adapted from Emerson & Anemone, 2012.

The Wasatchian NALMA is sub-divided into four biostratigraphic levels. These are the Sandcoulean, Graybullian, Lysitean, and Lostcabinian in chronological order from the earliest to the latest. The presence of the perissodactyl Hyracotherium but absence of the perissodactyl Homogalax as well as the presence of primates and artiodactyls are the defining characteristics of the Sandcoulean (Granger, 1914, cited in Johnson, 2005). The Graybullian is defined by the presence of Homogalax as well as Hyracotherium, primates, and artiodactyls (Johnson, 2005). The Sandcoulean and Graybullian are considered to be early Wasatchian. The next biostratigraphic zone is the Lysitean, which corresponds with the middle Wasatchian. It was defined by Sinclair and Granger (1911, cited in Johnson, 2005) on the presence of perissodactyl *Heptodon*. Sinclair and Granger also defined the Lostcabinian (late Wasatchian) based on the presence of the perissodactyl *Lambdotherium.* The earliest level, the Sandcoulean, has been disputed by subsequent workers, with Gingerich (1983) being the most important, however, the other three divisions have been adopted.

The biostratigraphic sequence of the Wasatchian NALMA has been extensively studied throughout this region of the American West. Significant work has been done in the Clark's Fork and Bighorn Basins, located to the north of the GDB, by Gingerich (Bloch & Gingerich, 1998; Gingerich, 1980, 1989, 1991, 2001; Gingerich & Smith, 2006) and K. Rose (Rose, 1981; Rose et al., 2012). These Basins have been heavily prospected and analyzed and have detailed faunal assemblages published. The entire Green River Basin was analyzed by McGrew (1971) and was geologically explored by Roehler (1991, 1992, 1993) and Sullivan (1980). The Washakie Basin to the south was

examined by Morris (1954) and later by Johnson (2010). Early Eocene fossil faunas were explored by Burger & Honey (2008) in northwest Colorado. Comparisons were made between Eocene fauna from Wyoming and New Mexico by Beard (1988) and Beard later detailed the Eocene fauna from Mississippi (Beard, 2008; Beard & Dawson, 2009). There are plenty of faunal assemblages from regions around the GDB to compare it to, and plenty of Wasatchian faunal assemblages exist with which to compare those found within the GDB.

The Wasatchian NALMA is the period in time when several important mammalian orders first appear. They are the Perissodactyla, Artiodactyla, Euprimates, and hyaenodontid Creodonts. The perissodactyls were used to define the biostratigraphic divisions of the Wasatchian NALMA, therefore, *Hyracotherium, Homogalax, Heptodon,* and *Lambdotherium* are index fossils for the early Eocene. Other taxa that are typical of the Wasatchian are the Artiodactyl *Diacodexis*, the Carnivora *Viverravidae*, and omomyid *Teilhardana* and Adapiform *Cantius* euprimates. Other typical taxa are the pantodont *Coryphodon* and the condylarth *Haplomylus*, however, these taxa had their origins in the Clarkforkian period of the late Paleocene and continued into the Wasatchian. The condylarths *Hyopsodus* and *Meniscotherium* are also typical of the Wasatchian NALMA as well as the primate *Notharctus* and the tillodont *Esthonyx* (McGrew, 1971; Anemone & Dirks, 2009).

Early paleontological work in the GDB was performed by Smith and Veatch (Veatch, 1907) and later by Pipiringos (1955, 1962) and several fossil localities were identified. The assemblages from these localities were later described in publications by Gazin (1952, 1962, 1965). The first locality was named the Great Divide and included

the genus *Esthonyx, Notharctus, Coryphodon,* and *Heptodon,* which suggest a Lostcabinian age for this locality (Johnson, 2005). The Red Desert assemblage was described by Gazin (1962) and included genus such as *Omomys, Esthonyx, Haplomylus, Meniscotherium,* and *Hyracotherium,* which suggests an early Wasatchian time frame (Johnson, 2005). The Tipton Buttes fossil assemblage was first discussed by Gazin (1962) and was dated to the Lysitean biozone based on the presence of genus *Microsyops, Hyopsodus, Meniscotherium,* and *Hyracotherium.* An updated faunal assemblage based on a series of fossil localities around Tipton Buttes was detailed by Johnson (2005) that reflected more recent work in the Great Divide Basin by R.L. Anemone (Anemone & Dirks, 2009; Emerson & Anemone, 2012). Johnson detailed a similar fossil assemblage as Gazin's earlier publications, including typical Wasatchian NALMA genus like *Cantius, Viverravus, Coryphodon, Diacodexis, Hyracotherium, Hyopsodus, Homogalax, Paramys, Haplomylus,* and *Meniscotherium* (Johnson, 2005).

Some areas of the GDB have late Paleocene geology called the Fort Union Formation. This is the geologic formation directly underlying the earliest Wasatch Formation, as discussed previously. This geologic formation corresponds with the late Paleocene biostratigraphic zone called the Clarkforkian. A brief discussion of the Clarkforkian NALMA is necessary as some surveying is performed in these portions of the GDB. The Clarkforkian NALMA was detailed by Rose (1981) in which he described the assemblage from the Clark's Fork Basin. The Clarkforkian begins with the first appearances of the rodent *Paramys,* the pantodont *Coryphodon,* the condylarth *Haplomylus,* and the tillodont *Esthonyx* and ends with the appearance of the perissodactyl *Hyracotherium,* the artiodactyl *Diacodexis,* the primate *Cantius,* and the omomyid

Teilhardana in the earliest portion of the Wasatchian NALMA (Anemone & Dirks, 2009).

The Clarkforkian is further divided into three biostratigraphic zones. The first two are defined by two species of *Plesiadapis*, with *P. gingerichi* defining the oldest zone and *P. cookei* defining the next, while the third zone is defined by the abundance of the condylarth genera *Phenacodus* and *Ectocion* (Rose, 1981). The Clarkforkian is important because many of the genus that continued into the Wasatchian first appeared during this period of time. It is also important because plesiadapiformes are possibly the earliest ancestors of the primate order.

Fossils in the Great Divide Basin

A brief discussion of the actual fossils recovered from the GDB will aid in understanding the difficulties of fossil recovery in this portion of the American west. The fauna of the early Eocene were not large mammals. It has also been suggested that this might be due to a certain amount of dwarfing that occurred during the transition from the Paleocene to Eocene epochs (Gingerich, 2001). Since the animals themselves were relatively small, the resulting fossils that they left behind are small as well. The remains also degrade over time as they undergo the fossilization process. The result of these two factors is that the fossils found in the GDB are quite small. The fossils found within the GDB are typically the denser portions of the bones, such as teeth, mandibles, and the distal ends of long bones. Figure 6 shows an example of a fossil recovered from the GDB and exhibit the size of the fossils recovered.

The fossils are actively eroding out of the various geologic formations of the GDB. The mammalian fossils are typically preserved in the fluvial sandstones of the Wasatch Formation. As the fossils erode out of the sandstones due to the action of wind and water, they become deposited in the loose sands found at the base of the sandstone outcrops. The simplest method of searching for mammalian fossils is to locate the sandstone outcrops in the landscape and then search the bases of those outcrops. Some fossils are also found still encased within the sandstone matrix and can be carefully removed from the surrounding rock using dental picks. Dry and wet screening can also be incorporated in the search for small fossils.

Figure 6. Fossil recovered from the GDB, photo by author.

Another technique for locating fossils in the landscape is to intensely survey anthills. The size of small mammalian fossils, such as teeth, are approximately the same

as the size of the material used by ants in the construction of their homes. This results in ants collecting small teeth and incorporating them into their anthills and concentrating large numbers of fossils in one location. By scrutinizing these locations, large numbers of small fossils can be recovered in a relatively quick manner. This technique is frequently utilized in the GDB, especially at the Virgin Hills locality that was composed of several anthills that yielded 1460 fossils during the 1995 field season (Johnson, 2005).

Using these methods, large numbers of fossils can be recovered from localities within the GDB. However, many of these fossils are unidentifiable fragments, therefore; only fossils that can be used to identify the genus and possibly the species are collected. This is why it is so important to locate fossil remains of teeth, mandibles, and long bones, as these are the easiest to identify.

CHAPTER III

LITERATURE REVIEW

A complete understanding of previous work concerning GIS, GEOBIA and predictive modeling is required in order to know where new research is fruitful. An exhaustive literature review of these topics follows. The following sections will include: a section reviewing the literature concerning GEOBIA, a discussion of the literature concerning applications of GIS and RS to a variety of fields, and finally a review of the literature of past GIS and remote sensing applications applied to the search for fossils in the GDB.

Geographic Object Based Image Analysis (GEOBIA)

History. GEOBIA is a term coined by Hay and Castilla (2008) to differentiate the geospatial sub-discipline of object based image analysis from other applications. The basic concepts and potential of GEOBIA was recognized in the 1980's, however, the technology to apply object based analyses was not available until the 1990's (Aplin & Smith, 2011). This new method of RS imagery analysis was constrained due to the limitations in technology, specifically in computational power and lack of high resolution satellite imagery (Blaschke, 2003). Advances in computer power, data storage, and databases in the late 1990's through the early 2000's resolved the issues of being able to process imagery (Blaschke, 2010).

The spatial resolution of satellite imagery is the physical size on the ground that each pixel in the image represents. An example of low resolution images would be those collected by the Moderate Resolution Imaging Spectroradiometer (MODIS) aboard the Terra and Aqua satellites which has 250 meter, 500 meter, and 1000 meter spatial resolutions or the Advanced Very High Resolution Radiometer (AVHRR) which has approximately one kilometer spatial resolution. Medium resolution imagery is typified by the Landsat spatial resolution of 30m. Newer satellites have a higher resolutions, i.e. each pixel is a smaller area of the ground. In the past, medium spatial resolution imagery collected by satellites like Landsat and SPOT and higher resolution aerial photography were the only means of remotely analyzing landscapes (Lang, 2008). With the launching of new satellites, like IKONOS (launched in 1999), QuickBird (2001), and OrbView (2003), high resolution imagery became far more accessible for research (Aplin & Smith, 2011; Blaschke, 2010). With the launch of Worldviews 1 and 2 in 2007 and 2009, respectively, commercial satellites were now capable of capturing images with a resolution of less than a half meter (Blaschke, 2010). With this confluence of technological advances in computing and increases in availability of very high resolution satellite imagery, a shift from pixel based to object based analysis began to occur.

Theoretical framework. The theoretical framework that has been adapted to GEOBIA is a combination of two theories in ecology; patch dynamics and hierarchy theory. Ecological theory in the past assumed that there is a balance in nature, or an inherent equilibrium. This is questioned today and alternative theories have been developed to explain issues in ecology such as non-equilibrium, heterogeneity of landscape, and hierarchical linkages (Wu & Loucks, 1995). Patch dynamics explains

issues of homogeneity and heterogeneity of landscape by discussing how landscapes are composed of patches, which are spatial units that are different from its surroundings in either nature or appearance (Wu & Loucks, 1995). A patch can be composed of anything in a landscape, depending on the context and scale of what is being examined. Ecological patches are often shifting in form, transitioning from potential, active, and degraded, and combine together in a shifting mosaic to create a landscape (Pickett & White, 1985). Patches can be composed of a variety of aspects of the landscape, including both biological and physical patches (Wu & Louck, 1995). Patches are also known as holons in hierarchy theory (Burnett & Blaschke, 2003) and are called geons by Lang (2008). Hierarchy theory attempts to explain the connections in ecological systems across different scales and how ecological behavior changes depending on the scale being examined and the concepts of equilibrium. These two theories have been synthesized into Hierarchical Patch Dynamics (HPD) and adopted to GEOBIA (Burnett & Blaschke, 2003).

An important part of HPD is the concept of scale. Scale is defined by Allen & Starr (1985) as a "period of time and space over which signals are integrated or smoothed to give a message" (cited in Burnett & Blaschke, 2003, p. 235), and is measured in either absolute units or units relative to what is being examined. This is known as the 'focal scale' (Burnett & Blaschke, 2003). Scale is broken down into two aspects, grain and extent. Grain is the smallest sampling unit in space that is used to gather observations while extent is the total area in which observations at a particular grain are collected (Blaschke, et al., 2005). Grain can be thought of as the data collected in each grid cell of a RS image and extent would be the ground footprint of the image.

The focal scale of analysis is the scale at which the phenomenon a researcher is interested in is best examined. There is not one correct scale for any given phenomenon, therefore, it is critical to choose the scale of analysis as carefully as possible. Patches are hierarchically linked to levels above and below the focal scale, with higher levels imposing top-down constraints and lower levels providing 'initiating conditions and mechanistic explanations' to higher levels (Blaschke, et al., 2005). Figure 7 is an example of focal scale and how patches change over scale. In this example trees are used and it can be seen that the patchiness of the image changes depending on the scale that the imagery is examined. At level -1, individual trees can be seen while the focal scale (Level 0) consists of stands of trees. Level +1 shows entire forests. Figure 8 shows how the segmentation process results in a hierarchical relationship of image objects in a GEOBIA methodology.

Combining these two theories into HPD results in four core concepts which inform the methods of GEOBIA. These concepts are succinctly described by Burnett & Blaschke (2003, p. 239) in the following list:

1. Ecological systems can be perceived as spatially nested patch hierarchies, in which larger patches are made up of smaller, functioning patches.

2. The dynamics of a given ecological system can be derived from the dynamics of interacting patches at adjacent hierarchical levels. Patches at higher levels impose top-down constraints to those lower levels by having slower or less frequent processes, while lower levels provide initiating conditions and mechanistic explanations for, and give apparent identity to, higher levels through interactions among patches. Distinctive characteristic time scales of patches at lower versus higher levels are the fundamental reason for the near-decomposability of ecological systems.

3. Pattern and process have components that are reciprocally related, both pattern and process, as well as their relationship, change with scale.

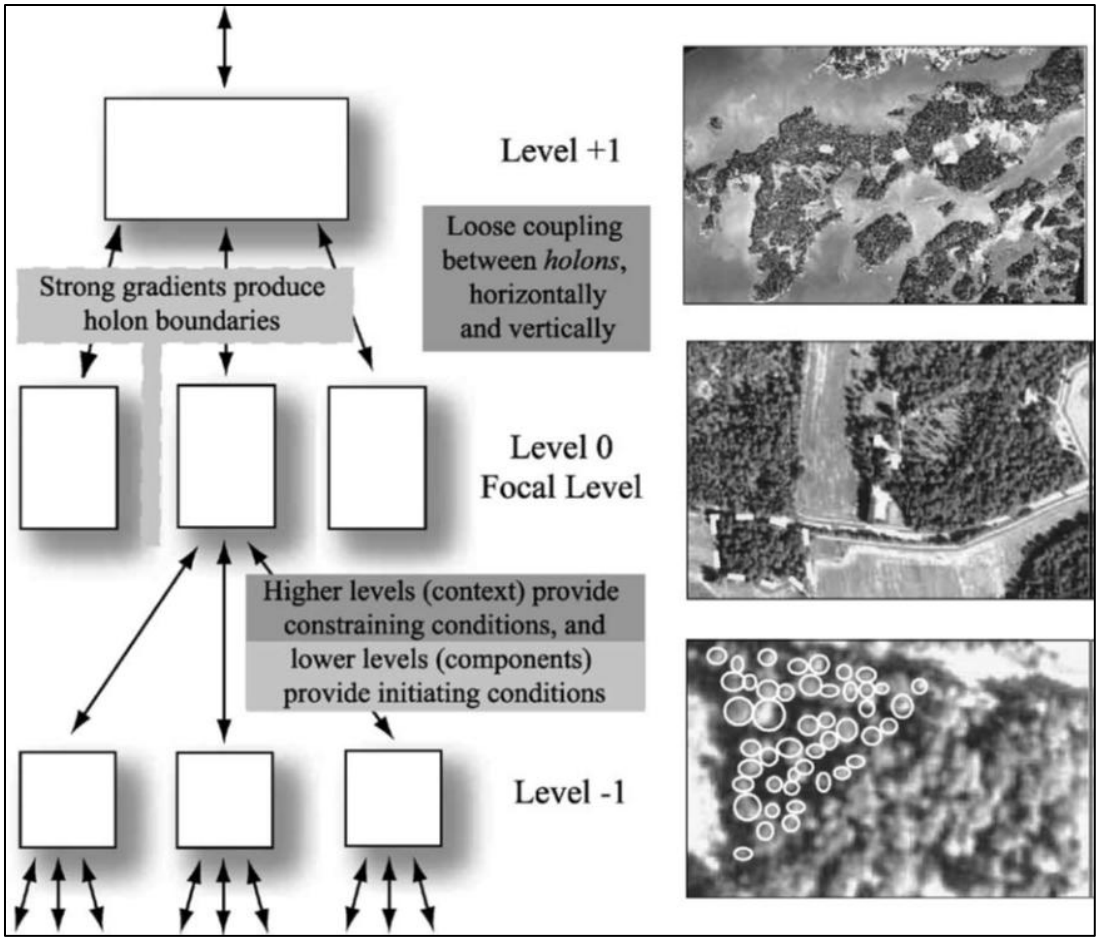

Figure 7. Focal scale and hierarchical interactions of patches depending on scale, from Burnett & Blaschke, 2003.

4. Non-equilibrium and stochastic processes are common in ecological systems. In general, small scale processes tend to be more stochastic and less predictable.However, non-equilibrium and stochastic processes do not necessarily work against stability. They usually constitute mechanisms that underlie the apparent stability of systems.

These concepts sum up the previously discussed concepts of patchiness, hierarchical links between scales, interaction of higher and lower levels with focal scales, and how processes change when the scale changes. The last concept listed here concerns equilibrium in systems. It simply states that at lower level scales there is frequently states of non-equilibrium, however, this does not mean that the entire system will be unstable.

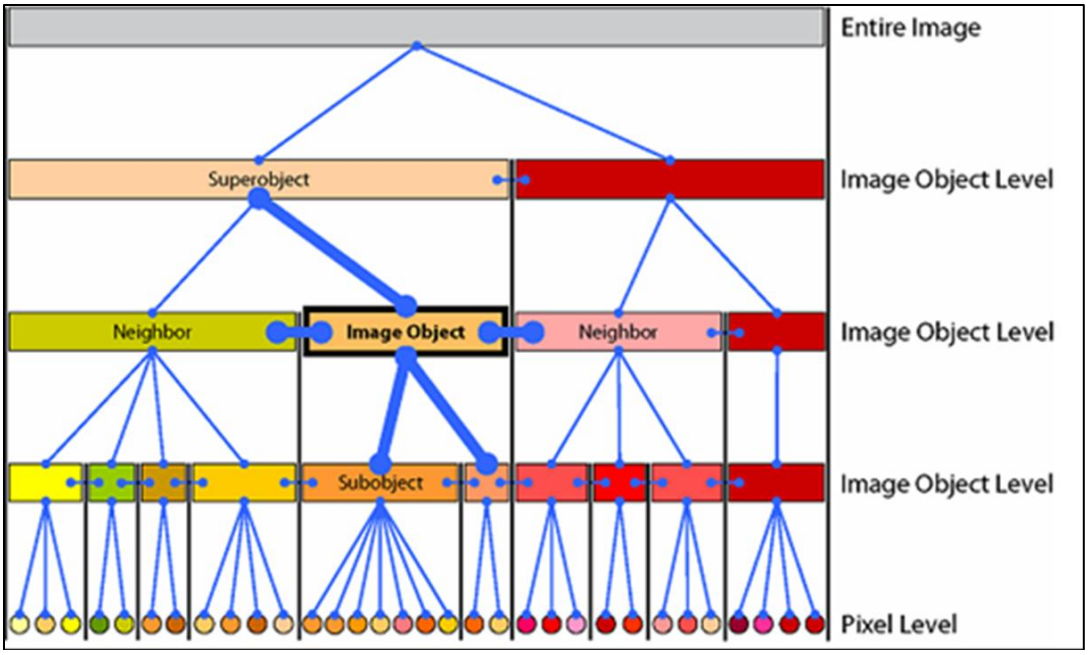

Figure 8. Hierarchy of pixels and image objects achieved through segmentation, from Definiens User Guide, 2006.

Contrarily, the lower level non-equilibrium may actually work to create metastability in the system (Wu & Loucks, 1995). These are the core principles of HPD that have been adopted by GEOBIA and form the theoretical background of the methodology in analyzing imagery in this fashion.

Problems with pixels. The primary difference between GEOBIA methods and pixel based methods is that the scale of analysis is different. In pixel based methods, analysis is performed on individual cells, or pixels, which form an arbitrary and abstract grid over the image and have no direct correlation with real world objects (Burnett & Blaschke, 2003). In a geographic object based image analysis, an image segmentation process groups pixels into homogenous 'image objects' that correspond with real world objects (Aplin & Smith, 2011; Blaschke & Strobl, 2001), thereby allowing for inclusion of contextual relationships in the analysis of the image objects (Blaschke, 2003,2005;

Mahmoudi, Samadzadegan & Reinartz, 2012). Another flaw with pixel based methods is that "a substantial proportion of the signal apparently coming from the land area represented by a pixel comes from the surrounding pixels." (Blaschke & Strobl, 2001, p.13). Object oriented techniques partially overcome this flaw in pixel based methods by grouping the pixels into homogenous areas and then generating statistical averages of information for the image object. The digital numbers for each band of the pixels are combined together and then averaged, thereby overcoming the influence of surrounding pixels on any one pixel.

Scale is an important concept in GEOBIA. The scale of imagery is very important to the accuracy of the analysis, which is why the object based method has only come to fruition with the advent of higher resolution satellite imagery. The resolution of the satellite imagery needs to be high enough that the objects of analysis, the real world objects that are being analyzed at the 'focal scale' (Blaschke, 2010), are larger than the pixels. This mitigates the mixed-pixel problem of lower resolution imagery (Blascke, 2003, 2005). Mixed pixels are when a single pixel, such as a 30 meter by 30 meter Landsat pixel, encompasses more than one type of land cover. The finer resolution imagery also reduces mis-classification due to shadowing effects because the smaller pixel size allows for better differentiation of shadows from other elements of the landscape (Zhu, Guo, Li & Harmon, 2011).

Higher resolutions also allow for grouping of pixels into image objects that represent objects on the ground (Blaschke, et al., 2005). If the resolution of the pixels is larger than actual objects on the ground, then those objects will not be visible when pixels are segmented into image objects. Therefore, pixel size is of utmost importance when

analyzing imagery using the GEOBIA technique. Image resolution must be finer than the objects on the ground that are being classified.

The pixel based method is thought of as 'uni-scale' while the object based method is multi-scale (Burnett & Blaschke, 2003). Uni-scale refers to the fact that pixel based analysis is constrained to only the scale of the spatial resolution of the imagery. What Burnett and Blascke (2003) mean by multi-scale is the fact that in object-based methods images can be segmented into image objects on a variety of scales. This allows for analysis of the landscape at different scales, whichever is most appropriate for the task at hand.

Segmentation and classification. The primary difference between a GEOBIA based technique and a per-pixel based technique is the process of multi-resolution segmentation. Instead of relying on analysis of single pixels, the image is deconstructed into image objects, which are groups of pixels that are spectrally similar. This has been deemed the "building block of object based image analysis" (Blaschke, 2010, p.3).

The advantages of using image objects as opposed to pixels are reductions in computational loads and therefore faster processing times (Johansen, Tiede, Blaschke, Arroyo & Phinn, 2011), application of more complex analyses, reduced impact of the Modifiable Areal Unit Problem (MAUP, a problem of spatial analysis of aggregated data where the results differ when the same analysis is applied to the same data but with different aggregation techniques) (Hay & Castilla, 2008), and reduction in mis-registration and shadowing effects (Johansen, Arroyo, Phinn & Witte, 2010). Also, 'salt and pepper' effects that often occur in pixel-based methods are not a problem (Zhu, et al., 2011). The most important advantage to this research is the fact that the image objects

created can directly correspond to a real world object (Lang, 2008), such as a known highly productive fossil site like Tim's Confession.

The first step in the creation of an object based analysis is the fractal net evolution approach to segmentation in the eCognition software (Baatz & Schäpe, 2000). This is done by selecting random seed pixels in the image and growing a region (image object) based on the increase in heterogeneity when pixels are merged together (Benz, Hofmann, Willhauck, Lingenfelder & Heynen, 2004). The primary features of the image that are used to determine heterogeneity are color and shape (Benz, et al., 2004). Color is derived directly from the digital numbers for each electromagnetic band of each pixel, while shape is determined by a combination of 'smoothness' and 'compactness' heterogeneity (Benz, et al., 2004). Smoothness heterogeneity is a ratio of the border length of the image object and the border length of the bounding box of that image object, while compactness heterogeneity is the ratio of the border length of the image object and the square root of the number of pixels in the object (Benz, et al., 2004). In practical terms, the shape parameter affects the segmentation by weighting the importance of shape over color and compactness determines how compact resulting image objects will be (Definiens Professional User Guide, 2006).

A user defined 'scale' parameter in eCognition sets the threshold at which region growing ends and limits the image objects to a particular level of heterogeneity, and subsequently determines the general size of all image objects (eCognition Developer User Guide v8.8.2, 2013). These three parameters, scale, shape, and compactness, are the user defined parameters that dictate the shape and size of image objects from segmentation. When another scale of segmentation is performed in this hierarchical

method, existing image objects are further segemented with a new, smaller scale value, therefore changing the threshold for heterogeneity (Baatz & Schäpe, 2000; Benz, et al, 2004). The precise equations for the image segmentation process are described in multiple articles (primarily Baatz & Schäpe, 2000 and Benz, et al, 2004; but also Blaschke, 2003 and Burnett & Blaschke, 2003).

Another of the advantages of GEOBIA analysis is the ability to incorporate expert knowledge in both the segmentation and classification processes (Platt & Rapoza, 2008). An understanding of the scale of the phenomenon in the landscape that you wish to extract will guide the heuristic segmentation process (Blaschke, 2005) and understanding of the problem domain will aid in classification. As discussed earlier, HPD explains how processes change when scale changes. The focal level of the phenomenon needs to be set, which can only be determined if the phenomena itself is understood. Appropriate scales of segmentation will be heuristically determined based on the focal scale that is required for the analysis of any particular phenomena.

Since image objects are groups of homogenous pixels as opposed to single pixels, certain statistical parameters can be generated for the object and used in the classification process. Statistics like mean, median, variance, and standard deviation, can be used (Blaschke, 2010). Also, contextual relationships can be incorporated. Relationships between individual image objects on the same and different hierarchical levels can be computed and used to drive the classification process. For example, image objects that have a certain length of shared border with a particular class of image object can be classified.

Aspects of texture can also be incorporated into the classification process. Texture is the coarseness or smoothness of the image objects. A study by Kim, Warner, Madden & Atkinson (2011) incorporated the grey-level co-occurrence matrix (GLCM, after Haralick, Shanmugam, & Dinstein, 1973) in the classification process of wetlands in Georgia, U.S. The results of their study were that the model that incorporated texture had the highest accuracy; eighty-six percent with a Kappa of 0.78 (Kim et al., 2011). Another study used object based analysis and GLCM in California to aid in land classification for population estimation. This study found that the incorporation of texture in the analysis was only marginal with an overall accuracy of fifty-eight percent and a Kappa of 0.45 (Liu, 2004).

These advantages of GEOBIA, incorporation of expert knowledge, statistics, and texture, lead to more complex methods of classification as compared to per-pixel based methods. Statistics and contextual relationships can be used with a variety of classification algorithms to assign each image object to a class (Platt & Rapoza, 2008). There are several classification techniques incorporated into the eCognition software, such as the supervised nearest neighbor technique and a simple Boolean class assignment tool. In the nearest neighbor technique, the spectral characteristics of a group of training pixels are selected to represent whatever classes the user wishes to create. Image objects are then assigned to particular classes based on the training locations and the image objects that are closest to it. The Boolean tool assigns image objects to classes based on a particular parameter of one of the statistical values of the image objects, such as mean brightness being greater than or equal to a particular threshold value. The Boolean class

assignment tool allows for parameters such as contextual relationships and texture to be incorporated into the classification.

Classification schemes such as nearest neighbor and the Boolean tool are considered crisp classifications, where an image object is either a member of a class or not. These binary techniques do not incorporate any concepts of uncertainty in the classification scheme. Image objects often are potentially members of multiple classes, and fuzzy classification techniques take into account uncertainty by calculating probabilities for membership to multiple classes. The image object is assigned to the class with the highest probability, however, the probability score shows how likely that image object belongs to that class. Probabilities for other class membership can also be examined when using a fuzzy logic technique. Fuzzy classification takes into account: uncertainty in sensor measurement, parameter variations due to limited sensor calibration, vague class descriptions, and aspects of mixed pixels (Benz, et al., 2004). Fuzzy classification methods are also available in the eCognition software.

Applications of GIS and Remote Sensing

The application of Geographic Information Systems, RS techniques, and the newer methodology of GEOBIA have been widespread throughout a multitude of disciplines. Research that has any inherent spatial aspect can take advantage of the complex analytical tools that are now available. Disciplines that have adopted these tools are as varied as environmental analysis, archaeology, geology, and now paleontology and paleoanthropology.

Environmental analysis. GIS and remote sensing have been found to have many uses in the analysis of the biosphere of our planet. Recent advances in technology have allowed these things to become more prevalent in research. Advances in computing power and data storage capabilities have made it possible to map and analyze data in more complex ways. Ecologists and biologists have been able to develop more sophisticated methods of mapping and predicting habitats of plant and animal species. Element distribution models, also known as habitat suitability models, have been developed that incorporate vast amounts of environmental data and presence/absence data in a GIS environment to predict species habitats (Beauvais, Keinath, Hernandez, Master & Thurston, 2006; Engler, Guisan & Rechsteiner, 2004; Franklin, 1995).

Often in the construction of these habitat models remotely sensed data is used as ancillary information. As satellite technology has become more sophisticated, studies of the environment have begun to use RS data in a more primary fashion. A variety of methods have been developed to classify RS data for various purposes. Chubey, Franklin, and Wulder (2006) used high resolution Ikonos 2 imagery to develop forest inventories in Alberta, Canada. They compared a per-pixel based classification technique to a GEOBIA method for the purpose of differentiating tree species. They found "that image objects delineated through segmentation are carriers of important forest-related information in the form of image object metrics derived from the inherent spectral and spatial characteristics of forest stand components" (p. 393). The GEOBIA technique allowed them to generate 87 statistical metrics for their image objects which they then analyzed using a decision tree method. They found that they could differentiate tree

species, specifically pine from other species, using only four metrics with an overall accuracy of 0.86 (Chubey, Franklin, & Wulder, 2006).

Another application of RS techniques was done by Chen & Hay (2011) where they used light detection and ranging (Lidar) data combined with high resolution Quickbird satellite imagery to determine above ground biomass and timber value in a forest inventory. They analyzed this data with a GEOBIA technique to estimate canopy heights and to determine the optimal Lidar transect coverage required to perform their estimations. They used a size constrained region merging segmentation method combined with regression modeling and found that the optimal transect coverage was only 17.6% (Chen & Hay, 2011). These are just two examples of the applications of RS and GEOBIA techniques to forest inventory management.

There are plenty of other examples of ecological and agricultural uses for RS classification. Johansen et al. (2011) used Lidar data and a GEOBIA technique to classify streambed and riparian areas in a complicated landscape in Australia. They generated a Digital Terrain model from the Lidar data and combined this with slope data and a polyline of the stream center and then performed a multi-threshold segmentation. It was found that the inclusion of contextual relationships reduced errors in classification and minimized shadowing effects, resulting in an accuracy of over ninety percent with the GEOBIA method as compared to the approximately fifty percent accuracy in the pixel based method (Johansen, et al., 2010; Johansen, et al., 2011).

A combination of aerial photos and Quickbird imagery were used to analyze the change in distribution of shrubs and grasslands in the arid environment of the Chihuahuan Desert, New Mexico. Due to the high resolution of the QuickBird images

and the image object analysis, small shrubs were able to be accurately classified in a hierarchical, multi-scale method. The statistically significant variables for the larger scale image objects tended to be spectral and the lower levels of the hierarchy's variables tended to be contextual and textural (Laliberte, Fredrickson, & Rango, 2007; Laliberte, et al., 2004).

Lucas, Rowlands, Brown, Keyworth & Bunting (2007) used both pixel-based and object-based techniques in developing a rule based classification of a complex landscape. They found that the object-based technique was more accurate in classifying the complex portions of their research area and the pixel-based method was adequate in classifying the homogenous areas (Lucas, et al., 2007). A classification of wetlands in Alberta, Canada incorporated GEOBIA, decision tree classifiers, and textural measures in a multi-scale analysis (Powers, Hay & Chen, 2012). The results of their work suggest that the incorporation of textural measures significantly increase the accuracy of their classification when compared to pixel-based methods.

Remote Sensing techniques are also found to be important in management of agricultural land. Analysis of agricultural land in Bulgaria was achieved through the application of a combination of unsupervised classification with a neural network called Self Organizing Maps (SOM) and object based image analysis to RapidEye imagery (Taşdemir, Milenov & Tapsall, 2012). This technique resulted in over ninety percent accuracy in identifying good agricultural land, which was similar in accuracy to using just the GEOBIA technique. However, the SOM and GEOBIA combination, due to the automated nature of the SOM, decreased the amount of computational time and user interaction involved in the classification (Taşdemir et al., 2012). Another agricultural

example is the use of Landsat Thematic Mapper (TM) and Enhanced Thematic Mapper (ETM+) images to analyze sugar cane crops in Brazil by Vieira et al. (2012). They used a GEOBIA methodology with data mining techniques and a time sequence of images to classify the varying stages in sugar cane crop development. They achieved an overall accuracy of 93.99 % with a Kappa of 0.87 with this technique and found that texture attributes, such as GLCM homogeneity, were of considerable importance to correct classification (Vieira et al., 2012).

Archaeology. Archaeologists have readily adopted GIS and RS techniques, primarily for the creation of predictive models of potential archaeological sites. This application of GIS began primarily in the 1980's (Kvamme, 1992) and has continued to the present day. Applications of GIS, GPS, RS, and Lidar in archaeology have been reviewed by Kvamme (1999), McCoy and Lagdefoged (2009), and a useful edited volume on archaeological predictive modeling was done by Wescott and Brandon (2000).

The majority of archaeological predictive modeling involves environmental information organized in a GIS and then analyzed statistically to create maps of areas of the landscape that are predicted to contain archaeological materials. Examples of these would be the work by Kvamme (1992), Brandt, Groenewoudt, & Kvamme (1992), Fletcher & Winter (2008), and Hildebrandt-Radke & Jarosław (2009). All of these studies examined the environmental variables of the landscape and attempted to predict where archaeological material would be found in the future. More complicated statistical analysis of environmental variables has been incorporated as well. Finke, Meylemans, & Van de Wauw (2008) used Bayesian inference and classification and regression trees (CART) to analyze their environmental variables. Canning (2005) and Boos, Hornung,

Jung & Müller (2007) have also incorporated Bayesian theory into their predictive models. Paleoenvironmental reconstruction has also been attempted by Zwertvaegher et al. (2010).

Remote sensing has also been adopted by archaeologists to aid in locating sites. An interesting review of the history of NASA remote sensing data and archaeology was done by Giardino (2011). Carr & Turner (1996) used medium resolution (30m spatial resolution) Landsat Thematic Mapper (TM) images to create a predictive map of ancient chert quarries in southwest Montana. The images were analyzed using a maximum likelihood classification method. This per-pixel method resulted in a predictive map that was 66% accurate for quarry presence when field tested. Sever & Irwin (2003) used a variety of RS techniques to determine the extent and general shape of Mayan sites in Guatemala. They used both medium resolution Landsat TM and Enhanced Thematic Mapper (ETM+) and Ikonos imagery that was pan-sharpened to one meter resolution. The addition of a digital elevation model and STAR-3i radar imagery completed their data set and allowed them a clearer picture of the archaeological sites, specifically the causeways. This work showed the distinct advantages of using higher resolution data, the Ikonos image, over medium resolution images, such as Landsat (Sever & Irwin, 2003).

Remote sensing imagery was used to discover the location of a legendary river, *Sarasvati,* in India associated with the Harappan culture (Rajani & Rajawat, 2011). Low and medium resolution satellite imagery was combined with digital elevation models and analyzed using Principal Components Analysis (PCA). These paleochannels were mapped with known site locations to explore the spatial relationships between the two

and subsequently learn more about the spread and distribution of Harappan sites (Rajani & Rajawat, 2011).

Geology. Geologists have readily adopted GIS and RS applications to their work. A review of RS applications in geology was done by Goetz and Rowan (1981) that described the basic principles of remote sensing. This work explained the specifics of multispectral data, including describing the particular wavelengths and went on to explain how this data can be used for delineating regional geologic structures, lithologic mapping, and geobotanical applications. Goetz and Rowan also briefly discussed some applications of radar and airborne methods. This work is somewhat dated as the imagery discussed is medium resolution Landsat MSS, which has been surpassed in recent years with much higher resolution imagery.

Geologic applications of remotely sensed imagery are used for a variety of purposes. Geologic mapping is one of the primary purposes. K. Belt and S. Paxton (2005) used a GIS to create a digital elevation model overlaid with a bedrock geology map to create detailed geologic maps of Oklahoma. They found that by using these techniques, far more accurate maps can be made than by traditional field techniques (Belt & Paxton, 2005). A more complex technique was applied to the measurement of strikes and dips in Peru. By using aerial photographs and satellite imagery (SPOT and Landsat images) in a stereoscopic method, highly detailed descriptions of bedding attributes can be created in a digital elevation model (Bilotti, Shaw & Brennan, 2000). Mapping of carbonate platforms of various islands throughout the world using Landsat imagery and a statistical unsupervised classification led to a highly accurate result (Kaczmarek, Hicks, Fullmer, Steffen & Bachtel, 2010). Collection of sediment data to confirm the RS based

classification showed an 82-85% accuracy and the resulting maps "show a level of complexity and heterogeneity that is more realistic than shown in previously published maps..." (Kaczmarek, et al., 2010, p. 1581). Another mapping technique was explained by Bilotti et al. (2000). Their work used Landsat Thematic Mapper (TM) and SPOT imagery to develop stereoscopic images to accurately (less than 5º error) map surface bedding attitudes, including sub-surface geology formations.

Mineral mapping is another aspect of RS utilization in geology. A review of the techniques of determining surface minerals using multi- and hyperspectral imagery was done by Van der Meer et al. (2012). Detailed information about the methods of determining mineral composition using the various bands, or ratios of bands, of ASTER imagery was explained, followed by a description of hyperspectral techniques using visible and short wave infrared (VIS-SWIR) wavelengths of imagery (Van der Meer et al., 2012). Finally, a detailed analysis of Landsat Enhanced Thematic Mapper (ETM+) imagery of an upland area of Ethiopia was performed by Godebo (2005). In this work, detailed mapping of mineral composition was performed, as well as geologic mapping, hydrologic mapping, and soil analysis for the purpose of determining primary locations for groundwater.

Other uses for RS and GIS in geology are hazard analysis, glaciology, and predictive soil modeling. Pradhan and Lee (2007) used Landsat TM imagery and an artificial neural network (ANN) to perform a landslide hazard analysis in Malaysia. They found that areas of high risk for landslides could be mapped with an 82.92 % accuracy. Work performed by Clark (1997) explained how RS and GIS technology can be used in glacial geomorphology and paleoglaciology. Clark also explained the use of Synthetic

Aperture Radar (SAR) and digital elevation models (DEM's) for mapping glaciers past and present (Clark, 1997). A GIS of geologic data was analyzed using an ANN for the purpose of predicting sediment buildup in the harbor in Gothenburg, Sweden (Yang & Rosenbaum, 2001). The work by Yang and Rosenbaum shows how predictive models can be developed for future sedimentary deposition.

Paleontology and Paleoanthropology. While the adoption of GIS and RS techniques in paleontology and paleoanthropology has been slow, there have been some pioneers that have begun to incorporate these techniques into their search for fossils. An excellent review of the adoption of GIS and RS techniques to paleontological and paleoanthropological research is done by Anemone et al. (2011a). GIS techniques have been incorporated in paleoenvironmental reconstruction for the purpose of determining the habitat ranges of past species (Stigall-Rode, 2005, Stigall & Lieberman, 2006). This work mapped location information for fossil taxa and then converted the present map of the earth into what it looked like during the Devonian. These fossil presence points were then used to recreate the habitat range of Devonian species (Stigall-Rode, 2005). Another interesting application of GIS to paleontology was the work by Rayfield, Barrett, McDonnell & Willis (2005). They used a GIS to analyze middle and late Triassic Land Vertebrate Faunachrons (LFVs). LFVs are simply a method of dating fossil assemblages based on evolutionary processes and represented by certain index fossils. Rayfield et al. (2005) were testing the LVFs to determine if they were "temporally restricted, numerically abundant and spatially widespread" (p. 328) and found that for certain LVFs the index fossils did not meet these criteria. The work by Bailey, Reynolds and King (2011) incorporated Landsat ETM+ imagery with Shuttle Radar Topographic Mission

(SRTM-3) data to reconstruct the paleoenvironment. The authors argued that tectonics and volcanism play a pivotal role in the habitat suitability of early hominins. These are examples where geospatial technology has been incorporated into large scale, macroevolutionary research.

Other work has incorporated GIS techniques on a smaller scale. Ghaffar (2010) used a digital elevation model (DEM) to generate a triangulated irregular network (TIN), which is a network of non-overlapping triangles where the corners are determined by a set of x, y, and z coordinates, where x and y indicate coordinates in space and z indicates an elevation. TIN's are useful because they are a digital representation of the landscape that shows the topography, such as slopes, ridges, and valleys, very well. Ghaffar then created digital contour maps of the Dhok Bun Ameer Khatoon site in the Siwaliks of Pakistan. He then used these digital models to explore the fossil distribution of *Giraffokeryx punjabiensis* throughout this site. Sedimentary deposits from Plio-Pleistocine cave sites in Swartkrans, South Africa were spatially analyzed and a digital archive was created. A 3-D model of the cave site was created using a laser theodolite. Fossil remains and artifacts relating to hominin activity were mapped in this three-dimensional reconstruction of the cave sites (Nigro, Ungar, de Ruiter & Bergen, 2003).

The work by Conroy (2006) shows the utility of creating interactive maps of a larger research area. He shows how to use GIS, and ArcMap in particular to create maps of the Uinta Basin, Utah, showing various paleontological sites. DEM's and digital orthophoto quads (DOQ's) allow for very good visualization of the landscape, however, the true utility of the GIS is the ability to spatially map all the fossil find sites in the region and then to query the relational database, called the attribute table. Queries can be

performed based upon particular data attached to the fossil localities as well as spatially through the use of buffers and intersection (Conroy, 2006). This work shows the usefulness of displaying such data in a GIS and how the data can be queried and analyzed to aid in the guidance of survey work. However, it does not predict where future fossils will be found. Conroy, Anemone, Van Regenmorter & Addison (2008) developed a method to share paleontological information of the GDB using the functionality of Google Earth. Six map layers were created in a GIS (ArcGIS v. 9.2) and included: latitude and longitude coordinates of fossil localities, faunal lists for each locality, a list of localities that yield primate fossils, elevation derived from a 30 meter DEM, slope in degrees derived from the DEM, and a geologic map. Each of these map layers were exported into Keyhole Markup Language (KML) files which could then be compressed and easily distributed electronically. These files could then be visualized in Google Earth, thereby allowing this data to be shared with people that do not have access to expensive GIS software like ArcGIS.

A predictive model was developed by Kathryn Oheim (2007) to predict where fossils are located in the Two Medicine Formation (late Cretaceous) of north-central Montana. Oheim adopted the methodology of suitability analysis that is common amongst archaeologists (such as Kvamme, 1992) for the creation of predictive models. She incorporated several types of data into a GIS, including geologic maps, land cover maps, road networks, and elevation (based on a 30 meter spatial resolution DEM). She assigned classification values, ranging from zero to four with four being most suitable, and assigned them to particular values of the four types of data. Oheim then weighted each of the four data types based on importance, with geology weighted heaviest and

distance from roads weighted least because it is only a measurement of ease of access (Oheim, 2007). This analysis resulted in a raster data layer where each grid cell had a value based on environmental suitability and weighted by importance that predicted the possibility of locating fossils at that location. This model was field tested by systematically surveying areas of both high and low probability. The number of fossils sites found per km^2 was used to create a fossil density, which had an R^2 score of 0.905 (Oheim, 2007, p. 363) with the predicted score. This work shows how even a simple suitability model can be useful in creating a predictive model of fossil localities.

The incorporation of RS techniques into paleontological research is another aspect of the fusion of geospatial science with paleontology. An early project that pioneered this was the "Paleoanthropological Inventory of Ethiopia". This program was initiated in 1988 by Ethiopia's Ministry of Culture and was developed by B. Asfaw, an Ethiopian paleoanthropologist, and T. White, of NASA. Asfaw, Ebinger, Harding, White & WoldeGabriel (1990) worked primarily in the Main Ethiopian Rift and Afar depression using a combination of satellite imagery (Landsat Thematic Mapper (TM)), aerial photos, and space shuttle large format camera (LFC) photos to identify geologic formations and geologic structures for the purpose of finding locations of interest for paleontologists. The Landsat TM imagery, with seven spectral bands and 30 meter spatial resolution, was used to create false color images to differentiate the various lithologies on the ground and to pinpoint locations with similar geology to known fossil localities (Asfaw et al., 1990). These RS images were used to "determine the main features of each rift segment…and to identify the spectral characteristics of surficial geological deposits, including those known to be fossiliferous." (Anemone et al., 2011a, p. 28). This work was then used to

guide field survey throughout the region to sample the geology and search for paleontological and archaeological resources. This early work in Ethiopia led the way for the incorporation of RS technology into paleontology and paleoanthropology.

More recent work has utilized RS imagery to aid in the location of fossils. Haile-Selassie, Deino, Saylor, Umer & Latimer (2007) used a combination of aerial photography and RS images to pinpoint locations of interest for ground survey in Woranso-Mille study area in the central Afar region of Ethiopia. Aerial photographs with scales of 1:60,000 and 1:25,000 were used to aid in navigation through the study area and new fossil localities were documented using Global Positioning System (GPS) units. These RS products were used as visual references to aid in survey work and led to the cataloging of 77 new fossil localities and the recovery of over 1000 fossils during the field seasons of 2002-2006 (Haile-Selassie et al., 2007). Njau and Hlusko (2010) used high resolution imagery to aid in the location of new paleontological and archaeological sites in Tanzania. They used the freely available imagery from Google Earth (www.earth.google.com) and supplemented this with commercially available IKONOS satellite imagery. These sets of imagery reach spatial resolutions of as low as one meter. Njau and Hlusko were able to assess this high resolution imagery for erosional patterns and were able to identify sedminetary rock based on the spectral reflectance 'signatures' of the rock (Njau & Hlusko, 2010). They found that areas with high reflectance, i.e. spectrally brighter, were predictive of sedimentary rocks, and therefore targeted those locations for subsequent ground survey. These authors did reinforce the absolute need for ground verification of RS imagery interpretations as they found that in some cases the areas they interpreted as sedimentary rock based on spectral reflectance were in fact

metamorphic rocks that looked similar, spectrally, to sedimentary rocks (Njau & Hlusko, 2010). The RS imagery used here was also critical in aiding the survey teams in locating paths and roads while in the field.

The works previously discussed simply used visual inspection of RS imagery to aid in guiding ground surveys. Another method of predicting where fossils can be found is by classifying imagery. Supervised and unsupervised classification are the two primary methods for classifying an image. In unsupervised classification, computer software is used to determine clusters of the pixels, known as spectral classes, in the multi-band image, with no interaction by the researcher. Once the clusters are identified, the researcher needs to identify what each spectral class represents. In supervised classification the researcher classifies the image using the spectral signatures derived from training samples. Training samples are areas in the image that represent each type of land cover (such as water, shrubland, vegetation, fossil localities, etc…).

Work done by Malakhov, Dyke, and King (2009) used Landsat ETM+ imagery to create a predictive model for 'remote prospecting' of fossils in Kazahkstan. This imagery is medium resolution, 28.5 meters, which was pan-sharpened to 14.5 meters using the higher resolution pan-chromatic band. A series of analytical techniques were then applied to this image. The first was an unsupervised image classification algorithm called ISODATA in which pixels in the image are statistically clustered together. The authors found that this technique was not exceptionally useful because it showed topographic, and not geologic, aspects of the landscape (Malakhov et al., 2009). The next technique they employed was to calculate band ratios to display clay and ferrous minerals in the image. This was done because it is believed that ferrous minerals are characteristic

of weathered or disturbed areas (Malakhov et al., 2009). The final, and most successful, analytical technique employed was Spectral Angle Mapping of the entire multispectral Landsat image. Spectral Angle Mapping (SAM) is a spectral classification technique that uses an *n*-D angle to match pixels in an image to reference spectra and determines the spectral similarity between two spectra by calculating the angle between the spectra and treats them as vectors in a space with dimensionality equal to the number of bands (Kruse et al., 1993). SAM compares the angle between the reference spectrum vector and each pixel vector, with smaller angles representing closer matches to the reference spectrum, and assigns pixels to classes based on their similarity to the reference data (Kruse et al., 1993). This technique created five spectral classes of the landscape: yellow Late Cretaceous Clays, red Late Cretaceous clays, overlying Neogene and Paleogene sediments, Quaternary clay beds, and the dried bottom of a temporary lake. The Cretaceous clays areas were then prospected in the field and several new fossil localities were located. This shows the utility of using medium resolution imagery to predict highly fossiliferous locations prior to field survey.

Conroy, Emerson, Anemone & Townsend (2012) also used Landsat ETM+ imagery to remotely prospect for fossils in the Uinta Basin of Wyoming. The 30 m resolution imagery was pan-sharpened using the panchromatic band to a resolution of 15m. A supervised classification method was adopted and training sites were developed for six classes. The classes were: known fossil localities, oil/gas infrastructure, water, agricultural land, scrub/tree cover, and steep slopes (Conroy et al., 2012, p. 82). The fossil locality training sites were based on known fossil localities that were documented prior to 2005. A maximum likelihood method was then applied that took into account the

variances and covariances of the class signatures as determined by the training sites when assigning each pixel to a particular class. The mean vector and covariance matrix is used for each grid cell to generate a statistical probability of membership to a particular class. The grid cell is then assigned to the class that it has the highest probability of being a member. Conroy et al. (2012) then created a class probability map showing the grid cells that had a >98% probability of belonging to the class fossil locality. This was further refined by creating a mask of areas of Eocene geology so that the final map only showed areas of the basin that were classified as being >98% probable of being a fossil locality and fell within Eocene age geology. A post-hoc validation of this model was done by comparing the model to fossil localities documented after 2005 that were not included in development of the model. Every single fossil locality in the post-hoc validation was found to fall within predicted locations on the class probability map (Conroy et al., 2012).

Recent Research in the GDB

Recent research in the GDB has been done by R. Anemone and C. Emerson (Anemone et al., 2011b, Emerson & Anemone, 2012). Two scenes of Landsat 7 Enhanced Thematic Mapper (ETM+) imagery from August and September 2002 were acquired. The eighth band of this imagery, the panchromatic band, was used to pan-sharpen the image using a principle components method, resulting in a spatial resolution of 14.25 meters. GPS coordinates of 110 fossil localities were collected between 1991 and 2010 in the GDB. These locations were used to create regions of interest "using eight neighbours (queen's case) and a 0.5 SD [standard deviation] of the red band

reflectance as the cut-off tolerance" (Emerson & Anemone, 2012, p. 455). These regions of interest were between 0.4 and 1.6 hectares in size. Training sites for other land cover types were determined. There were three spectral classes designated for soils based on color of the soil (dark, white, and red) and four different types of vegetation (sagebrush, grassland, brushland and mixed) as well as forest and wetlands. A quarter of the training sites were randomly selected for post-hoc accuracy assessment while the remaining were used in the supervised classification of the image (Emerson & Anemone, 2012).

An artificial neural network (ANN) was used to classify the image. An ANN is an attempt to imitate the workings of biological networks of nerve cells in the brain. This particular research utilized a back-propagation multilayer perceptron model consisting of six input nodes, two hidden nodes and ten output nodes (Emerson & Anemone, 2012). Figure 9 gives a diagram of the layout of an ANN. The six input nodes are the Landsat ETM+ visible and reflective infrared bands (Bands 1-5 and 7), and the ten output nodes correspond with the land cover spectral classes. The ten output spectral classes were then condensed down into five informational classes: localities, barren, scrubland, forest, and wetland (Anemone et al., 2011b).

Post-hoc accuracy assessment was then performed using the 25% of training sites held out of training the ANN. A variety of measures of classification accuracy were generated, including overall accuracy, Kappa coefficient, and User's and Producer's accuracy. Overall accuracy is simply the total percentage of pixels that were accurately classified. Kappa coefficient is a more conservative measure that takes into account chance agreement. Producer's accuracy is a measure of errors of omission where pixels are incorrectly classified as something else. User's accuracy is a measure of errors of

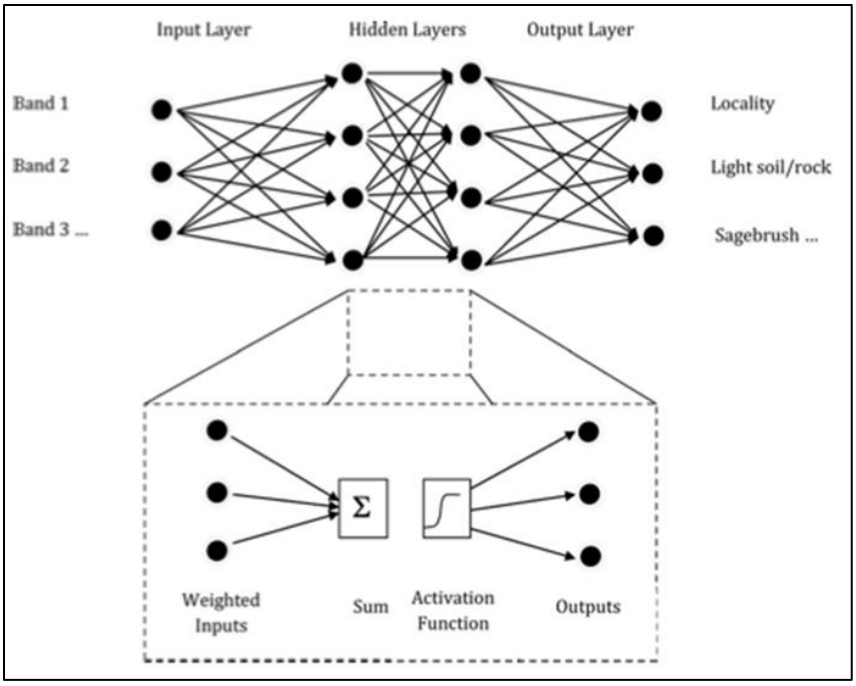

Figure 9. Diagram of an artificial neural network (ANN), from Emerson & Anemone, 2012.

commission where pixels predicted to be one particular class are actually something else. The model had an overall accuracy of 84.21 % with a Kappa of 77.44% (Anemone et al., 2011). Of distinct interest in this work is the Producer's and User's accuracy of the localities class, which were 79 % and almost 99 % respectively.

In this work, each predicted locality pixel had a probability of membership to that class ranging from high to low. In order to further refine the areas predicted as being highly fossiliferous, a 'Rule Image' was created where only pixels that were 95% probable of being a locality were included (Anemone et al., 2011b). This was further refined by only including pixels that had a slope of greater than 5%, as fossils are typically found actively eroding out of sandstone outcrops in the GDB and 80% of known fossil localities fall within areas of 5% slope or greater (Emerson & Anemone, 2012).

This resulted in figure 12, showing an image of the entire GDB with red pixels denoting the highly probable localities.

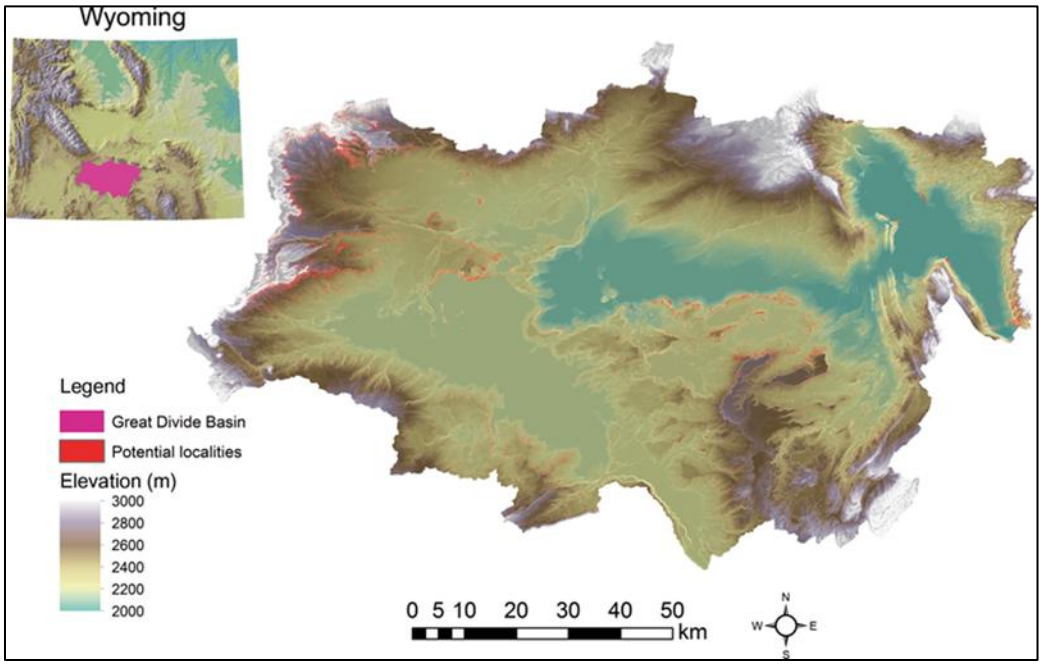

Figure 10. Results of the ANN classification, from Emerson & Anemone, 2012.

The model was further tested by extending the method to include the Paleocene (Fort Union Formation) Bison Basin just to the north of the GDB. Three known fossil localities within the Bison Basin were used to test the accuracy of this ANN method. The Bison Basin was included with the GDB and the ANN method was re-run. A similar >95% probable locality and >5% slope rule image was developed. It was found that all three of these Bison Basin localities were exactly predicted by the ANN model.

The results of this work are encouraging for the possibility of being able to remotely prospect the landscape for areas highly likely to contain fossils. This work used medium resolution imagery (pan-sharpened to 14.5m resolution) and encompassed the

entire 10,000 km² basin, and therefore was adequate as a general reconnaissance of the GDB. The work by Anemone and Emerson highlighted areas of the GDB that were of high interest for future work, utilizing higher resolution imagery on a finer scale.

CHAPTER IV

METHODOLOGY

The theory and methodology adopted by this thesis is based on the theoretical framework of Hierarchical Patch Dynamics, discussed in the previous chapter, as adapted by Burnett and Blaschke in the development of their MultiScale Segmentation and Object Relationship Modeling (MSS/ORM) methodology (Blaschke et al., 2005; Burnett & Blaschke, 2003). This methodology creates a five step process for performing GEOBIA analysis. The steps are as follows: GIS building, segmentation, classification, visualization, and finally quality assessment. A brief discussion of Hierarchical Patch Dynamics begins this chapter, followed by a discussion of the five methodological steps.

GIS Building

The first step in this research was the collection and preparation of the appropriate data. The primary data is RS imagery from the Worldview 2 and Quickbird 2 satellites of sections of the Great Divide Basin that were deemed high priority for exploration by previous research (Emerson & Anemone, 2012). A total of six images were acquired from the commercial satellite imagery company Digital Globe. This imagery is eight band multispectral for the Worldview 2 images and four band multispectral for the Quickbird 2 imagery with both sources having an approximately two meter spatial resolution (see table 4 for specifics).

Table 4

Specifications of satellite imagery

Satellite	Spatial Resolution (at nadir)	Bands
Worldview 2	0.46 m	Pan: 450-800 nm
	1.8 m	Coastal: 400-450 nm
		Blue: 450-510 nm
		Green: 510-580 nm
		Yellow: 585-625 nm
		Red: 630-690 nm
		Red Edge: 705–745 nm
		Near IR-1: 770–895 nm
		Near IR-2: 860-900 nm
Quickbird 2	61 cm	Pan: 450-900 nm
	2.44 m	Blue: 450-520 nm
		Green: 520-600 nm
		Red: 630-690 nm
		Near IR: 760-900 nm

Both images included higher resolution panchromatic bands, however, these bands were not used in the subsequent analysis. The six high resolution images are of sections of the Great Divide Basin that were of interest for field survey (see figure 11). The Salt Sage Draw image was acquired because the known productive fossil locality, Tim's Confession (WMU-VP-220), is located in this image and this locality was used in the development of the segmentation and classification technique. Therefore, only five of the six images were tested in the field, with the sixth image, Salt Sage Draw, being used to develop the methodology and for preliminary accuracy assessment.

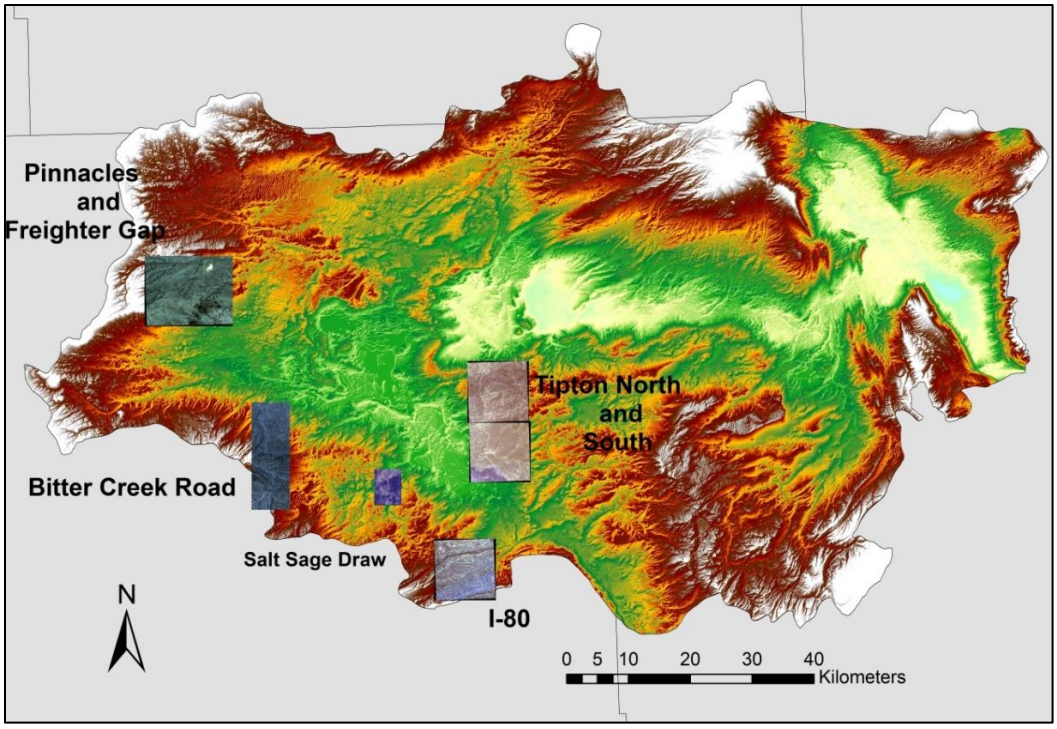

Figure 11. Location of satellite images in the GDB. Elevations of the GDB are shown in the background.

Tim's Confession is important because it is the most productive locality within the GDB. It was discovered in 2002 and has provided thousands of fossils, including important adapid and omomyid Primate species, over the past years. This one site has yielded so many fossils that it is the ideal location to use as the training site for this research. The goal is to find other locations within the GDB that are similar to this one location with the hopes of finding other, highly productive fossil localities.

Other acquired data included a digital elevation model (DEM), a surficial geology map, a map of Wyoming roads, and the watershed boundaries of the Greater Green River basin. All of these were acquired through the Wyoming Geospatial Library (wygl.wygis.org), with the exception of the watershed basin, which was acquired from the Wyoming State Water Plan (waterplan.state.wy.us). The DEM has a ten meter

resolution and was developed from the National Elevation Dataset created by the United States Geological Survey (USGS). The geologic map was created by the Wyoming State Geological Survey in 1998 at a 1: 500,000 scale. The road network was developed by the Wyoming Department of Transportation. A boundary of the Great Divide Basin was developed from the watershed boundary of the Greater Green River basin (acquired from the Wyoming State Water Plan, waterplan.state.wy.us). The Hydrologic Unit Code level 4 was used for this purpose. This basin boundary was then used to create subsets of the DEM, geologic map, and road network.

The 3-D Analyst extension of ArcMap 10.1 was used to generate a slope surface from the DEM. A slope surface is a measurement of the rate of change of a z-value, in this case elevation, as expressed in percent slope. A percent slope of 0 is flat while a percent slope of 100 represents a 45 degree slope, and the percent slope increases as the change in elevation becomes more vertical. Figure 12 shows an example of one of the slope surfaces that was generated. The final piece of data was a point feature of known fossil localities collected by Dr. Anemone and his field crews using GPS. All data were standardized in the Universal Transverse Mercator (UTM) coordinate system, zone twelve north projection with the World Geodetic System (WGS), 1984 datum, and were organized into a file geodatabase using ArcMap version 10.1.

Segmentation

The segmentation was accomplished using eCognition Developer 64™ version 8 software. For each image, the blue, green, red, and near infrared bands were imported

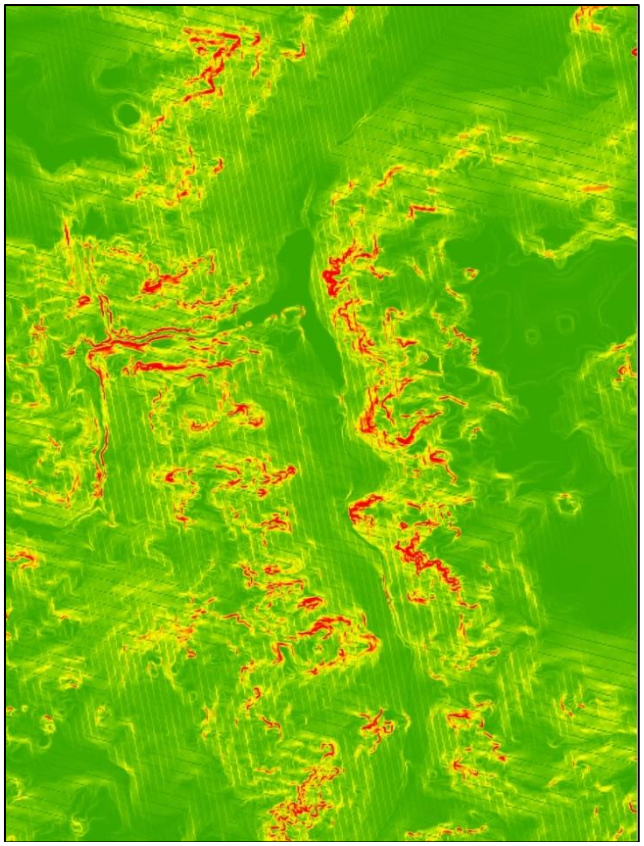

Figure 12. Slope surface of the Salt Sage Draw image.

into the software (bands 2, 3, 5, and 7 for the Worldview images; bands 1,2,3,4 for Quickbird). The slope surface developed from the DEM data was also imported as an additional band. The Salt Sage Draw image that contained the known highly productive fossil locality, Tim's Confession, was used to develop the rule set for both the segmentation and classifications. The multi-resolution segmentation algorithm was used and the segmentation parameters were developed using a heuristic process to determine the appropriate values. This process is hierarchical and iterative as each segmentation operates on previous segmentations, creating image objects that nest within larger supra-objects, and resulting in a multi-scale segmentation of the image. A total of four

hierarchical levels of segmentation were performed (a minimum of three levels as suggested by Burnett and Blaschke, 2003) using the parameters detailed in table 5.

Table 5

Segmentation parameters

Segmentation Level	Scale	Color	Shape	Shape settings	
				Smoothness	Compactness
Level 1	100	0.9	0.1	0.5	0.5
Level 2	50	0.9	0.1	0.5	0.5
Level 3	25	0.9	0.1	0.5	0.5
Level 4	10	0.9	0.1	0.5	0.5

.

As can be seen, the color variable (the digital numbers of the red, green, blue, and near infrared bands of the image) was primarily weighted in the segmentation. Shape was only marginally incorporated in the segmentation and both the smoothness and compactness aspects of shape were equally balanced. As the scale parameter increases, the size of the resulting image objects increases correspondingly. Therefore, the level 1 segmentation has the largest image objects and level 4 has the smallest. Each subsequent segmentation operated on the previous segmentation. Once level one was segmented, the level 2 segmentation was performed on the level 1 image objects, thereby creating a hierarchical relationship between each level. Figure 13 shows an example of a segmented image.

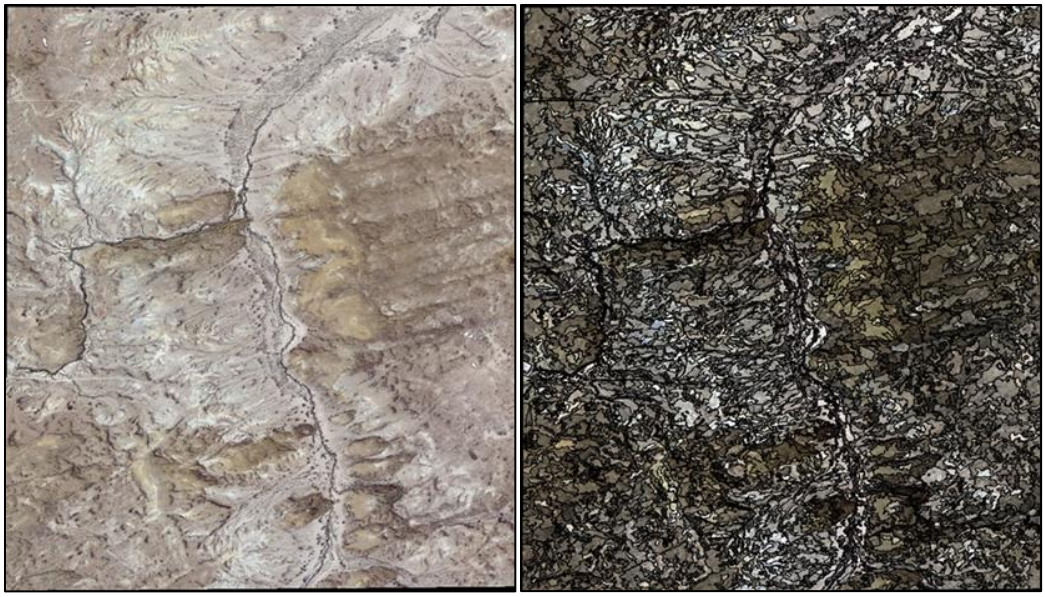

Figure 13. Salt Sage Draw image, RGB display on left and segmented on right.

Once each multi-resolution segmentation was completed a spectral difference segmentation was performed for each level. Each segmentation created a large number of individual image objects, often with neighboring image objects that were barely different from one another. The Spectral Difference segmentation algorithm merged neighboring image objects according to their mean image layer intensity values. Neighboring image objects were merged if the difference between their layer mean intensities was below the value given by the maximum spectral difference value. This algorithm is designed to refine existing segmentation results by merging spectrally similar image objects produced by previous segmentations. (Definiens Professional Reference Book, 2006). A maximum spectral difference value of 10 was heuristically chosen. This was performed to minimize the total number of image objects, specifically for the level 3 and 4 segmentations, and decrease total computation times.

The goal of the segmentation was to create an image object that closely fit with the known fossil locality, Tim's Confession, therefore it was very important to have a-priori knowledge of what specifically was being sought in the landscape (Blaschke, 2005). The level three and four segmentations (Scale parameters of 25 and 10) best delimited the areal extent of Tim's Confession, therefore, it was deemed that these two segmentations would be the focal scales for the model. Once the specific parameters for the multi-resolution segmentation were determined using the Salt Sage Draw image, the segmentation was applied to the other five images in the basin.

Classification

The segmented Salt Sage Draw image was then analyzed to develop the classification rule set. The precise image object that corresponded with Tim's Confession was located and the statistical values of that image object were used to determine the parameters for classification. This is another advantage of the GEOBIA technique as parameters like mean, variance, standard deviation, and textural measures like gray level co-occurrence matrix (GLCM after Haralick) (Haralick et al., 1973; Liu, 2004) can be calculated and used in the classification process (Blaschke, 2003; Frohn, 2006). Normalized difference vegetation index (NDVI) was also calculated for each image object (Rouse, Haas, Schell & Deering, 1973). NDVI is a simple band ratio of the Near Infrared and visible red bands of a multispectral image with values ranging from zero to one. NDVI is a standard used for classifying vegetation in imagery. Equation 1 details the equation used for generating the NDVI value. This equation creates a band ratio of the average values of the near infrared (NIR) and visible red bands (VIS) in each image

object. The Worldview 2 bands 7 (NIR) and 5 (VIS) and Quickbird band 4 (NIR) and band 3 (VIS) are the bands used for this purpose.

$$NDVI = \frac{NIR - VIS}{NIR + VIS} \quad (1)$$

The incorporation of expert knowledge is a significant advantage of the GEOBIA technique (Liu, Guo & Kelly, 2008; Mahmoudi et al., 2012; Platt & Rapoza, 2008). Expert knowledge can be defined as information used in decision making that is accumulated and refined over time. In this particular instance, the classification method is trying to mimic the decisions made by paleoanthropologists performing ground survey in the GDB. The classification was developed based on information provided by Dr. R. Anemone based on twenty years of field work in the GDB. There are five primary characteristics of the landscape that are sought out during field work. These are: steep slope, lighter colored geologic formations, lack of heavy vegetation, not on roads, and most importantly correct surface geology. The first four of these criteria were incorporated in this classification scheme with the last incorporated at a later stage.

The first landscape characteristic used in the classification was slope. Slope is important because fossils tend to be fragile and do not last long once exposed to the elements. While the GDB is a desert environment, occasional flowing or standing water destroys fossils. More important are the persistent winds in this region that tumble and scour fossils beyond recognition. The most productive localities in the GDB have been located along cliff faces, where a protective cap of sandstone overlies softer fossil-bearing mudstones (Emerson & Anemone, 2012) The landscape associated with

productive localities, therefore, is sandstone outcrops, which are typically areas with a higher percent slope. The second characteristic follows Njau and Hlusko (2010) who used high resolution imagery to visually pinpoint bright areas (i.e. high spectral values) that corresponded with sedimentary geologic formations in Tanzania. This concept was reinforced by the expert knowledge of R. Anemone.

Highly vegetated areas are also considered to be undesirable for fossil recovery. The primary vegetation in the GDB is sagebrush and fossils are typically not found in thick patches of sagebrush. Roads are also considered bad for fossil recovery because they are areas that have been disturbed by human activity. While many roads in the GDB are simple two-track trails, other roads have been graded or paved by the booming oil and gas companies in the region. Fossils are typically found in surface scatters, therefore, any human activity, i.e. grading, paving, frequent travel, will accelerate the decomposition of fossils. It is also probable that any interesting fossils, such as jaws, teeth, or more complete long bones, may be picked up by amateur fossil collectors. Therefore, areas of human disruption of the landscape are not generally good locations for prospecting for fossils. The most important aspect of the landscape that dictates areas that will be prospected is the correct surface geology. While searching for Wasatchian NALMA taxa in the GDB, the Eocene geology, the Wasatch formation, will be specifically targeted.

The three statistical values of the image objects that were used were the mean slope value derived from the slope surface, mean brightness, and the NDVI value (see equation 1). Brightness is defined as the "sum of the mean values of the layers containing spectral information divided by their quantity computed for an image object (mean value of the spectral mean values of an image object)" (Definiens Professional

User Guide, 2006, p. 42). The parameters of the equations in equation 2 are defined as: W_k^B: brightness weight of layer k, $c_k(v)$: mean intensity of layer k of an image object v.

$$w_k^B = \begin{cases} 0 \\ 1 \end{cases} \qquad w^B = \sum_{K-1}^{K} w_K^B$$

$$\bar{c}(v) = \frac{1}{w^B} \sum_{k-1}^{K} w_k^B \, \bar{c}_k(v) \qquad (2)$$

Source: Definiens Professional Reference Book, 2006.

An exclusionary classification scheme was adopted. Areas of the image were classified into crisp classes using Boolean descriptors based on the above parameters and then excluded in a step-wise manner until only the suitable areas of the image remained. A series of classes was generated including: Flatland, Sloped land, Vegetation, Road Candidate, Road, Cloud, and finally Sandstone (see figure 14). Refer to table 6 for the precise rule set. All classifications used the 'Assign Class' tool in eCognition.

The first two steps of the classification divided the image into areas of high and low slope based on the mean slope values of the image objects included by the addition of the slope surface as an additional band of the image. A value of six percent slope was chosen as the threshold based on a slightly more exclusive slope than that used by Emerson and Anemone (2012) in their Landsat analysis of the GDB. All areas with six percent mean slope or higher were classified as high slope and all below six percent were classified as low slope. The areas of low slope were then excluded from consideration.

Table 6

Classification rule set for all images

Classification Rule Set	
Step	Boolean rule
1	unclassified with mean Slope >6 = Slopedland
2	unclassified with mean Slope <6 = Flatland
3	Flatland and Slopedland with NDVI >= 0.16 = Vegetation
4	Flatland and Slopedland with Length/Width (geometry ratio) >4 and Mean Slope <= 4 =Road Candidate
5	Road Candidate with Brightness >340 and GLCM (all dir.) < 134 = Road
6	Road Candidate with Mean Slope > 6 = Slopedland
7	Road Candidate with Mean Slope <6 = Flatland
8	Slopeland with Brightness >= 390 = Sandstone

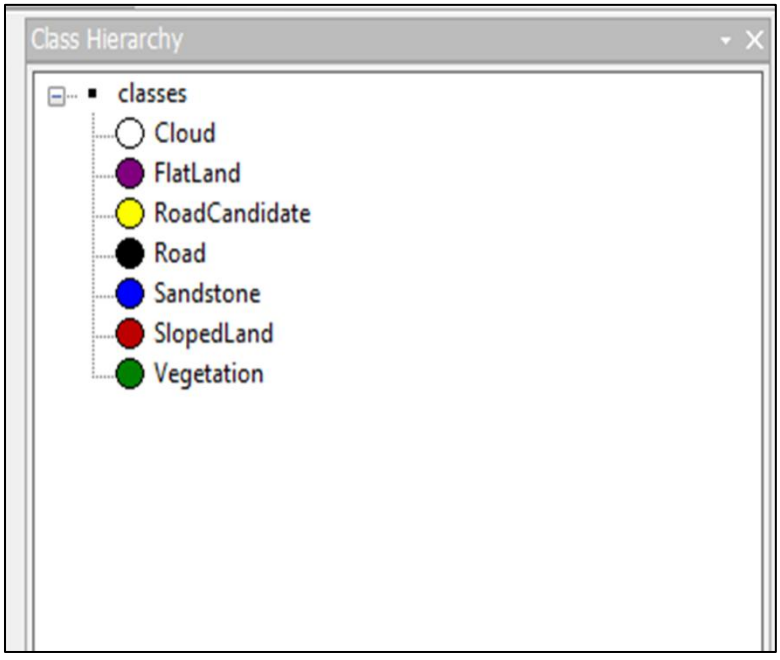

Figure 14. Class hierarchy developed in eCognition.

The third step was a classification of vegetated areas using the mean NDVI values for each image object. A threshold of 0.16 was adopted with image objects at or above this value being classified as highly vegetated areas and then excluded. This value, while somewhat low for typical NDVI values for heavy vegetation, was determined in a heuristic manner to adequately capture the sagebrush vegetation in the GDB. A variety of values were tested and visually inspected to determine if large patches of sagebrush were adequately classified.

The next step was to classify the roads within the image. A three step (steps 4 and 5) classification was adopted for this process as the 'assign class' tool in eCognition only allows for the use of two parameters. This was found to be inadequate to correctly classify roads in the images. The first step (step 4) was to create a road candidate class based on the length/width ratios and mean slope of the image objects. The length/width ratios identified the image objects that were thin in shape, as road image objects tended to be, and the low mean slope represented the relative flat areas where roads were built. Image objects for roads tend to be long and narrow in shape. By using a low length/width ratio and a low mean slope, potential roads were extracted from the image. The next step (step 5) was to refine the road classification using a texture parameter, the gray level co-occurrence matrix (GLCM after Haralick) and a refined mean brightness value to classify the roads. A high brightness value reflected the fact that the bare soil of the dirt roads in the images was significantly brighter than their surroundings. The low GLCM value was representative of the fact that the roads were significantly smoother than the surrounding rough terrain in the images. All other remaining areas of road

candidates were then converted back into either the low or high mean slope classes (steps 6 and 7).

A couple of modifications were made to this rule set for particular images. The I-80 image is dominated by the Interstate running east-west through the northern part of the image. This is a black top asphalt highway and is therefore significantly darker in brightness than the typical dirt roads in the images. An additional road classification was performed on this image to accurately classify the Interstate for exclusion. The same two steps (# 4 and 5) were applied to the image classification only with step 5 set to 'mean Brightness < 284 and GLCM (all dir.) < 134. The second modification is the fact that in the Pinnacles and Freighter Gap image, roads are not readily visible. All attempts to classify roads in this image were extremely flawed; therefore, road classification was not performed on this image. Also in the Pinnacles and Freighter Gap image, there is a small patch of cloud cover in the north-eastern portion of the image. This cloud was manually classified for exclusion.

At this stage of the classification there were five classes: Flatland, Slopedland, Vegetation, Clouds, and Roads. These classes were areas not considered potentially fossiliferous and were now excluded from the remaining areas of the image that had a high slope. The final step (Step 8) in the classification was applied to the remaining high slope areas with a mean brightness value of greater than or equal to 390. Any image object remaining in the high slope classification that met this mean brightness parameter was then classified as being a potentially fossiliferous location. One modification to this parameter was required. In the Pinnacles and Freighter Gap image there is a large region of shadow resulting from cloud cover. This made this entire region darker than the rest

of the image. In order to be able to include this region in the classification, a modification to the rule set was applied. This region was masked out and the rule set was re-run for this sub-region with the brightness value for this last step (step 8) lowered to 220. A completely segmented and classified image for all images was now completed; examples can be seen in figures 15 through 18.

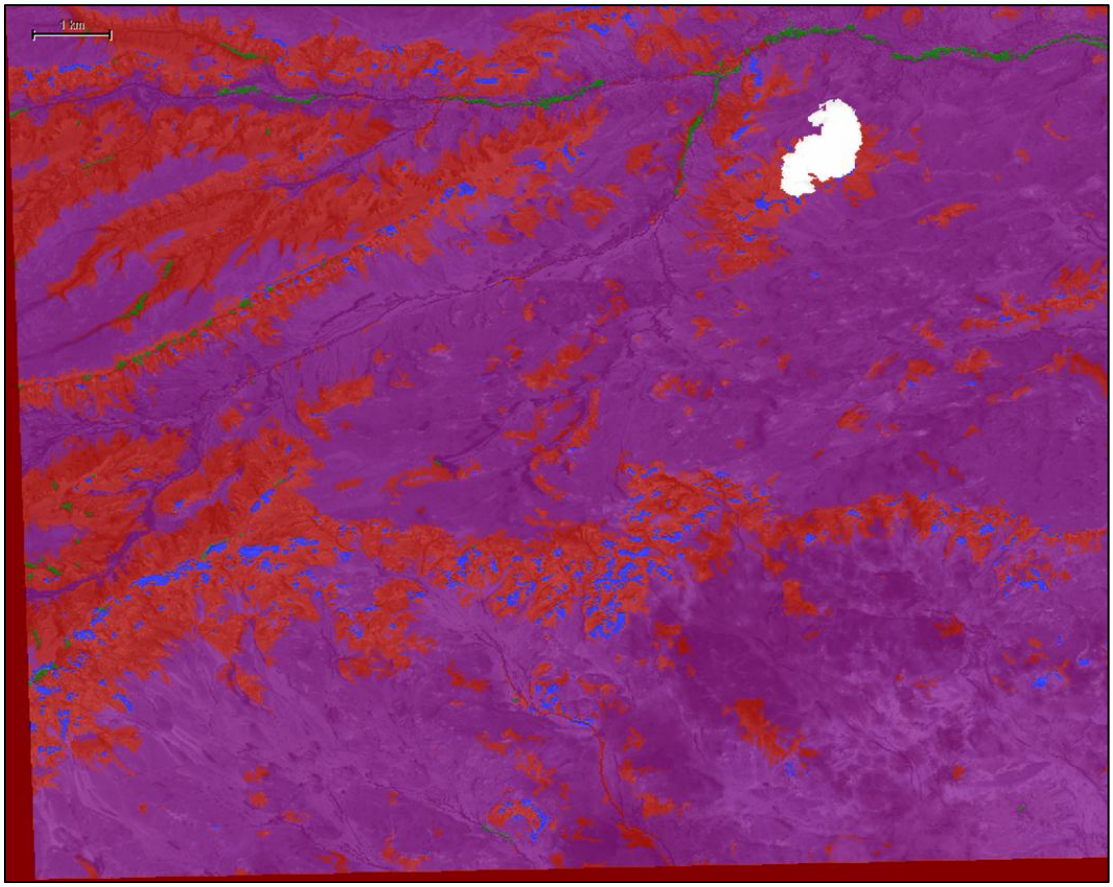

Figure 15. Classified Pinnacles and Freighter Gap image. Refer to figure 14 for legend.

Figure 16. Classified I-80 image. Refer to figure 14 for legend.

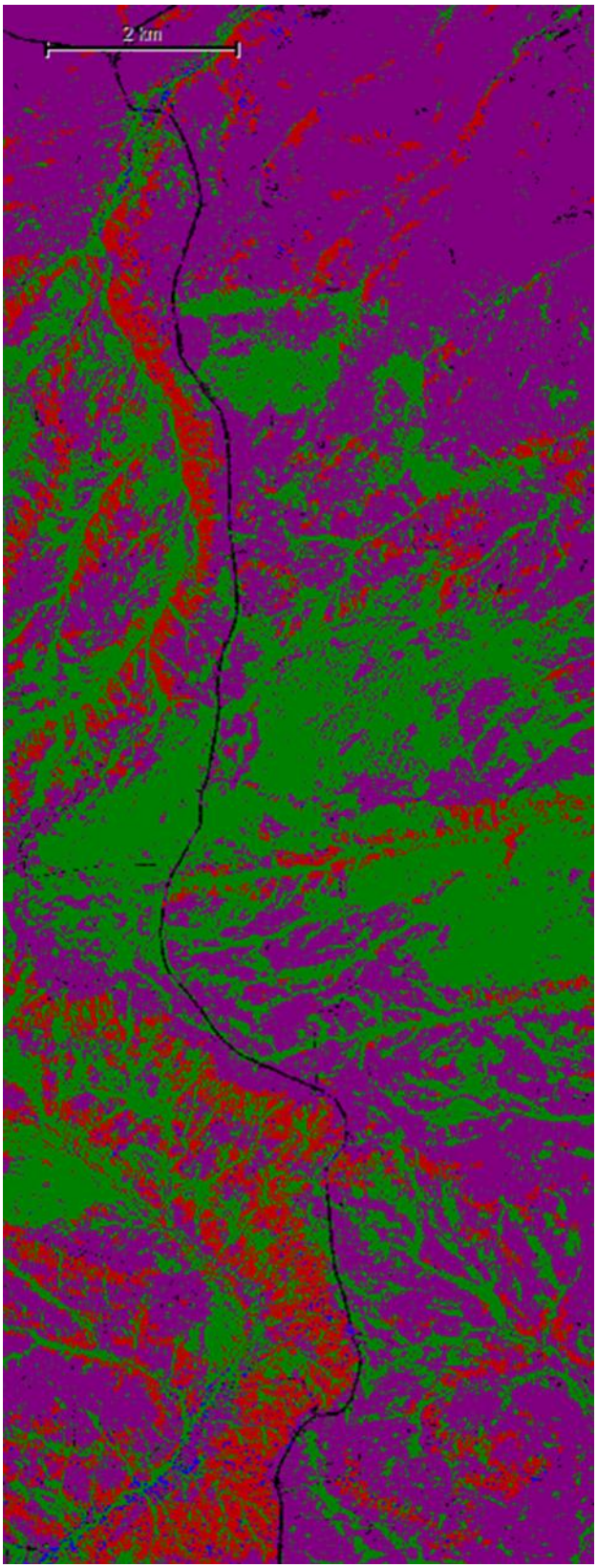

Figure 17. Classified Bitter Creek Road image. Refer to figure 14 for legend.

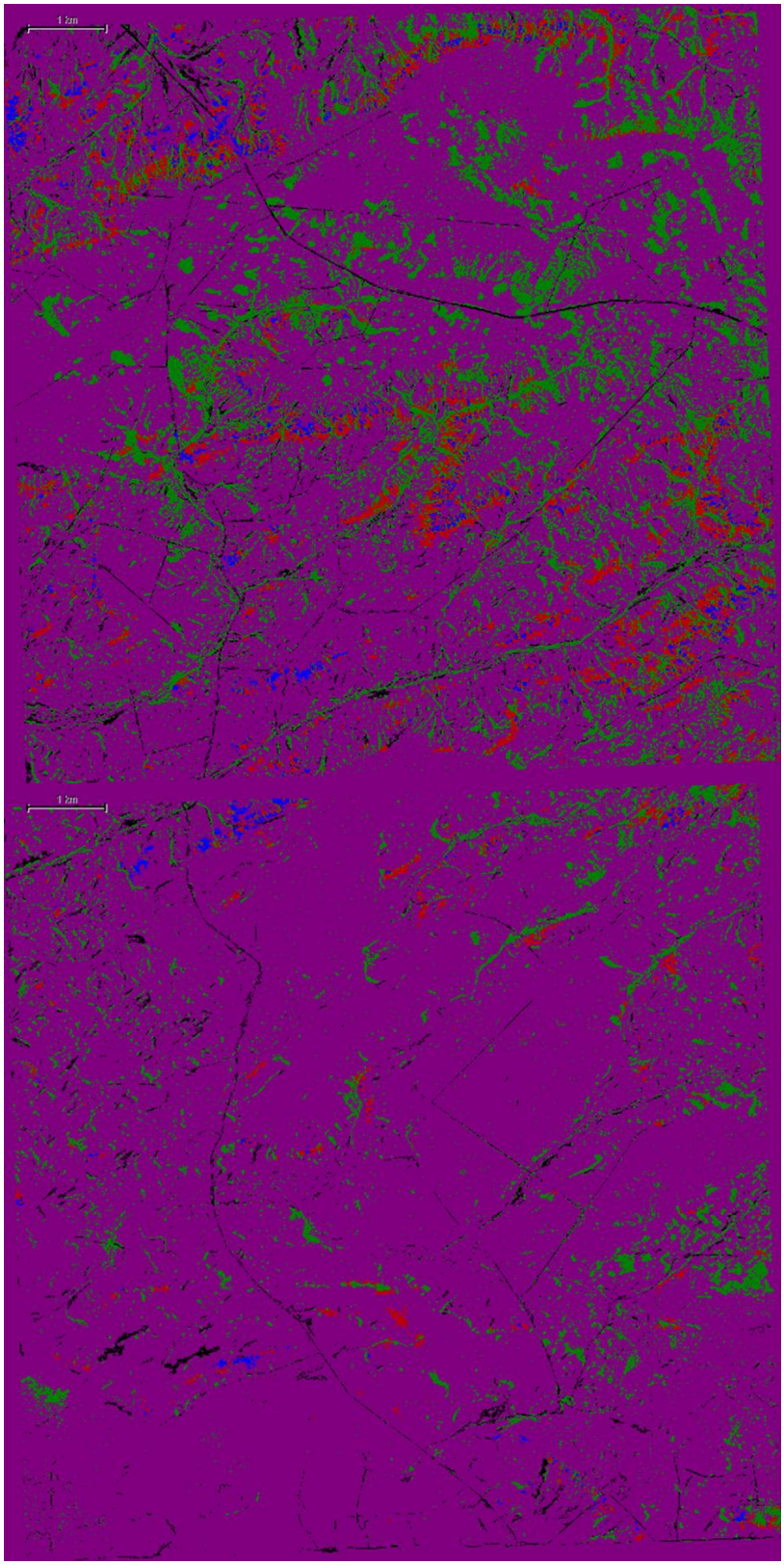

Figure 18. Classified Tipton North and South images. Refer to figure 14 for legend.

Visualization

The final classified image objects were then exported from the eCognition software as vector data models. Only the image objects classified as potential localities were exported for all four levels of segmentation. This vector data was imported into a file geodatabase in ArcMap 10.1. The surface geology map was added to these maps and any classified image objects that did not fall within the correct geology, the Wasatch formation, were excluded. The one exception to this rule is the fact that Tim's Confession, the known highly productive fossil locality, is mapped as Quarternary sand (see figure 5). It is obvious that this sandstone formation is not of Quarternary age as Wasatchian NALMA fossils are recovered from this location. It is possible that this area of the landscape was incorrectly mapped or more likely that the sandstone outcrops that comprise Tim's Confession are smaller than the minimum mapping unit of the geologic maps. This would result in a generalized mapping of the area as Quarternary sand with patches of Wasatch formation outcrops. This was the final step in the classification process and resulted in six maps (refer to figures 19 through 22) of each area of the satellite images with polygons indicating areas of the image that met all criteria for being potentially fossiliferous. The road network of the basin was added to each map, as well as a point feature of all known fossil localities from previous field seasons.

The purpose of this segmentation and classification scheme was to guide field survey during the field season of 2013. The maps that were created indicated locations within the satellite images that met the criteria for containing fossils. However, there were thousands of individual predicted image objects within each image and it would be

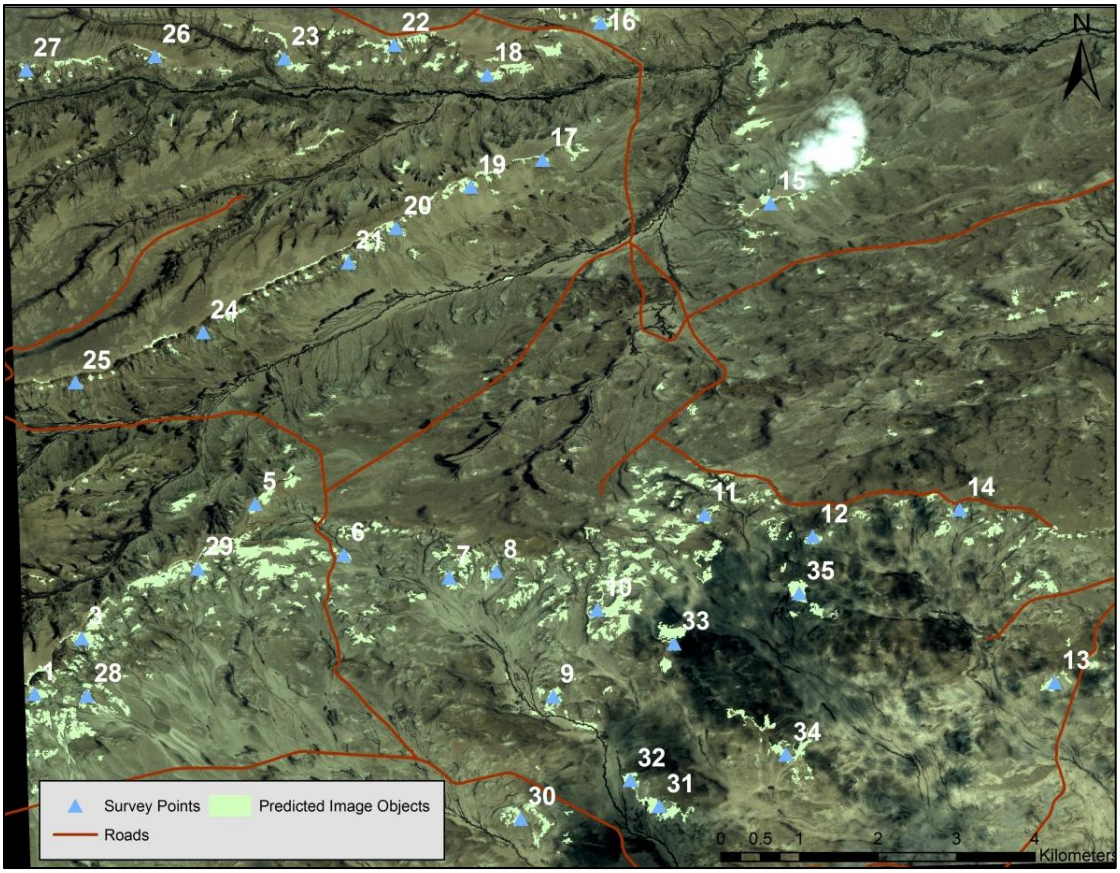

Figure 19. Survey map of Pinnacles and Freighter Gap.

impossible to survey each individual image object in the limited time allotted. In order to further refine the areas to be surveyed, points of particular interest, called survey points, were created. Approximately twenty to thirty points were selected based on certain criteria for each image with the exception of the Salt Sage Draw image. The Salt Sage Draw image had been heavily surveyed and little survey time was allotted for this area during the 2013 field season. The Pinnacles and Freighter Gap image had the most survey points with 35, the I-80 image had 33, the Bitter Creek Road image had 22, and the Tipton North and South images had 23 and 22 respectively. The maps were visually

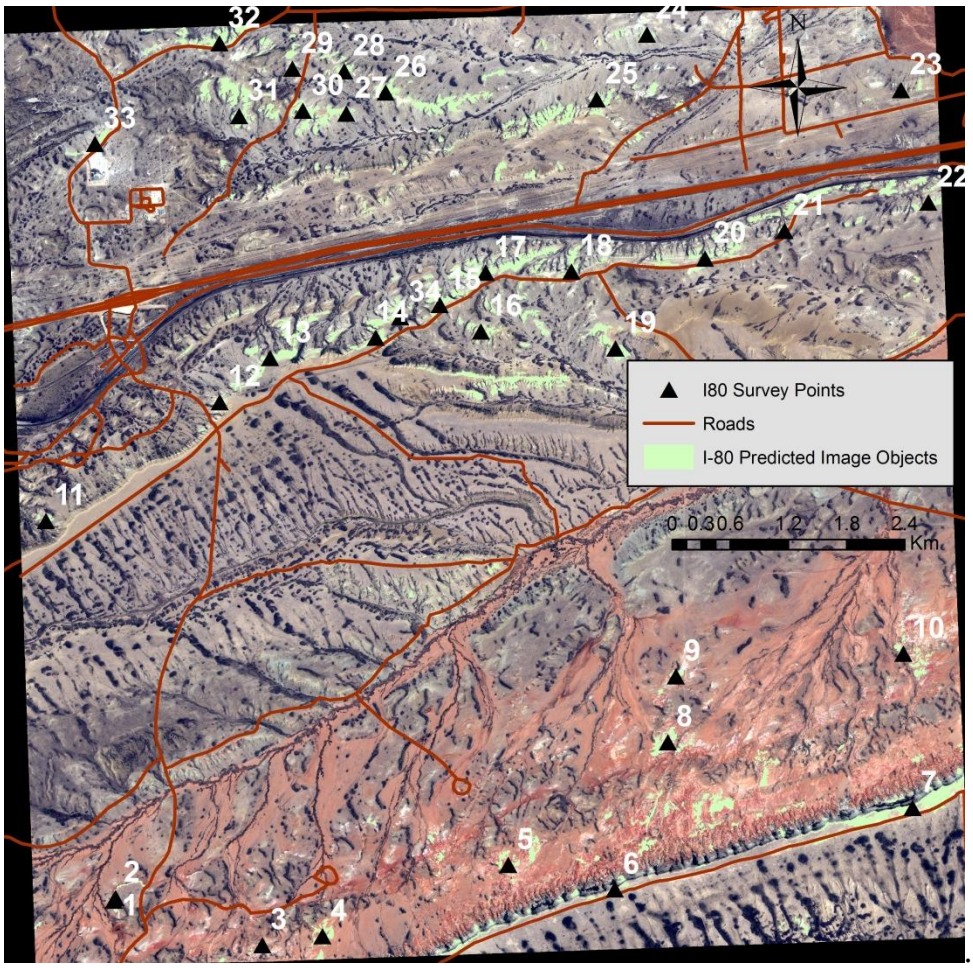

Figure 20. Survey map of the I-80 image.

inspected and areas with clusters of predicted image objects were located that were also not within close proximity of known fossil localities. This would maximize the number of image objects that could be surveyed while also focusing on areas of the landscape that had not been previously surveyed.

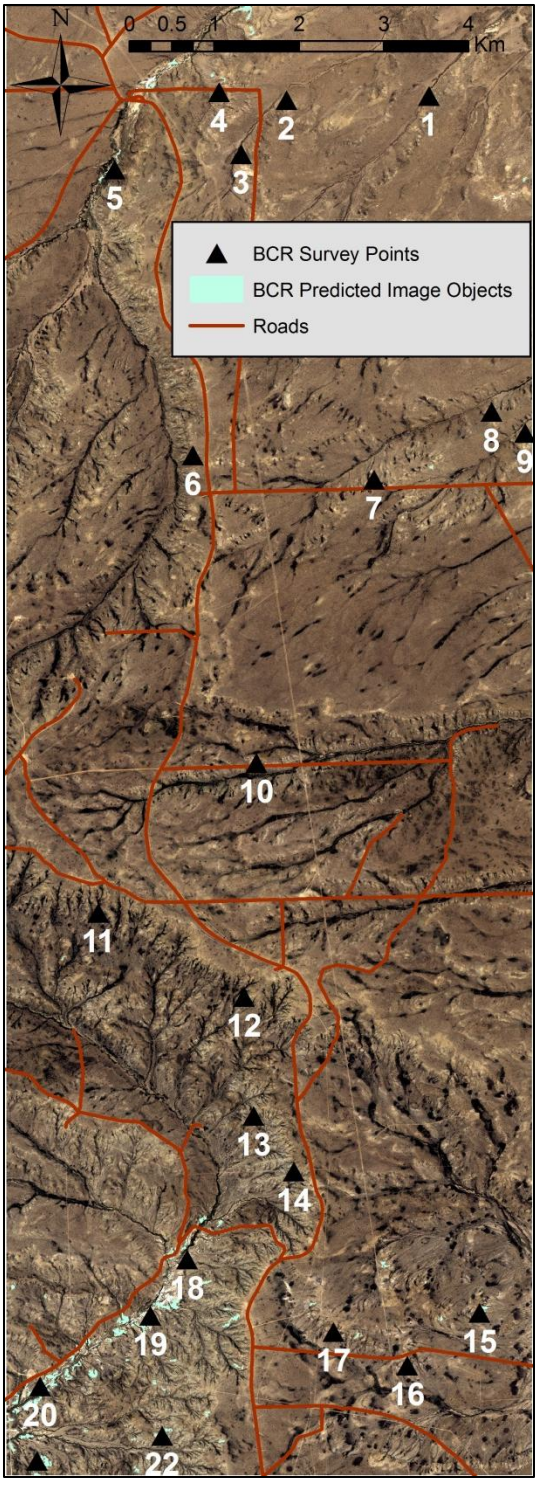

Figure 21. Survey map of Bitter Creek Road image.

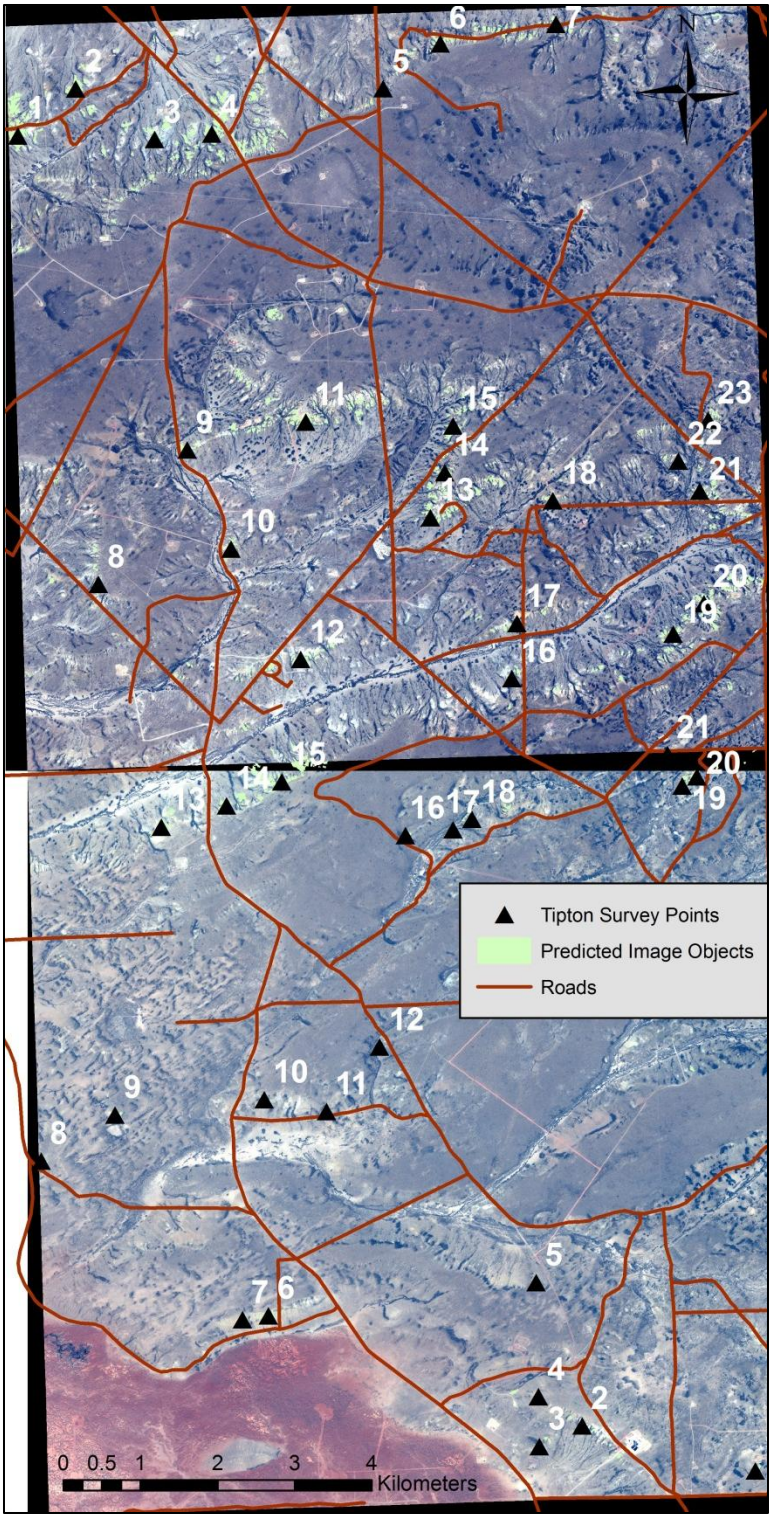

Figure 22. Survey map of the Tipton North and South images.

Quality Assessment

A quality assessment of the classifications was necessary prior to field testing the model. The best method to determine preliminary accuracy was by assessing how well the classification scheme correctly classified known fossil localities. The Salt Sage Draw image was chosen for this purpose as limited field time was to be spent in this area and the training site for the classification was located on this image. The map for the Salt Sage Draw image (see figure 23) was displayed with the classified image objects for the level three and four segmentations (refer to explanation in segmentation section) and the locations of known fossil localities were overlayed on the map.

The point feature of known fossil localities was created from field collected global positioning system (GPS) coordinates. These coordinates may be somewhat inaccurate and often represent a fixed point in the center of an area considered to be a locality. To compensate for this, a fifty meter buffer was created around all known localities within the Salt Sage Draw image. These buffer areas represented the actual area of the known localities, and fifty meters was chosen because this would accommodate inaccuracy in the GPS coordinates. There were thirteen known localities within the image, including Tim's Confession, which was excluded from the preliminary accuracy assessment as it was the training site used in the development of the classification scheme. The GEOBIA predicted image objects were then compared to the other twelve localities in the image to see how well the method predicted those known locations. The GEOBIA image objects correctly predicted eleven of the twelve localities. To provide comparison for this accuracy assessment the results of previous work in this

area (Anemone et al., 2011b) was checked in a similar manner. A raster data file of the Artificial Neural Network (ANN) results was mapped in a similar fashion. The ANN results were found to correctly classify nine out of the twelve known localities within the image (see figures 23 and 24).

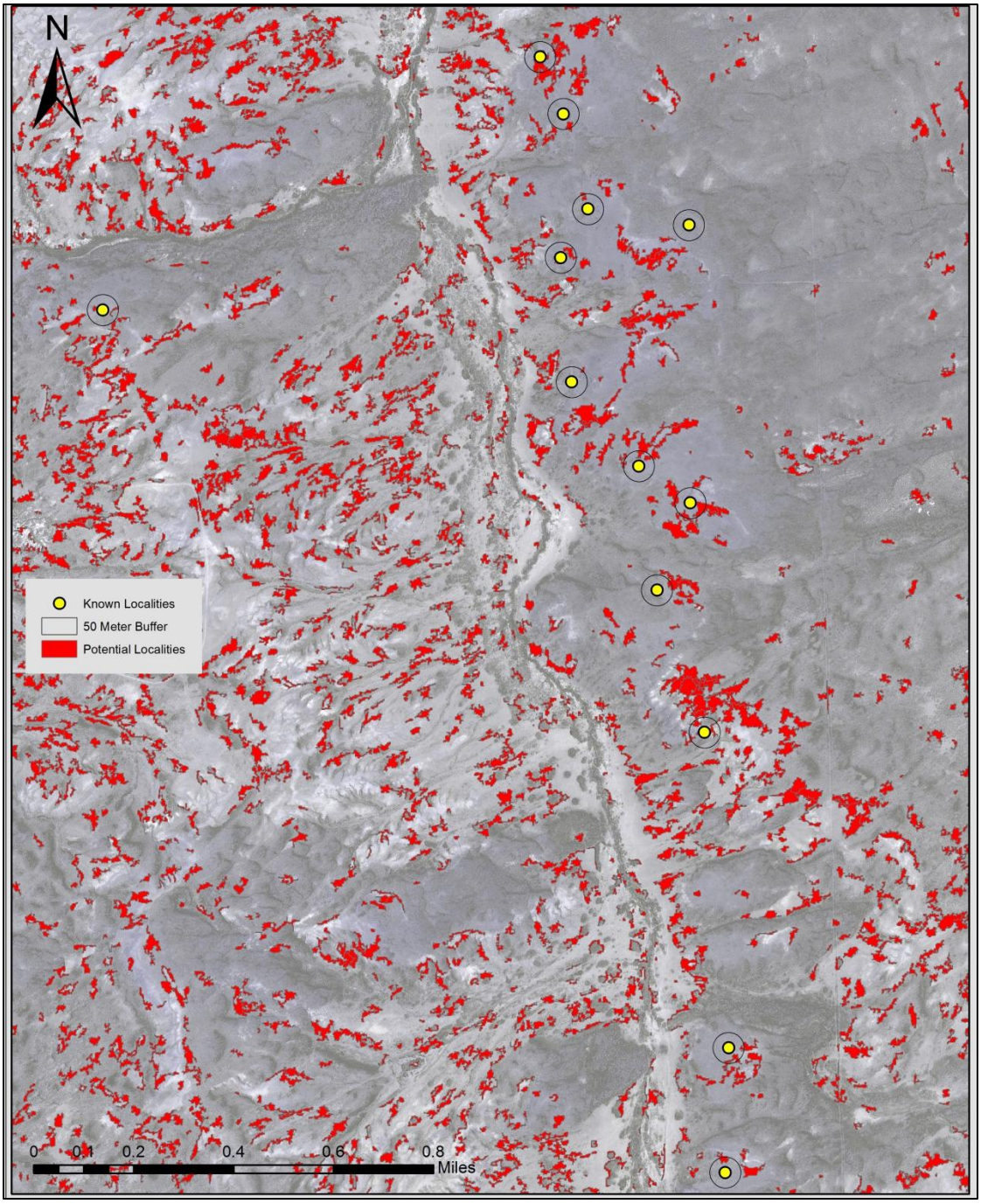

Figure 23. Salt Sage Draw Geobia Potential Localities. 11 out of 12 localities were correctly classified.

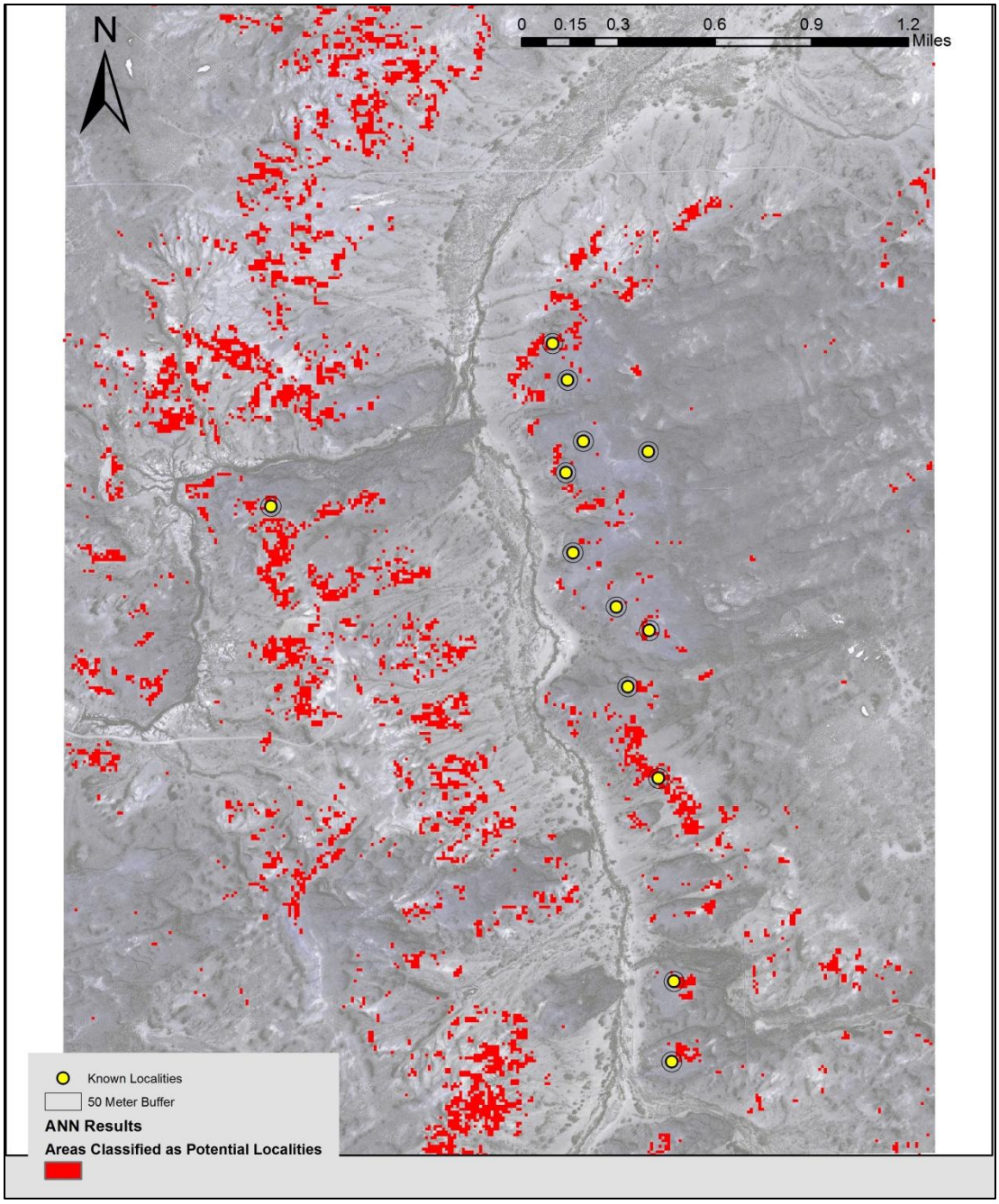

Figure 24. Salt Sage Draw ANN potential localities. This method accurately classified 9 out of 12 fossil localities.

CHAPTER V

RESULTS

This thesis was designed to predict areas of the landscape in the GDB that are potentially fossiliferous. The predictions were tested (ground-truthed) in the field during the 2013 field season. The maps that were created in ArcMap (refer to figures 19 through 22) were exported into ArcPad and then loaded onto three Topcon GRS-1 GPS receivers. These ArcPad maps included the four classified segmentation levels, a road map, geology map, the satellite image, a point feature of known fossil localities, and finally a point feature of the selected survey points. These GPS receivers were then used in the field to navigate to selected survey points. Any fossil localities found in the field were recorded in the map with a new, sequentially numbered point feature that included information such as: latitude and longitude coordinates, date, and a brief description of the types of fossils recovered. The segmentation level three and four classified image objects were the most appropriate for display on the maps and were primarily used to determine if particular locations in the field were within a predicted image object.

Five satellite images were surveyed during field work. They will be discussed in the sequential order in which they were surveyed. The first area worked in was the area labeled I-80, because of the presence of Interstate 80 running east-west through the image. The next area that will be discussed is the Tipton North and South images. After that is the Bitter Creek Road image followed by the Pinnacles and Freighter Gap area (refer to figure 11). A summary of the results of the field work will conclude this chapter.

I-80 Area

The I-80 image lies in the south central area of the Great Divide Basin. Interstate-80 crosses the image in an east-west path through the northern portion of the image. The image extends to the south to the Laney Rim, which is the southern border of the Basin in this area (see figures 20 and 25). This image was the most complex geologically (see figure 5). According to the geologic map, this area included several alternating inter-tongued geologic formations (Pipiringos, 1962). The areas of interest to us, which are of the correct geologic age, are the mapped units of the Wasatch Formation, the main body, the Niland tongue, and the Cathedral Bluffs Member. These units were oriented roughly east-west and alternated with the Green River formations (such as the Laney, Tipton and Luman tongues). Of primary interest were the Niland tongue and main body of the Wasatch formation, which are both of early Eocene age and are fluvial deposits and potentially fossiliferous. Refer to figure 25, which depicts the overall survey results in the I-80 image.

The first survey point navigated to on this image was SP-10 in the southeast portion of the image (see figure 26). This area is in the Cathedral Bluffs unit, which historically is not particularly fossiliferous in southwest Wyoming (Pipiringos, 1962; Honey, 1988). This location was a sandstone outcrop north of the Laney Rim and contained reptilian fossils, such as crocodile and turtle, as well as mammal fossils like the condylarth *Meniscotherium*. Other fossils typical of the Wasatchian NALMA were recovered from this location, which was labeled point 901 and named Bryan's Folly.

This locality is significant because fossils were recovered from geology that is typically non-fossiliferous.

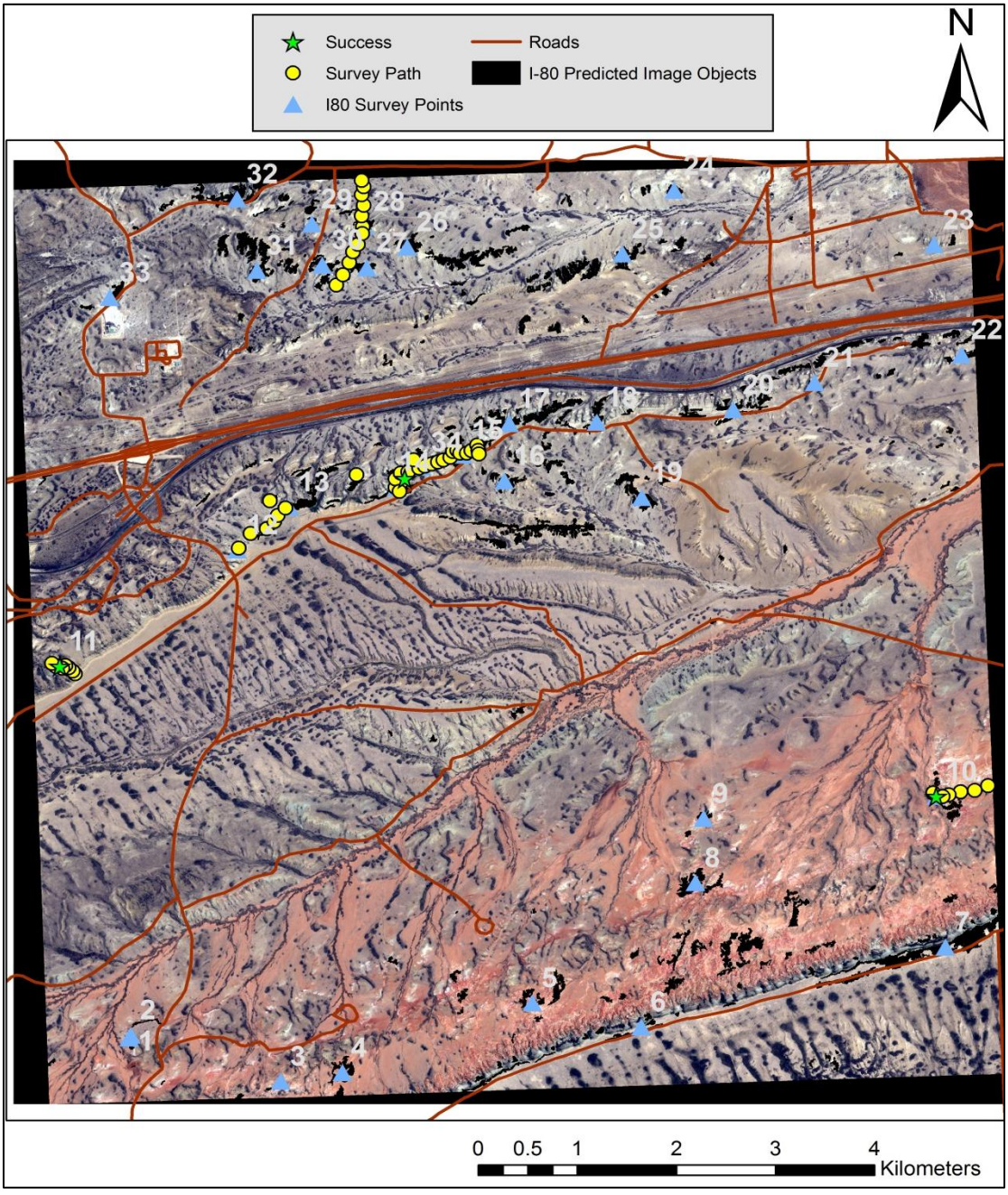

Figure 25. I-80 image survey results.

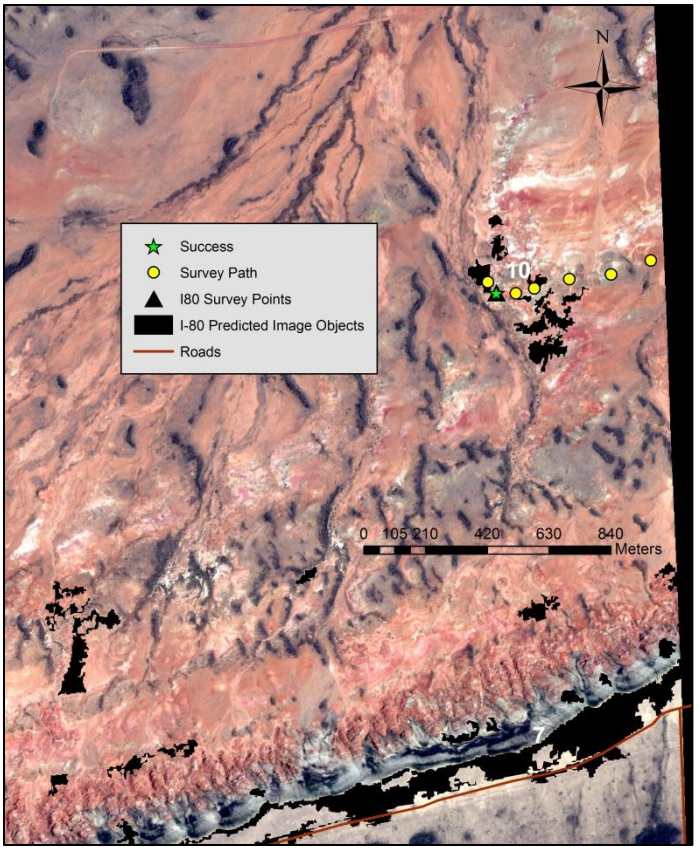

Figure 26. I-80 image survey, SP-10.

The next area surveyed was along an east-west ridgeline south of the Interstate that was believed to be part of the Niland tongue (see figure 27). The vicinity of SP-12 and SP-13 were surveyed without success. The ridgeline was composed primarily of mudstone and claystone. At SP-11, further to the west, some reptilian fossils, primarily turtle, were recovered from the mudstone and claystone slopes there. The next area surveyed was in the vicinity of SP-14, 15, and 34. Nothing was recovered from the area of SP-14 and only a small scatter of reptilian fossils was recovered from the vicinity of SP-15.

The lack of success in recovering mammalian fossils in this area is believed to be due to inaccuracies in the geologic mapping of this area. The geologic map indicates

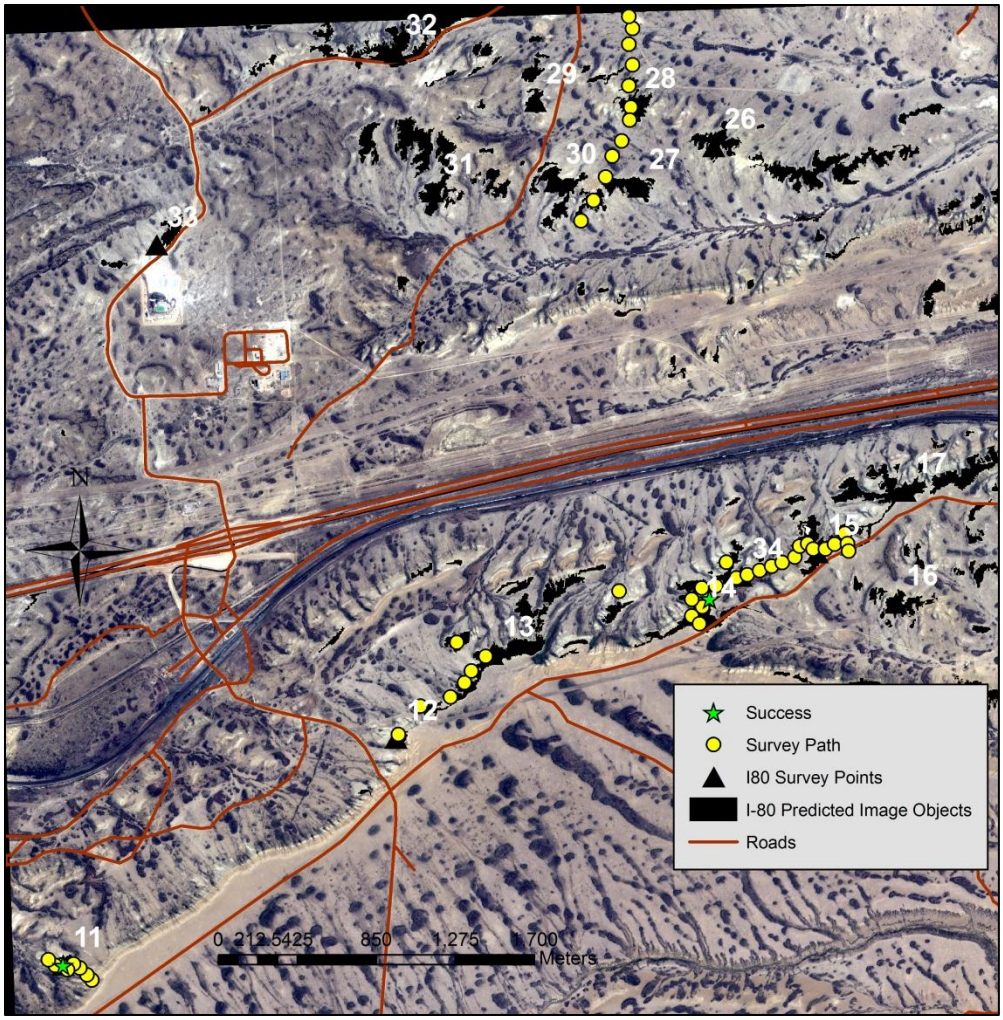

Figure 27. I-80 image survey, Northwest.

that this area is part of the Niland tongue, however, it appears that large portions of this area is actually part of the Tipton tongue of the Green River formation, an unlikely place to find mammalian fossils due to the lacustrine nature of these beds.

The last area of this image that was surveyed was in the north portion of the image in the vicinity of SP-27, 28, and 30. A path was surveyed directly between SP-27 and 30 while the predicted image object at SP-28 was more thoroughly surveyed. This

area consisted of claystone and mudstone outcrops that were found to not contain any fossils.

Tipton South and North Areas

The next area that was surveyed was the Tipton South area (see figure 28). This image lies on the edge of the Red Desert, as can be seen in the south west corner of the image. The geology within this image is mapped as being entirely main body of the Wasatch formation. This area is predominantly flat with only small areas with any kind of slope, with more topography to the north. This resulted in very few predicted image objects in this image and only in small clusters. The first area surveyed was in the vicinity of SP-2, 3, and 4. This area was briefly examined and found to consist primarily of mudstone and claystone and no fossils were recovered from this area. Following this, the vicinity of SP-6 and 7 was also briefly examined and determined to be unsuitable locations for extensive ground survey. The southern portions of this area were too flat and did not contain the kinds of weathered outcrops that are conducive to fossil recovery.

The next area surveyed in the Tipton South area was in the north of the image where there was more significant topography. The areas of SP-13, 14, and 15 were surveyed extensively (see figure 29). This area was composed of primarily sandy siltstones. The predicted image objects around SP-13 and 14 were found to be sterile of fossils. A small reptile scatter was found approximately 90 meters due west of SP-15.

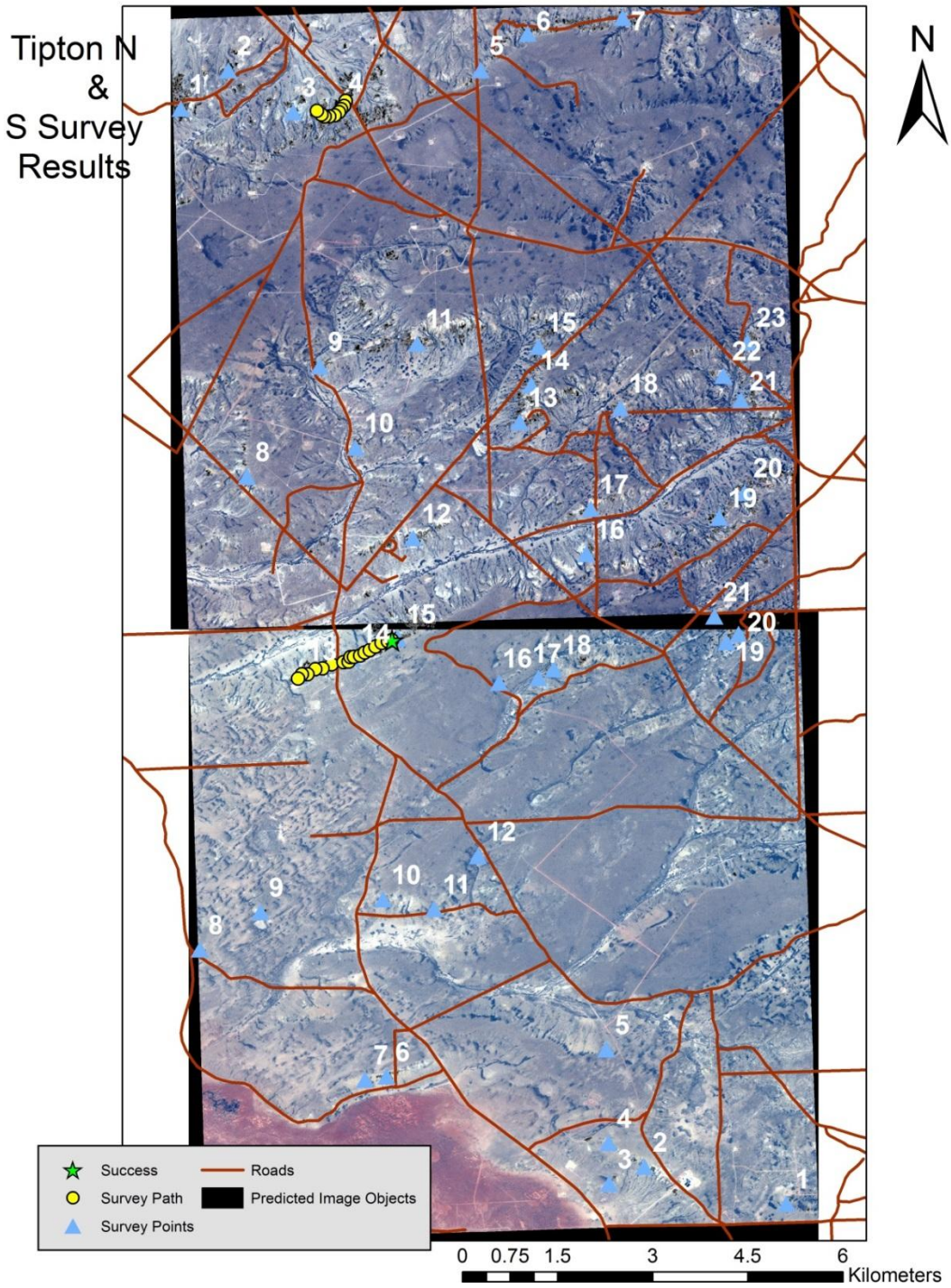

Figure 28. Tipton North and South images survey results.

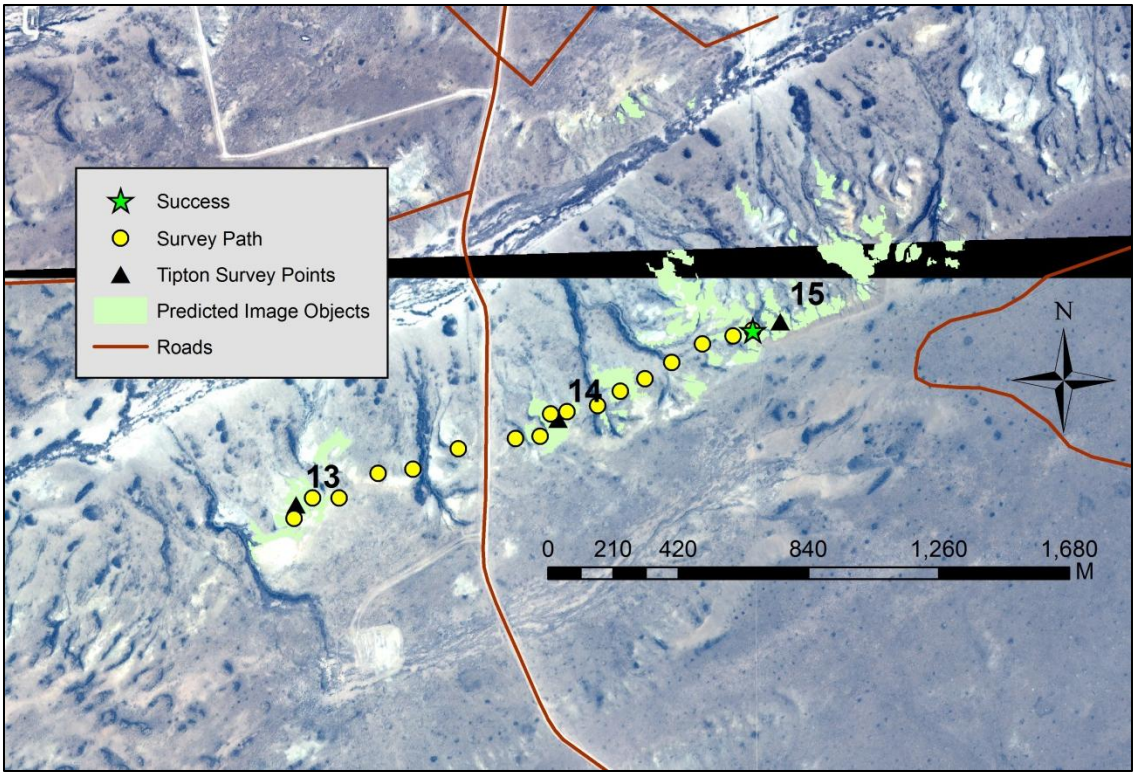

Figure 29. Tipton South image survey, SP-13, 14, 15.

Later in the field season a limited amount of time was spent in the Tipton North area. Due to limited success in the Tipton South area, less time was allocated to extensive ground survey in this area. In the northern portion of the image, the vicinity of SP-4 and predicted image objects west of this location were ground surveyed (see figure 30). This area consisted of claystone and mudstone outcrops and was devoid of fossils. The areas around SP-9 and 10 were briefly examined and determined to be unsuitable locations for further survey due to the limited slope and predominance of claystone/mudstone in these areas.

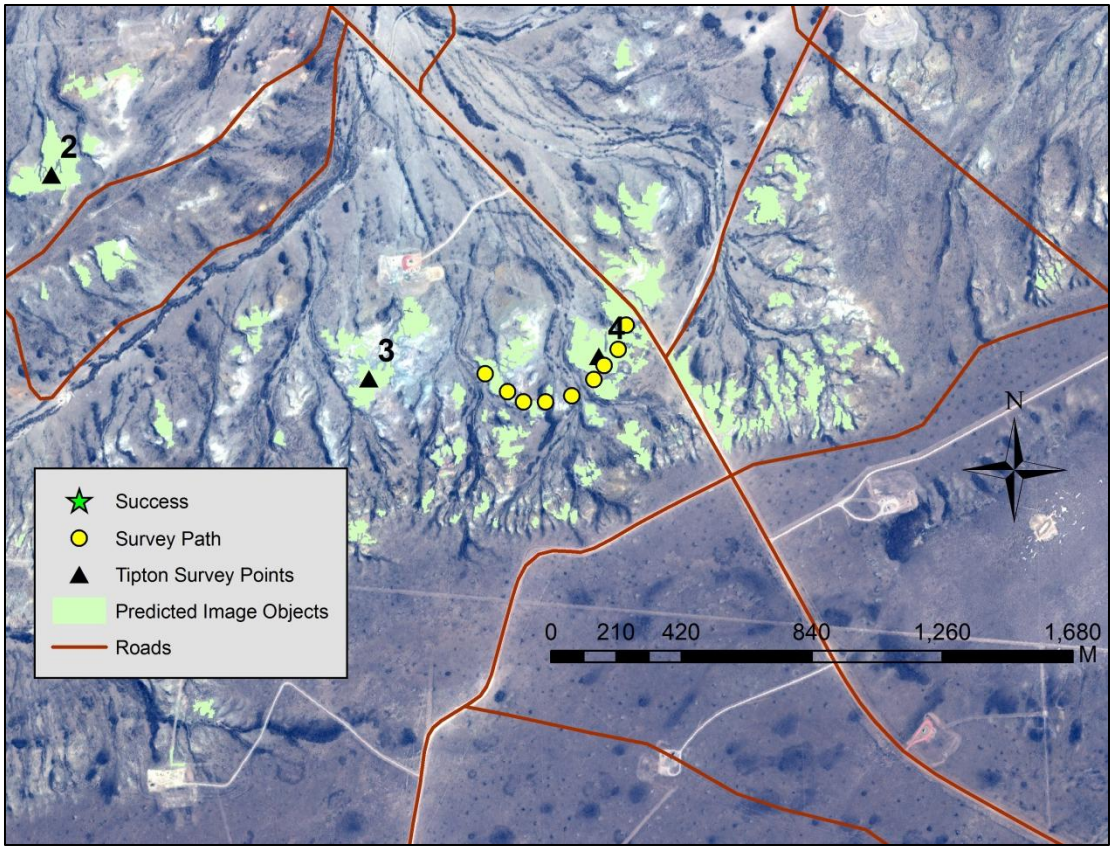

Figure 30. Tipton North image survey, SP-4.

Bitter Creek Road Area

The area of Bitter Creek Road was the next location to be surveyed. Only two locations were surveyed in this image due to time constraints and the fact that this area has been heavily surveyed in past seasons. The first location was in the southwest of the image. This area is not within the boundary of the GDB, and is mapped geologically as the Fort Union Formation of Paleocene age (see figures 4 and 5). Figure 31 shows details of the ground survey performed in the southern portion of Bitter Creek Road. The area around SP-22 was surveyed extensively and consisted of primarily mudstone and

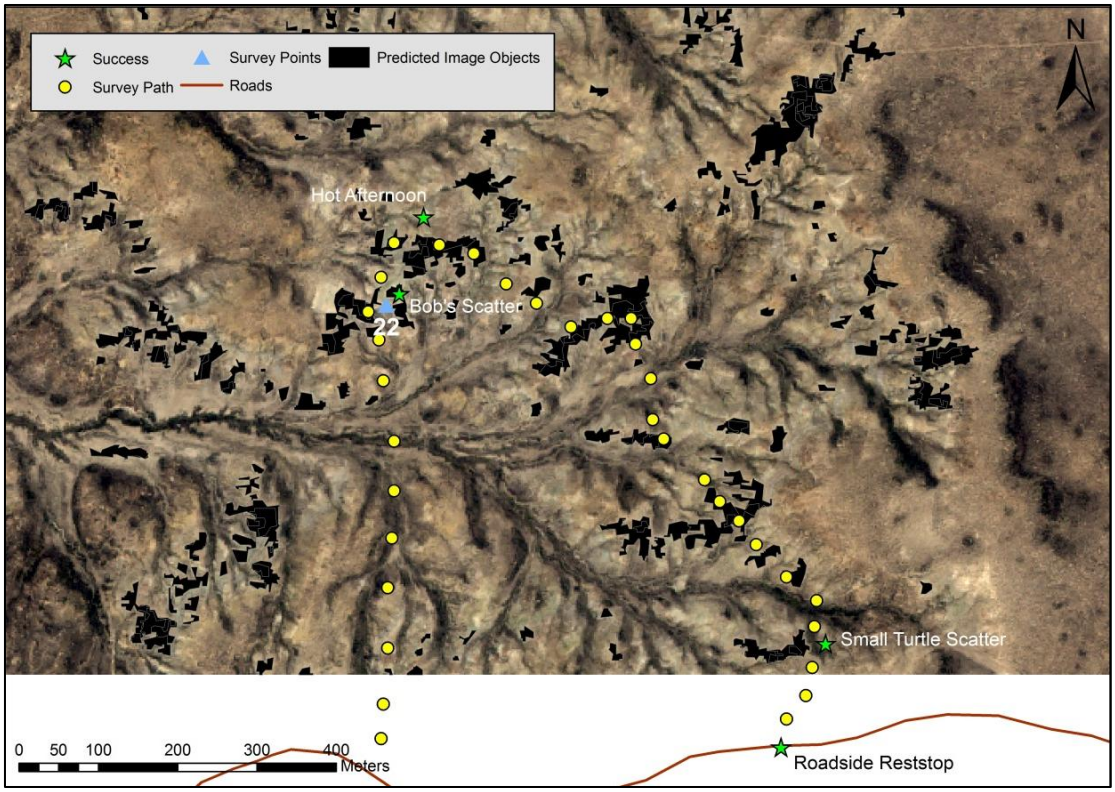

Figure 31. Bitter Creek Road South survey results.

claystone outcrops. The survey path took a horseshoe pattern, travelling from the road due north to SP-22 then further north before turning east and then south-east and heading back to the road. Two new localities were recorded in the vicinity of SP-22. These were point 909, 'Bob's Scatter' and 910, 'Hot Afternoon'. At both of these locations reptilian fossils were recovered, with point 909 consisting of crocodile fossils.

The survey path continued to the south across several more predicted image objects. A small scatter of turtle shell fossils were recovered near the edge of the image and were marked as point 911. As the survey team continued back to the road, a large scatter was located directly north of the road. This point is just south of the edge of the RS image and can therefore not be considered a success for this methodology. This

scatter contained a large number of fossils, including mammal and primate (possibly Plesiadapiform) fossils. This discovery is interesting for two reasons. The first is that fossils are difficult to locate within areas of Paleocene geology (Fort Union Formation) and primate fossils are rare. Even the reptilian fossils recovered from this area are potentially significant. The second reason is that the locality was directly next to the road, which questions the concept of road classification for exclusion adopted in this research.

After completing survey in the southern area of the image the team moved to the northern portion. Ground survey was completed in the vicinity of SP-5 (see figure 21). The area north east of the road was examined and found that it had recently been disturbed by pipeline construction, which would decrease the possibility of locating fossils, therefore, we surveyed to the south (see figure 32). The predicted image objects around SP-5 consisted of significant sandstone outcrops along the northeast-southwest oriented ridgeline. These sandstone outcrops are typical of what paleontologists look for while searching for fossils in this region. These sandstone outcrops, however, were sterile of fossils.

Pinnacles and Freighter Gap Area

The Pinnacles and Freighter Gap area was surveyed the most heavily during the 2013 field season and with the most success. Figure 33 shows details of survey results for the entire Pinnacles and Freighter Gap area. This area covers the largest areal extent,

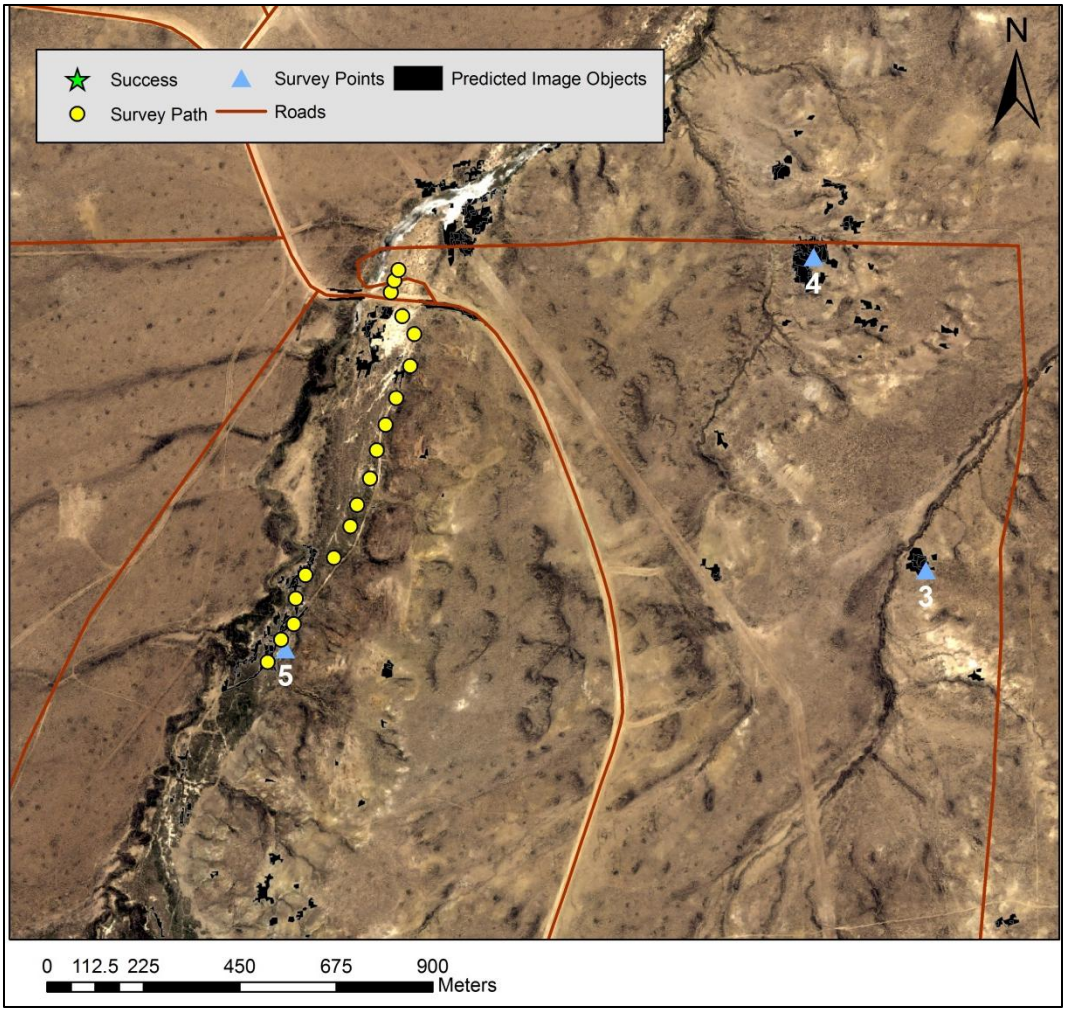

Figure 32. Bitter Creek Road North survey results.

and has a large number of known fossil localities but also contains many locations that had not been surveyed. The first area that was surveyed was in the vicinity of the known fossil localities, Lightning Park and FG-165 (see figure 34). The survey path followed a large east-west oriented ridgeline to the west of these locations before turning north and surveying the area to the south of SP-5. The team then moved east toward several small sandstone outcrops, which turned out to be sterile, prior to returning to the starting point. A small scatter of mammal teeth was recovered at point 916 and an isolated reptile jaw was found at point 915.

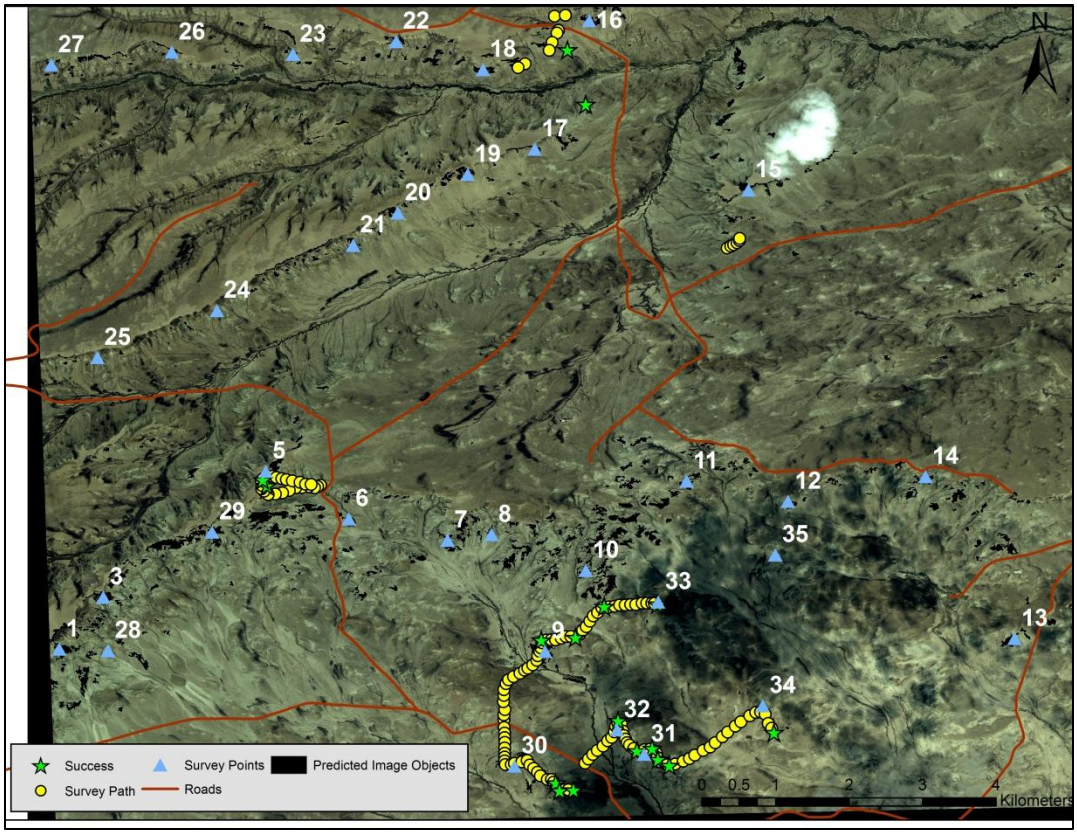

Figure 33. Pinnacles and Freighter Gap survey results.

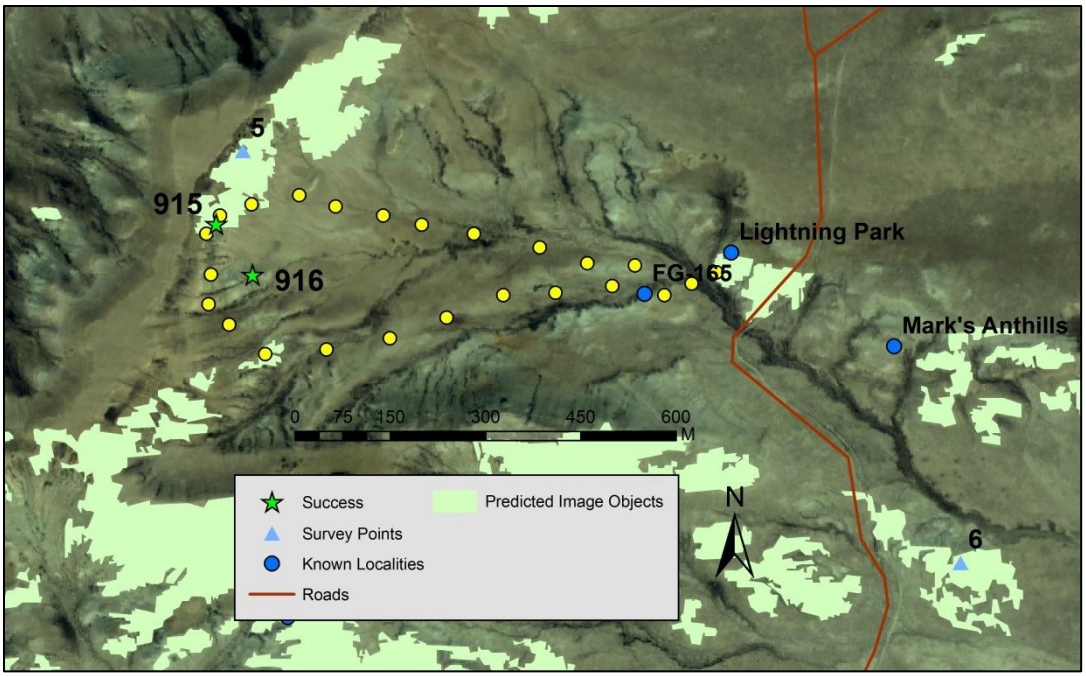

Figure 34. Pinnacles and Freighter Gap, SP-5.

The next area that was surveyed was in the southeast portion of the image. A highly productive locality was located, named 'Broke Duck SS', however, this locality was not predicted by the GEOBIA method. This locality contained a massive quantity of mammalian fossils, including primate jaws and teeth. This locality was within a line of sandstone outcrops running east-west approximately due north of a road (see figure 35) and was composed of dark red sandstone. This area of the image was excluded from the classification because of the dark red color of the sandstone.

The next area that was surveyed was to the east and north of 'Broke Duck SS', in the area of SP-9 (see figure 35). We surveyed the image objects to the south of SP-9, then moved along the western edge of the survey point and continued to the north. We discovered a productive locality at point 920, named 'Cactus', which contained a large number of reptilian and mammalian fossils. From this location there was a visible sandstone outcrop to the east. We moved to that location and discovered more fossils at point 931. This locality was named 'Balls' after the ball shaped stone formations covering the area. Fewer fossils were recovered from this location; however, a mammalian femur was uncovered here. This locality was just east of a predicted image object.

From the location of point 931 more sandstone outcrops were visible to the north east. We moved to that outcrop and found more fossils at point 932. This location, named 'Afternoon Spot', yielded a large number of turtle shell, gar spines, and some mammalian fossils. This locality was approximately 100 meters to the south of predicted image objects around survey point 10. More sandstone outcrops were visible to

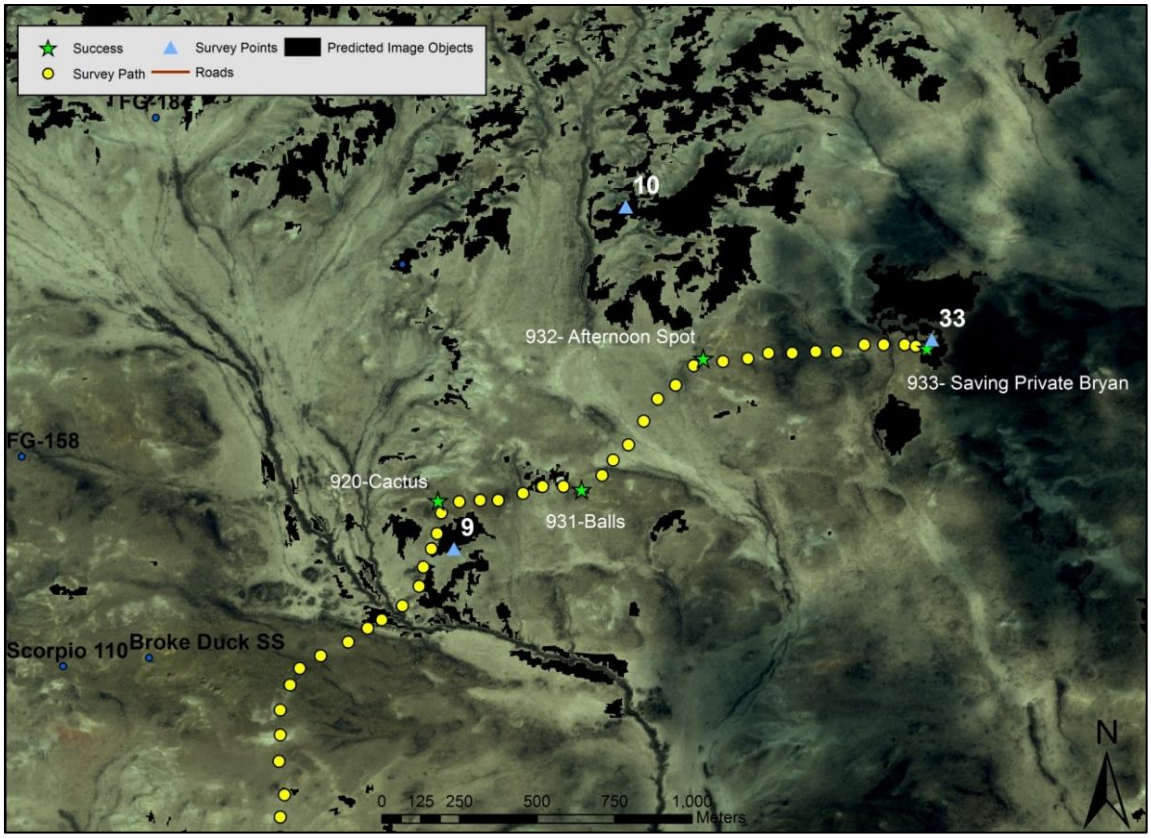

Figure 35. Pinnacles and Freighter Gap, SP-9, 10, 33.

the east from this location. We moved in that direction and discovered another locality at point 933, which corresponded precisely with the predicted image objects at SP-33. This locality yielded several mammal teeth and was named 'Saving Private Bryan'. Figure A32 in the Appendix details the vicinity of localities 931, 932, and 933.

The next area that was surveyed was south of the previous area surveyed, i.e. SP-9, 10, and 33 (see figure 36). The predicted image objects around survey point 30 were examined. A path was surveyed due south from the road and covered the predicted areas around SP-30, as well as the predicted ridgeline to the east. The survey team continued to the east and discovered a series of large sandstone bowls that corresponded with predicted image objects to the east. Fossils were recovered from points 934, 935, and

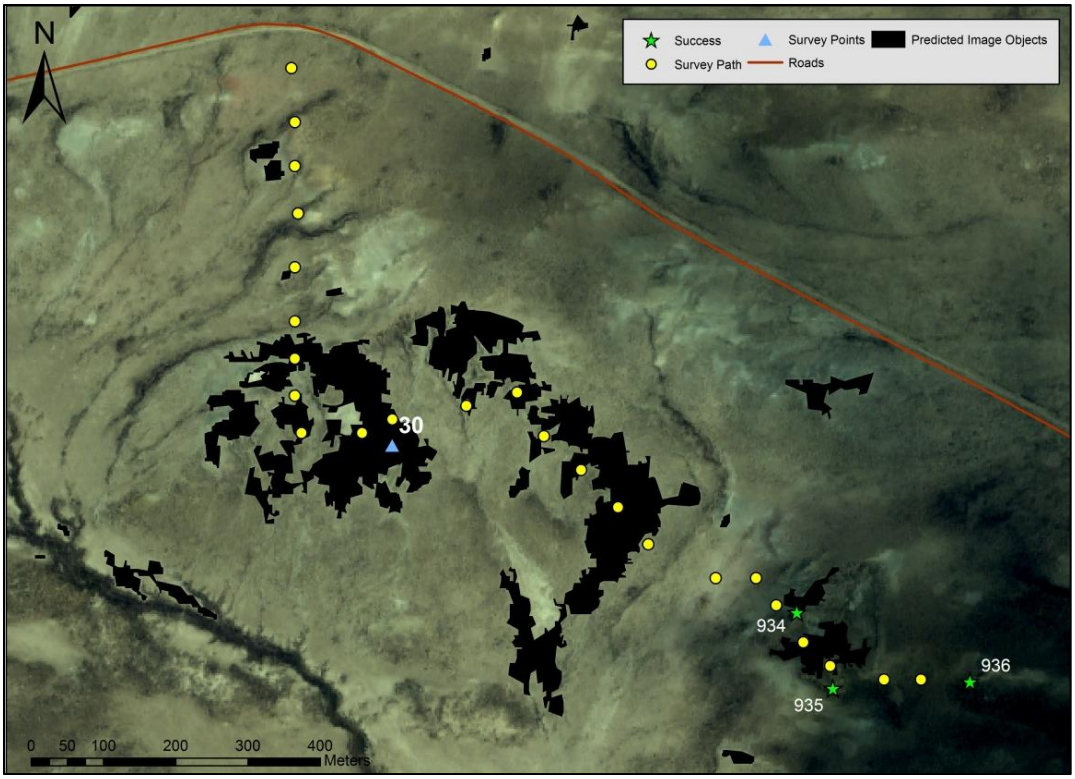

Figure 36. Pinnacles and Freighter Gap, SP-30.

936. The points recorded at 934 and 935 were both contained within a single sandstone bowl and yielded reptilian and mammalian fossils. This locality was collectively named 'Eagle Bowl'. The survey continued to the east to another sandstone bowl formation that did not correspond with a predicted image object. At point 936 more fossils were recovered from an area of anthills, including a large number of mammal teeth.

The survey team then moved to the northeast from point 936 and continued to SP-32 (see figure 37). The predicted image objects at SP-32 and to the south east to SP-31 were extensively surveyed. Fossils were recovered from point 940, 'Fish Hill', in the vicinity of SP-32 and included a large number of turtle fossils as well as some mammalian fossils. Near SP-31 there were four recorded points where fossils were

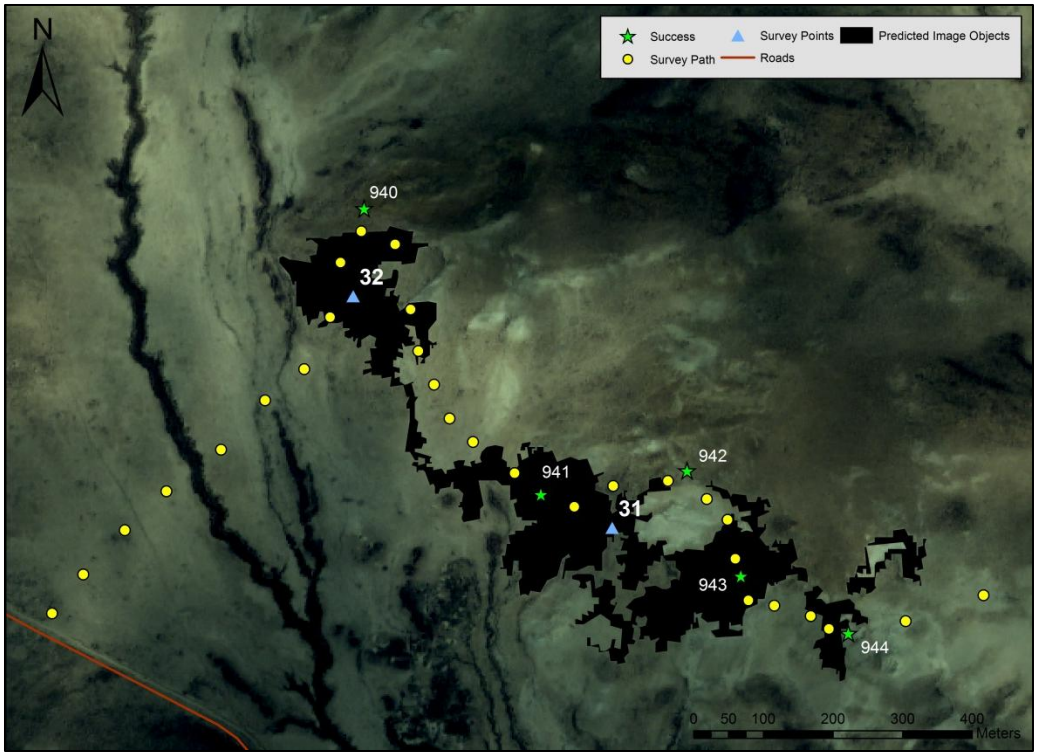

Figure 37. Pinnacles and Freighter Gap, SP-31 and 32.

recovered: 941, 942, 943, and 944. At point 941 a single mammal jaw was recovered. At point 942 more mammal fossils were found. Continuing to the south east, more mammalian fossils were recovered from points 943 and 944. The team continued to the north and east to SP-34 (see figure 38) and surveyed the predicted image objects to the south of that point. A single mammal jaw was recovered from point 945.

After heavily surveying in the south east portion of the area, the team moved to the north-west area of the RS image in an area known as Alkali Draw (see figure 39). Several predicted image objects were surveyed to the west of SP-16. These locations consisted of primarily claystone and mudstone, no sandstone, and did not contain any fossils.

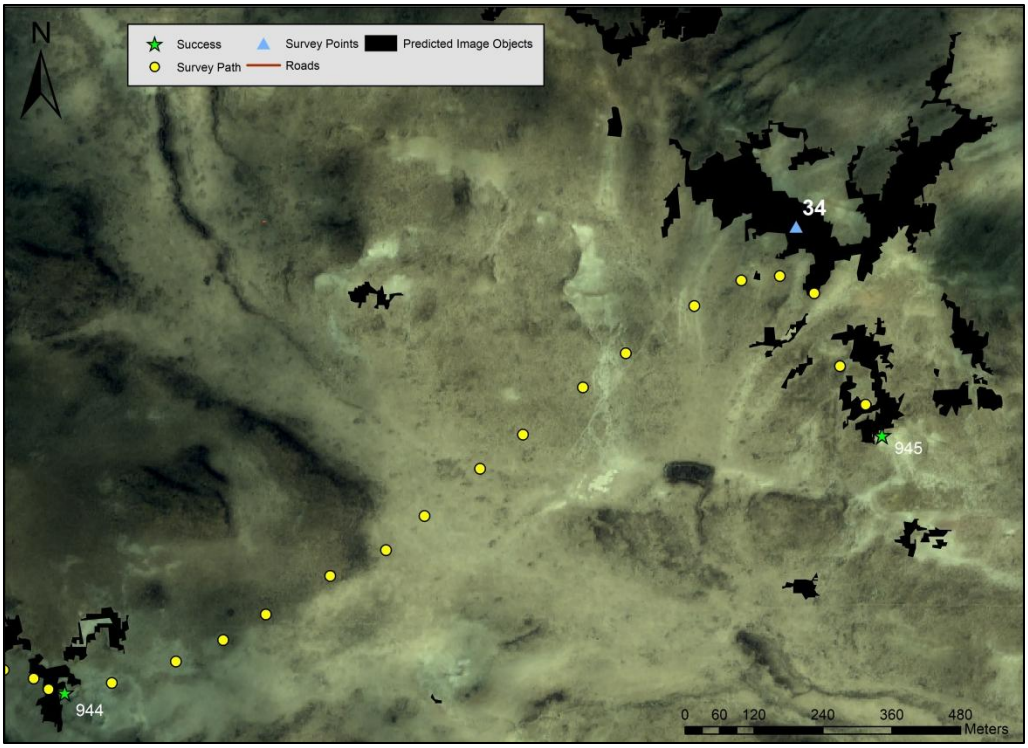

Figure 38. Pinnacles and Freighter Gap, SP-34.

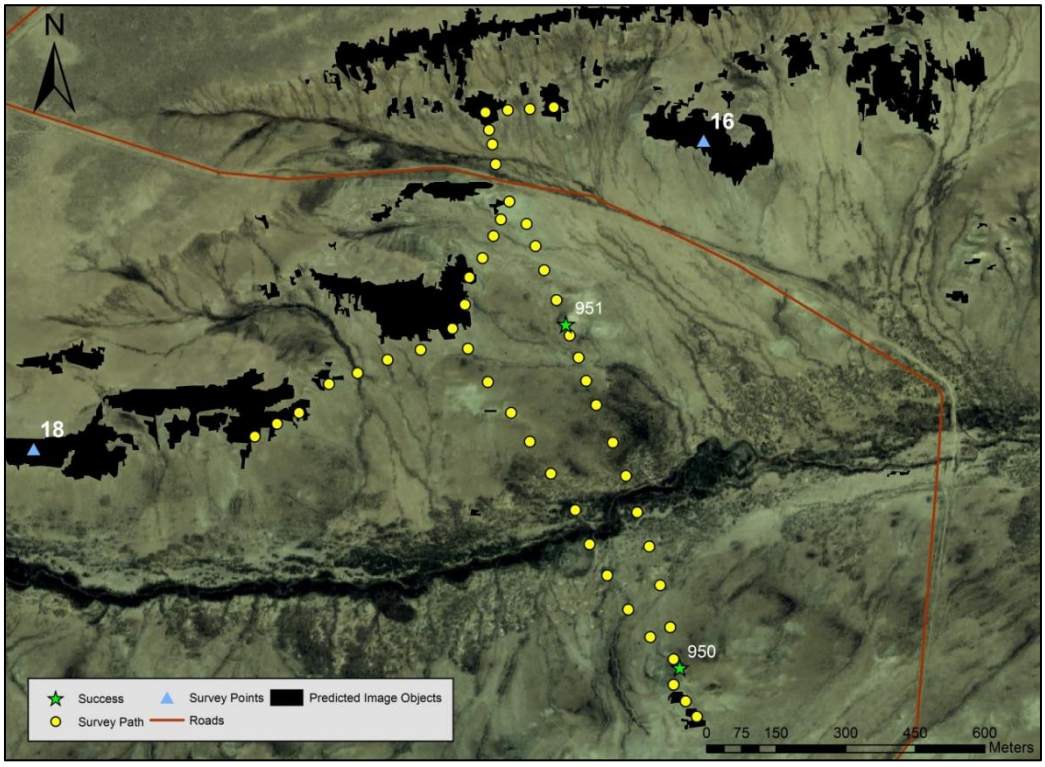

Figure 39. Pinnacles and Freighter Gap, SP-16 and 18.

The team moved to the south and surveyed several predicted image objects south of the road and continuing to the west toward SP-18. Similar geology was found here and no fossils were recovered. A prominent sandstone feature was visible to the south and the team moved there and found mammal fossils at point 950, named 'Pyramid'. The sandstone outcrop here corresponded with the small predicted image objects due south of point 950, however, the bulk of the fossils were recovered from the northern slope of this outcrop, where the GPS coordinates were recorded. On the trip back to the road, another fossil locality was discovered in a relatively flat area marked as point 951. Mammal fossils were recovered from this location, which is interesting because the locality is in a completely flat area.

Summary of Results

In summation, a total of 31 survey points in five different satellite images were surveyed during the course of the field season (see table 7). In the I-80 area, ten survey points were covered and three of these locations yielded fossils. Two were primarily reptile scatters while the third contained mammal fossils. The Tipton North and South images were not very productive. Tipton North had three survey points examined with no success. The Tipton South area had eight locations surveyed with only one location yielding a small reptile scatter. The Bitter Creek Road area had two locations surveyed with one yielding fossils. Finally, the Pinnacles and Freighter Gap area had eight survey points covered with all eight yielding fossils. Some of the survey points in the Pinnacles and Freighter Gap area yielded more than one new fossil locality (i.e. discrete GPS

coordinates of where fossils were recovered). A total of thirteen of the survey points yielded fossils giving a success rate of approximately 42%. A total of 22 new fossil localities were documented.

Table 7

Overall results of field work in GDB

Image Area	Points Surveyed	Successes	New Localities
I-80	10	3	3
Tipton South	8	1	1
Tipton North	3	0	0
Bitter Creek Road	2	1	1
Pinnacles and Freighter Gap	8	8	17
Totals	31	13	22

CHAPTER VI

CONCLUSIONS

Interpretation of Results

The primary goal of the survey work performed in the Great Divide Basin was the recovery of Eocene vertebrate fossils. Of particular interest were mammalian fossils, specifically primates (such as adapids and omomyids). Over the past twenty years of field work in this area, it has been recognized that sandstone outcrops are highly likely locations to contain mammalian and primate fossils (Emerson & Anemone, 2012). The goal of this predictive model is to recognize these potentially fossiliferous locations remotely and pinpoint them within the landscape. Survey teams can then be guided to locations in the landscape that possibly have been overlooked during previous field seasons. The overall success rate of this method, approximately 42%, is a moderate success. The location of 22 new fossil localities (17 of which were found near the 8 survey points in the Pinnacles and Freighter Gap area) is a success for this method. The classification scheme of this method is rather simplistic but refinement of this will increase the accuracy, and subsequent success, of this methodology.

Previous methods of survey relied on visual inspection of topographic and geologic maps to locate areas of interest. The survey team would then travel to these areas and physically search for visible sandstone outcrops, which were relatively close to roads. By using a RS method, locations that are further away from the road network, or possibly not visible from the road, can be located and survey teams can navigate to them.

By focusing survey work to areas that have been analyzed by this methodology and found to be probable of being fossiliferous, time can be used more efficiently in the field. The survey results of this research have shown that this methodology is capable of locating sandstone outcrops in the landscape, and is adept at locating locations that are not visible from nearby roads. The survey work done in the northern portion of the Bitter Creek Road area (vicinity of SP-5, see figure 21) located a string of sandstone outcrops which were, unfortunately, non-fossiliferous. The southern portion of Bitter Creek Road (see figure 20) is on the border between Paleocene and Eocene geology and is therefore less likely to be productively prospected due to uncertainties in the geologic maps. Work done in the Pinnacles and Freighter Gap area (see figures 22 through 27) located several locations of sandstone outcrops that were fossiliferous. The most important aspect of these successes is that these outcrops were not visible from the road, and using typical survey techniques, would be overlooked.

Another aspect of this methodology that can be considered a success is the location of fossils in areas of geology in which fossils are rarely found. Survey work was performed in the Cathedral Bluffs tongue of the Wasatch formation in the I-80 area (see figures 4, 25, 26) and fossils were recovered. Past paleontological work has found this tongue to be particularly non-fossiliferous (Pipiringos, 1962); therefore, survey may not have otherwise been performed in this area. Another example of this is the survey performed in the southern portion of the Bitter Creek Road area (see figure 31). This area consists of Fort Union formation geology (late Paleocene) and fossils are rarely found in this geology. Fossils were recovered from the Fort Union formation while surveying this area. This methodology led the survey team to areas of geology that are

not considered to be productive for fossil recovery, and fossils were recovered from these locations.

Potential Issues

There are some issues that have come to light in the execution of this research. The first of these is that the classification method relies solely on the mean brightness of the image objects to classify the sandstone outcrops. This is a rather simplistic method that doesn't take full advantage of the spectral signature of the image. The result of this is that there were quite a few 'false positives' in the classification. Many areas that were surveyed were found to consist primarily of claystones and mudstone, as opposed to sandstones. Also, there was some over-prediction of sandstone outcrops in the image. Incorporating other aspects of the spectral signature of the image objects may decrease the over-prediction and subsequent false positives in the classification.

The second issue with this methodology is the appropriateness of the landscape characteristics, and the particular parameters used, in the classification method. Survey work has resulted in particular aspects of the classification coming into question. Roads were classified in the image for the purpose of exclusion. While surveying the southern portion of the Bitter Creek Road area (see figure 31), a highly productive fossil locality (Roadside Reststop) was found directly next to a dirt road. The second example of road proximity is Tim's Confession, the highly productive fossil locality used to determine parameters for classification, has a dirt road that runs directly into the fossiliferous sandstone outcrops there. While the road classification was intended to extract only the

road itself, there is a possibility that potentially fossiliferous locations next to roads may be inadvertently excluded.

Another aspect of the classification scheme that has come into question is the appropriateness of the slope parameter of greater than six percent slope. Areas of the I-80 image, particularly in the Cathedral Bluffs tongue along Laney Rim, were predicted as potentially fossiliferous, however, they were part of an extremely steep slope and high elevation. These locations would be impractical to survey as a near vertical climb would be involved. An upper threshold of slope would need to be incorporated to exclude these kinds of areas. The second issue with slope is that areas of relative flat terrain were pinpointed as potentially fossiliferous. The majority of the Tipton North and South images were flat and only small areas were pinpointed based on slope values barely above the six percent threshold. Adjusting the slope parameters slightly upward and limiting the percent slope to an upper threshold would correct these two issues. However, there was one fossil locality discovered that shows that flat areas and low slope do not preclude the existence of fossils. While prospecting in the northern portion of the Pinnacles and Freighter Gap area (see figure 39), a new fossil locality was discovered in a completely flat area. This shows that, while steep slope is typically sought out in surveying for fossils, it does not mean that areas of low slope do not contain fossils.

The geology of the landscape is one of the most important indicators for fossils. Eocene fossils are only found in Eocene deposits and mammalian fossils are found almost exclusively in Wasatch formation geology. Searching for these geologic formations on the landscape can only be as accurate as the geologic maps that are available. Inaccuracies in the geologic maps will result in inaccuracies in the model.

This was found to be the case while surveying the Niland tongue, of the Wasatch formation, found in the I-80 area (see figures 25, 26, 27). It was found that this area was most likely part of the Tipton tongue of the Green River formation. This was based on the fact that the sedimentary deposits and fossils found here were more indicative of a lacustrine depositional environment. A second aspect of inaccuracies in geologic maps is the fact that Tim's Confession is mapped as Quarternary sand. These younger sand deposits were obviously deposited, probably by wind, over Eocene bedrock. The geology underlying these sand deposits is impossible to ascertain, therefore, either all Quarternary sand deposits should be included in the predictive model, which would potentially increase over-prediction, or should be excluded, which also has its detriments.

Future Work

Several modifications and improvements to this methodology would greatly enhance the accuracy and utility of this model. The first would be to use a supervised classification algorithm, such as the Nearest Neighbor functionality of the eCognition software, as opposed to the simple Boolean classifiers. Using a supervised method would allow Tim's Confession to be used as a training site to establish a more complex example of the spectral characteristics of a fossil locality. Training sites for other aspects of the landscape could be established and the images could be classified based on the entire spectral response patterns of the image objects, as opposed to only the mean brightness of the image objects. This would minimize the over-prediction of sandstone outcrops in the images and would decrease the number of false positives in the classification.

Incorporation of distinct spectral response patterns collected by a spectroradiometer for a variety of land cover classes would also improve that accuracy of this model. Another improvement that could be incorporated is a more robust ground truthing of the resulting classification. In this research, only the areas of the landscape that were classified as being potentially fossiliferous were surveyed due to time constraints. A better ground truthing would examine areas of the landscape that were classified as other classes, such as vegetation and roads, to determine the overall accuracy of the classification.

An updated and refined geologic survey of the GDB would greatly improve the accuracy of this predictive model. Corrections to the complicated inter-tonguing portions of the GDB would greatly increase the accuracy of any predictions made. A re-evaluation of the slope parameters of the model would also refine the model. Areas of extremely high slope or of relativly low slope (just above 6%) could be excluded to decrease the sheer number of predicted image objects. Another improvement would be to increase the spatial resolution of the imagery used. The Worldview 2 and Quickbird 2 imagery used here had a spatial resolution of 2 meters, however, a pan-sharpening technique, such as Principle Components Analysis, could be used with the pan-chromatic band for this imagery to refine the resolution down to 0.5 meters.

The visibility of sandstone outcrops is an important aspect of this research. In order to assess visibility, a viewshed analysis could be incorporated in future work. This would require a much more accurate road network to be developed as the majority of the dirt roads in the area are not accurately mapped, or mapped at all. A series of viewshed analyses from points on the road network could be accomplished in areas of the GDB to determine potentially fossiliferous sandstone outcrops that are not visible from the road.

This research has shown that the GEOBIA methodology of analyzing high resolution RS imagery has great potential for guiding paleontological and paleoanthropological survey in the field. The methodology developed here is a fairly simple segmentation and classification scheme that was shown to have moderate success in locating fossils in the field. With further refinement of this methodology, more accurate predictive models can be developed and the success rate of fossil recovery can be greatly increase. This will result in a saving of time and money while performing field work and will ultimately lead to the recovery of more fossils.

BIBLIOGRAPHY

Anemone, R., Conroy, G., & Emerson, C. (2011a). GIS and Paleoanthropology: Incorporating New Approaches From the Geospatial Sciences in the Analysis of Primate and Human Evolution. *Yearbook of Physical Anthropology*, *54*, 19-46.

Anemone, R., Conroy, G., & Emerson, C. (2011b). Finding Fossils in new Ways: An artificial neural network approach to predicting the location of productive fossil localities. *Evolutionary Anthropology*, *20*, 169-180.

Anemone, R., & Dirks, W. (2009). An anachronistic Clarkforkian mammal fauna from the Paleocene Fort Union Formation (Great Divide Basin, Wyoming, USA). *Geologica Acta*, *7*, (1-2), 113-124.

Aplin, P., & Smith, G. M. (2011). Introduction to object-based landscape analysis. *International Journal of Geographical Information Science*, 25(6), 869-875. doi:10.1080/13658816.2011.566570.

Asfaw, B., Ebinger, C., Harding, D., White, T., & WoldeGabriel, G. (1990). Space based imagery in paleoanthropological research: an Ethiopian example. *National Geographic Research*, *6*. 418–434.

Baatz, M., & Schäpe, A. (2000). Multiresolution segmentation- an optimisation approach for high quality multi-scale image segmentation. In J. Strobl, T. Blaschke, & G. Griesebner (Eds.), *Angewandte geographische informationsverarbeitung* (Vol. 12). Karlsruhe, Germany: herbert Wichman.

Bailey, G. N., Reynolds, S.C., & King, G. C. P. (2011). Landscapes of human evolution: models and methods of tectonic geomorphology and the reconstruction of hominin landscapes. *Journal of Human Evolution*, *60*. 257-280.

Beard, K. C. (1988). New notharctine primate fossils from the early Eocene of New Mexico and southern Wyoming and the Phylogeny of notharctinae. *American Journal of Physical Anthropology. 75*, 439-469.

Beard, K. C. (2008). The oldest North American primate and mammalian biogeography during the Paleocene-Eocene Thermal Maximum. *Proceedings of the National Academy of Sciences*. *105* (10). 3815-3818.

Beard, K. C., & Dawson, M. R. (2009). Early Wasatchian mammals of the Red Hot Local Fauna, Uppermost Tuscahoma Formation, Lauderdale County, Mississippi. *Annals of Carnegie Museum*, *78*(3). 193-243.

Beauvais, G. P., Keinath, D. A., Hernandez, P., Master, L., & Thurston, R. (2006). *Element Distribution Modeling: A primer, Version 2* [White paper]. Retrieved from www.natureserve.org/prodServices/pdf/EDM_white_paper_2.0.pdf

Belt, K., & Paxton, S. T. (2005). GIS as an aid to visualizing and mapping geology and rock properties in regions of subtle topography. *GSA Bulletin, 117*(1/2), 149-160. doi:10.1130/B25463.1.

Benz, U. C., Hofmann, P., Willhauck, G., Lingenfelder, I., & Heynen, M. (2004). Multi-resolution, object-oriented fuzzy analysis of remote sensing data for GIS-ready information. *ISPRS Journal of Photogrammetry & Remote Sensing, 58*, 239-258. doi:10.1016/j.isprsjprs.2003.10.002.

Bilotti, F., Shaw, J. H., & Brennan, P. A. (2000). Quantitative Structural Analysis with Stereoscopic Remote Sensing Imagery. *AAPG Bulletin, 84*(6), 727-740.

Blaschke, T. (2003). Continuity, complexity and change: A hierarchical Geoinformation-based approach to exploring patterns of change in a cultural landscape. In Ü. Mander & M. Antrop (Eds.): *Multifunctional Landscapes Vol. III: Continuity and Change. Advances in Ecological Sciences* (Vol. 16, pp. 33-54). Boston, MA: WIT Press.

Blaschke, T. (2005). Towards a framework for change detection based on image objects. In S. Erasmi, B. Cyffka, & M. Kappas (Eds.) *Remote Sensing & GIS for Environmental Studies*. (Vol. 113, pp. 1-9) Göttingen, Germany: Göttingen Geographische Abhandlungen.

Blaschke, T. (2010). Object based image analysis for remote sensing. *ISPRS Journal of Photogrammetry & Remote Sensing, 65*, 2-16. doi:10.1016/j.isprsjprs.2009.06.004

Blaschke, T., Lang, S., & Möller, M. (2005). Object-Based Analysis of Remote Sensing Data for Landscape Monitoring: Recent Developments. *12th Annual Symposium of Remote Sensing, Goiania, Brazil*, 2879-2885.

Blaschke, T., & Strobl, J. (2001). What's wrong with pixels? Some recent developments interfacing remote sensing and GIS. *GIS – Zeitschrift für Geoinformationssysteme, 14*(6), 12–17.

Bloch, J. I., & Gingerich, P. D. (1998). *Carpolestes simpsoni*, new species (Mammalia, proprimates) from the late Paleocene of the clarks fork basin, Wyoming. *Contributions from the museum of paleontology, The University of Michigan, 30*, (4), 131-162.

Boos, S., Hornung, S., Jung, P., & Müller, H. (2007). GIS as a tool for processing hybrid prospection data in landscape archaeology. *International Journal of Humanities and Arts Computing*, *1*(2), 137-149.

Bradley, W.H. (1925). A contribution to the origin of the Green River Formation and its oil shale. *American Association of Petroleum Geologists Bulletin*, *9*(2), 247-262.

Bradley, W. H. (1929). The varves and climate of the Green River epoch. *U.S. Geological Survey Professional Paper, 158-E*, 1-110.

Brandt, R., Groenewoudt, B. J., & Kvamme, K.L. (1992). An experiment in archaeological site location: Modeling in the Netherlands using GIS techniques. *World Archaeology*, *24*(2), 268-282.

Burger, B. J., & Honey, J. G. (2008). Plesiadapidae (Mammalia, Primates) from the late Paleocene fort union formation of the Piceance Creek Basin, Colorado. *Journal of Vertebrate Paleontology*, *28*(3), 816-825.

Burnett, C., & Blaschke, T. (2003). A multi-scale segmentation/object relationship modelling methodology for landscape analysis. *Ecological Modelling*, *168*, 233-249. doi:10.1016/S0304-3800(03)00139-X.

Canning, S. (2005). 'BELIEF' in the past: Dempster-Shafer theory, GIS and archaeological predictive modelling. *Australian Archaeology*, *60*, 6-15.

Carr, T. L., & Turner, M. (1996). Investigating regional lithic procurement using Mulit-spectral imagery and geophysical exploration. *Archaeological Prospection, 3*, 109-127.

Chen, G., & Hay, G. J. (2011). An airborne lidar sampling strategy to model forest canopy height from Quickbird imagery and GEOBIA. *Remote Sensing of Environment*, *115*, 1532-1542.

Chubey, M. S., Franklin, S. E., & Wulder, M. A. (2006). Object-based Analysis of Ikonos-2 Imagery for Extraction of Forest Inventory Parameters. *Photogrammetric Engineering & Remote Sensing*, *72*(4), 383-394.

Clark, C.D. (1997). Reconstructing the evolutionary dynamics of former ice sheets using multi-temporal evidence, remote sensing and GIS. *Quaternary Science Reviews*, *16*, 1067-1092.

Conroy, G. C. (2006). Creating, Displaying, and Querying Interactive Paleoanthropological Maps Using GIS: An Example from the Uinta Basin, Utah. *Evolutionary Anthropology*, *15*, 217-223. doi:10.1002/evan.20111.

Conroy, G. C., Emerson, C. W., Anemone, R.L., & Townsend, K. E. B. (2012). Let your fingers do the walking: A simple spectral signature model for "remote" fossil prospecting. *Journal of Human Evolution, 63*, 79-84.

Conroy, G. C, Anemone, R. L., Van Regenmorter, J., & Addison, A. (2008). Google Earth, GIS, and the Great Divide: A new and simple method for sharing paleontological data. *Journal of Human Evolution, 55*, 751-755.

Definiens Professional User Guide. (2006). Munich, Germany: Definiens AG.

Definiens Professional Reference Book. (2006). Munchen, Germany: Definiens AG.

eCognition Developer User Guide v8.8.2. (2013). Munchen, Germany: Definiens Imaging GmbH.

Emerson, C. W., & Anemone, R. L. (2012). An artificial neural network-based approach to identifying mammalian fossil localities in the Great Divide Basin, Wyoming. *Remote Sensing Letters*, *3*(5), 453-460.

Engler, R., Guisan, A., & Rechsteiner, L. (2004). An improved approach for predicting the distribution of rare and endangered species from occurrence and pseudo-absence data. *Journal of Applied Ecology*, *41*, 263-274.

Finke, P. A., Meylemans, E., & Van de Wauw, J. (2008). Mapping the possible occurrence of archaeological sites by Bayesian inference. *Journal of Archaeological Science, 35*, 2786-2796.

Fletcher, R., & Winter, R. (2008). Prospects and problems in applying GIS to the study of Chalcolithic archaeology in southern Israel. *Bulletin of the American Schools of Oriental Research*, *352*, 1-28.

Franklin, J. (1995). Predictive vegetation mapping: geographic modelling of biospatial patterns in relation to environmental gradients. *Progress in Physical Geography, 19*(4), 474-499.

Frohn, R. C. (2006). The use of landscape pattern metrics in remote sensing image classification. *International Journal of Remote Sensing*, *27*(10), 2025-2032. doi:10.1080/01431160500212229.

Gazin, C.L. (1952). The lower Eocene Knight Formation of western Wyoming and its mammalian faunas. *Smithsonian Miscellaneous Collections*, *117*, 1-82.

Gazin, C.L. (1962). A further study of the lower Eocene mammalian faunas of southwestern Wyoming. *Smithsonian Miscellaneous Collections*, *144*, 1-98.

Gazin, C.L. (1965). Early Eocene mammalian faunas and their environment in the vicinity of the Rock Springs Uplift, Wyoming. *Wyoming Geologic Association Guidebook, 19th Annual Field Conference*, 171-180.

Ghaffar, A. (2010). GIS and paleontology of Dhok Bun Ameer Khatoon fossil site, Pakistan. *Pakistan Journal of Science*, *62*(3), 163-167.

Giardino, M.J. (2011). A history of NASA remote sensing contributions to archaeology. *Journal of Archaeological Science, 38,* 2003-2009.

Gingerich, P. D. (1980) Evolutionary patterns in early Cenozoic mammals. *Annual Reviews of Earth and Planetary Sciences, 8,* 407-424.

Gingerich, P. D. (1983). Paleocene-Eocene faunal zones and a preliminary analysis of Laramide structural drformation in the Clark's Fork Basin, Wyoming. *Wyoming Geological Association Guidebook, 34th Annual Field Conference*, 185-195.

Gingerich, P. D. (1989) New earliest wasatchian mammalian fauna from the Eocene of northwestern Wyoming: composition and diversity in a rarely sampled high-floodplain assemblage. *University of Michigan papers on paleontology, 28*.

Gingerich, P. D. (1991) Systematics and evolution of early Eocene perissodactyla (mammalia) in the clarks fork basin, Wyoming. *Contributions from the Museum of Paleontology, The Univerisity of Michigan, 28*(8), 181-213.

Gingerich, P. D. (2001). Paleocene-Eocene Stratigraphy and Biotic Change in the Bighorn and Clarks Fork Basins, Wyoming. *University of Michigan Papers on Paleontology, 33*.

Gingerich, P. D. (2006) Environment and evolution through the Paleocene-eocene thermal maximum. *Trends in Ecology and Evolution, 21*(5), 246-253.

Gingerich, P. D., & Smith, T. (2006) Paleocene-Eocene land mammals from three new latest clarkforkian and earliest wasatchian wash sites at polecat bench in the northern bighorn basin, Wyoming. *Contributions from the Museum of Paleontology, The University of Michigan, 31*(11), 245-303.

Godebo, T. R. (2005). *Application of remote sensing and GIS for geological investigation and groundwater potential zone identification, southeastern Ethiopian plateau, Bale Mountains and the surrounding areas* (Master's thesis). July. Retrieved Febuary 12, 2014, from http://dmzone.org/papers/RangoGodebo2005.pdf

Goetz, A. F. H., & Rowan, L. C. (1981). Geologic Remote Sensing. *Science, 211*(4484), 781-791.

Haile-Selassie, Y., Deino, A., Saylor, B., Umer, M., & Latimer, B. (2007). Preliminary geology and paleontology of new hominid-bearing Pliocene localities in the central Afar region of Ethiopia. *Anthropological Science*, *115*, 215-222.

Haralick, R. M., Shanmugam, K., & Dinstein, I. (1973). Textural Features for Image Classification. *IEEE Transactions on Systems, Man and Cybernetics*, *SMC-3*(6), 610-621.

Hay, G. J., & Castilla, G. (2008). Geographic Object-based Image Analysis (GEOBIA): A new name for a new discipline. In T. Blaschke, S. Lang, & G. J. Hay (Eds.), *Object-Based Image Analysis: Spatial Concepts for Knowledge-driven Remote Sensing Applications* (pp. 75-90). Berlin, Germany: Springer-Verlag.

Hayden, F.V. (1869). Preliminary report (3rd annual) of the U.S. Geological Survey of Colorado and New Mexico, 3, 91-92.

Honey, J. G. 1988. A mammalian fauna from the base of the Eocene Cathedral Bluffs Tongue of the Wasatch Formation, Cottonwood Creek Area, southeast Washakie Basin, Wyoming. *U.S. Geological Survey Bulletin*. *1669*, C1-C14.

Hildebrandt-Radke, I., & Jarosław, J. (2009). Using multivariate statistics and fuzzy logic system to analyse settlement preferences in lowland areas of the temperate zone: An example from the polish lowlands. *Journal of Archaeological Science*, *36*(10), 2096-2107.

Johansen, K., Arroyo, L. A., Phinn, S., & Witte, C. (2010). Comparison of Geo-Object-Based and Pixel-based change detection of riparian environments using high spatial resolution Multi-spectral imagery. *Photogrammetric Engineering & Remote Sensing*, *76*(2), 123-136.

Johansen, K., Tiede, D., Blaschke, T., Arroyo, L. A., & Phinn, S. (2011). Automatic Geographic Object Based Mapping of Streambed and Riparian Zone Extent from LiDAR Data in a Temperate Rural Urban Environment, Australia. *Remote Sensing*, *3*, 1139-1156. doi:10.3390/rs3061139.

Johnson, E. M. (2005) *A new early eocene mammalian fauna from the great divide basin, southwestern Wyoming: vertebrate paleontology, paleoclimatology, and biostratigraphy* (Master's thesis).

Johnson, M. R. (2010). *Paleoclimate and paleoenvironment reconstruction of the middle Eocene in the Washakie Basin, southwest Wyoming* (Master's thesis).

Kaczmarek, S. E., Hicks, M. K., Fullmer, S. M., Steffen, K. L., & Bachtel, S. L. (2010). Mapping facies distributions on modern carbonate platforms through integration of multispectral Landsat data, statistics-based unsupervised classifications, and surface sediment data. *AAPG Bulletin*, *94*(10), 1581-1606. doi:10.1306/04061009175.

Kim, M., Warner, T. A., Madden, M., & Atkinson, D. S. (2011). Multi-scale GEOBIA with very high spatial resolution digital aerial imagery: scale, texture and image objects. *International Journal of Remote Sensing*, *32*(10), 2825-2850. doi:10.1080/01431161003745608.

King, C., (1878). Systematic geology, U.S. Geological Survey exploration of the 40th parallel. Washington, D.C., v. 1, section 4, 444-458.

Kolbert, E. (2014). *The Sixth Extinction: An Unnatural History*. New York, NY: Henry Holt and Co.

Kruse, F. A., Lefkoff, A. B., Boardman, J. B., Heidebrecht, K. B., Shapiro, A. T., Barloon, P. J., & Goetz, A. F. H. (1993), The Spectral Image Processing System (SIPS) - Interactive Visualization and Analysis of Imaging spectrometer Data. *Remote Sensing of the Environment*, *44*, 145 - 163.

Kvamme, K. (1992). A predictive site location model on the high plains: An example with an independent test. *Plains Anthropologist*, *37*(138), 19-40.

Kvamme, K. (1999). Recent Directions and developments in Geographical Information Systems. *Journal of Archaeological Research*, *7*(2), 153-201.

Laliberte, A. S., Fredrickson, E. L., & Rango, A. (2007). Combining Decision Trees with Hierarchical Object-oriented Image Analysis for Mapping Arid Rangelands. *Photogrammetric Engineering & Remote Sensing*, *73*(2), 197-207.

Laliberte, A. S., Rango, A., Havstad, K. M., Paris, J. F., Beck, R. F., McNeely, R., & Gonzalez, A. L. (2004). Object-oriented image analysis for mapping shrub encroachment from 1937 to 2003 in southern New Mexico. *Remote Sensing of Environment*, *93*, 198-210. doi:10.1016/j.rse.2004.07.011.

Lang, S. (2008). Object-based image analysis for remote sensing applications: modeling reality- dealing with complexity. In T. Blaschke, S. Land, & G. Hay (Eds.), *Object-Based Image Analysis: Spatial Concepts for Knowledge-driven Remote Sensing Applications* (pp. 3-28). Berlin, Germany: Springer-Verlag.

Liu, X. (2004). Dasymetric Mapping with Image Texture. *ASPRS Annual Conference Proceedings*. Denver, Colorado.

Liu, Y., Guo, Q., & Kelly, M. (2008). A framework of region-based spatial relations for non-overlapping features and its application in object based image analysis. *ISPRS Journal of Photogrammetry & Remote Sensing*, *63*, 461-475. doi:10.1016/j.isprsjprs.2008.01.007.

Lucas, R., Rowlands, A., Brown, A., Keyworth, S., & Bunting, P. (2007). Rule-based classification of multi-spectral satellite imagery for habitat and agricultural land cover mapping. *ISPRS Journal of Photogrammetry & Remote Sensing*, *62*, 165-185. doi:10.1016/j.isprsjprs.2007.03.003.

Mahmoudi, F. T., Samadzadegan, F., & Reinartz, P. (2012). Object Oriented Image Analysis based on Multi-Agent Recognition System. *Computers & Geosciences*. doi:10.1016/j.cageo.2012.12.007.

Malakhov, D. V., Dyke, G. J. & King, C. (2009). Remote sensing applied to paleontology: Exploration of upper cretaceous sediments in Kazakhstan for potential fossil sites. *Palaeontologia Electronica*, *12*(2), 1935-3952. ISSN 1094-8074, http://palaeo-electronica.org/2009_2/164/index.html.

McCoy, M. D., & Ladefoged, T. N. (2009). New Developments in the Use of Spatial Technology in Archaeology. *Journal of Archaeological Research, 17*, 263-295. doi:10.1007/s10814-009-9030-1.

McGrew, P. O., (1971). Early and Middle Eocene Faunas of the Green River Basin. Department of Geology, University of Wyoming.

Morris, W. J. (1954). An Eocene fauna from the Cathedral Bluffs Tongue of the Washakie Basin, Wyoming. *Journal of Paleontology*. *28*, 195-203.

Nace, R. L. (1939). Geology of the northwest part of the Red Desert Basin, Sweetwater and Fremont Counties, Wyoming. *Geological Survey of Wyoming Bulletin, 27*, 1-51.

Nigro, J. D., Ungar, P. S., de Ruiter, D. J., & Bergen, L. R. (2003). Developing a Geographic Information System (GIS) for mapping and analyzing fossil deposits at Swartkrans, Gauteng Province, South Africa. *Journal of Archaeological Science*, *30*, 317-324.

Njau, J. K., & Hlusko, L. J. (2010). Fine-tuning paleoanthropological reconnaissance with high-resolution satellite imagery: the discovery of 28 new sites in Tanzania. *Journal of Human Evolution*, *59*, 680-684. doi:10.1016/j.hevol.2010.07.014.

Oheim, K. B. (2007). Fossil Site prediction using geographic information systems (GIS) and suitability analysis: The Two Medicine formation, MT, a test case. *Palaeogeography, Palaeoclimatology, Palaeoecology*, *251*, 354-365.

Pipiringos, G.N. (1955). Tertiary rocks in the central part of the Great Divide Basin, Sweetwater County, Wyoming. *Wyoming Geological Association Guidebook, 10th Annual Field Conference*, 100-104.

Pipiringos, G.N. (1962). Uranium-bearing coal in the central part of the Great Divide Basin. *Geological Survey Bulletin, 1099A*, 1-103.

Platt, R. V., & Rapoza, L. (2008). An evaluation of an Object-oriented Paradigm for Land Use/Land Cover Classification. *The Professional Geographer*, *60*(1), 87-100. doi:10.1080/00330120701724152.

Powers, R. P., Hay, G. J., & Chen, G. (2012). How wetland type and area differ through scale: A GEOBIA case study in Alberta's Boreal Plains. *Remote Sensing of Environment*, *117*, 135-145.

Pradhan, B., & Lee, S. (2007). Utilization of optical remote sensing data and GIS tools for regional landslide hazard analysis using an artificial neural network model. *Earth Science Frontiers, 14*(6), 143-152.

Rajani, M. B., & Rajawat, A. S. (2011). Potential of satellite based sensors for studying distribution of archaeological sites along palaeo channels: Harappan sites a case study. *Journal of Archaeological Science*, *38*, 2010-2016. doi:10.1016/j.jas.2010.08.008.

Rayfield, E. J., Barrett, P. M., McDonnell, R. A., & Willis, K. J. (2005). A geographical information system (GIS) study of triassic vertebrate biochronology. *Geological Magazine, 142*(4), 327-354. doi:10.1017/S001675680500083X.

Roehler, H. W. (1968). Redefinition of tipton shale member of green river formation of wyoming. *American Association of Petroleum Geologists Bulletin*, *52*(11), Pt. I, 2249-2257.

Roehler, H. W. (1991). Revised stratigraphic nomenclature for the wasatch and green river formations of eocene age, wyoming, utah, and colorado. *U.S. Geological Survey Professional Paper, 1506-B.*

Roehler, H. W. (1992). Description and correlation of eocene rocks in stratigraphic reference sections for the green river and washakie basins, southwest wyoming. *U.S. Geological Survey professional Paper, 1506-D.*

Roehler, H. W. (1993). Eocene climates, depositional environments, and geography, greater green river basin, wyoming, utah, and colorado." *USGS Professional Paper 1506-F*, 1-74.

Rose, K. D. (1981). Composition and species diversity in paleocene and eocene mammal assemblages: an empirical study. *Journal of Vertebrate Paleontology, 1*(¾), 367-388.

Rose, K. D., Chew, A. E., Dunn, R. H., Kraus, M. J., Fricke, H. C., & Zack, S. P. (2012). Earliest eocene mammalian fauna from the paleocene-eocene thermal maximum at sand creek divide, southern bighorn basin, wyoming. *University of Michigan Papers on Paleontology, 36.*

Rouse, J. W., Jr., Haas, R. H., Schell, J.A., & Deering, D.W. (1973). Monitoring the vernal advancement and retrogradation (green wave effect) of natural vegetation. *Progress Report RSC 1978-1*, Remote Sensing Center, Texas A&M Univ., College Station, 93 (NTIS No. E73-106393).

Sever. T. L., & Irwin, D.E. (2003). Landscape Archaeology: Remote-sensing investigation of the ancient Maya in the Peten rainforest of northern Guatemala. *Ancient Mesoamerica, 14*, 113-122.

Stigall-Rode, A.L. (2005). The application of geographic information systems to paleobiogeography: implications for the study of invasions and mass extinctions. *Paleontological Society Papers, 11*, 77-88.

Stigall, A.L., & Lieberman, B.S. (2006). Quantitative palaeobiogeography: GIS, phylogenetic biogeographical analysis, and conservation insights. *Journal of Biogeography, 33*, 2051-2060.

Sullivan, R. (1980). A stratigraphic evaluation of the Eocene rocks of southwestern Wyoming. *Geological Survey of Wyoming Report of Investigations, 20*.

Taşdemir, K., Milenov, P., & Tapsall, B. (2012). A hybrid method combining SOM-based clustering and object-based analysis for identifying land in good agricultural condition. *Computers and Electronics in Agriculture, 83*, 92-101. doi:10.1016/j.compag.2012.01.017.

Van der Meer, F. D., van der Werff, H. M. A., van Ruitenbeek, F. J. A., Hecker, C. A., Bakker, W. H., Noomen, M. F., van der Meijde, M., Carranza, E. J. M., de Smeth, J. B., & Woldai, T. (2012). Mulit- and hyperspectral geologic remote sensing: A review. *International Journal of Applied Earth Observation and Geoinformation, 14*, 112-128.

Veatch, A.C. (1907). Geography and geology of a portion of southwestern wyoming. *U.S. Geological Survey, Professional Papers, 56*, 1-178.

Vieira, M. A., Formaggio, A. R., Rennó, C. D., Atzberger, C., Aguiar, D. A., & Mello, M. P. (2012). Object based image analysis and data mining applied to a remotely sensed landsat time-series to map sugarcane over large areas. *Remote Sensing of Environment*, *123*, 553-562. doi:10.1016/j.rse.2012.04.011.

Wescott, K.L., & Brandon, R.J. (Eds.). (2000). *Practical Applications of GIS for Archaeologists*. London, England: Taylor & Francis.

Wu, J., & Loucks, O. L. (1995). From balance of nature to hierarchical patch dynamics: A paradigm shift in ecology. *The Quarterly Review of Biology, 70*(4), 439-466.

Yang, Y., & Rosenbaum, M.S. (2001). Artificial neural networks linked to GIS for determining sedimentology in harbours. *Journal of Petroleum Science and Engineering*, *29*, 213-220.

Zhu, J., Guo, Q., Li, D., & Harmon, T. C. (2011). Reducing Mis-registration and Shadow effects on Change detection in wetlands. *Photogrammetric Engineering & Remote Sensing*, *77*(4), 325-334.

Zwertvaegher, A., Werbrouck, I., Finke, P.A., De Reu, J., Crombé, P., Bats, M., Antrop, M., Bourgeois, J., Court-Picon, M., De Maeyer, P., De Smedt, P., Sergant, J., Van Meirvenne, M., & Verniers, J. (2010). On the use of integrated process models to reconstruct prehistoric occupation, with examples from sandy flanders, belgium. *Geoarchaeology: An International Journal*, *25*(6), 784-814.